THE PRODUCTION OF CHARGED PIONS BY PHOTONS.

BY

J.K. WALKER

PRESENTED TO THE UNIVERSITY OF GLASGOW AS A THESIS FOR THE DEGREE OF DOCTOR OF PHILOSOPHY, SEPTEMBER, 1960.

Preface

The following describes research work performed during the period September, 1957, to September, 1960, in the Department of Natural Philosophy, University of Glasgow, in candidature for a Ph.D. degree.

Chapter I contains a summary of the theoretical attempts to describe the fundamental photoproduction mechanism.

Chapter II is a review of previous experimental methods and results in the field of low energy pion physics.

Chapter III describes the apparatus which I have constructed and developed for the detection and identification of positive and negative charged pi-mesons. This work is new in the respect that this is the only electronic technique which has been able to detect both types of charged pion simultaneously. The work of designing the apparatus was shared with Dr. J.G. Rutherglen.

In conclusion I have described some experiments performed to test the apparatus under normal working conditions. The interpretation of these results was performed by myself.

In Chapter IV I have described an experiment in which the ratio of negative to positive pi-mesons photoproduced from denterium was measured. The liquid target used was constructed by Dr. W. Hogg. The experiment was performed in collaboration with Dr. J.G. Rutherglen with whom also the analysis of results was shared.

Chapter V contains a description of a threshold meson experiment which is the only experiment to date which shows clearly the non linear behaviour of the cross section as threshold is approached. The liquid target used in this experiment was constructed by Mr. D. Miller whose help was greatly appreciated. The collection of data during the experiment which lasted nearly one month was shared with Dr. J.G. Rutherglen and Mr. E. Paterson. The evaluation and analysis of the data was performed mainly by myself.

In Chapter VI an experimental determination of the energy spectrum of the bremsstrahlung beam from the Glasgow synchrotron is described. The gamma ray spectrometer was designed by Mr. A.L. Cockroft and I was concerned only with certain small modifications which had to be made and also with the design and construction of the counters and coincidence units.

In Chapter VII I have concluded by discussing the present state of our knowledge in the field of low energy pion physics.

Appendix A describes an experiment I have performed on the polarization of free relativistic electrons. The motivation for this experiment came from a recent proposal by Dr. K.M. Guggenheimer on the theory of relativistic fermions.

In Appendix B a description is given of a possible means of obtaining high energy plane polarized gamma rays with the use of a proposed electron accelerator. This work is entirely that of myself.

I should like to thank Dr. J.G. Rutherglen for his constant advice and close guidance in all phases of this work. In conclusion I would like to thank Professor P.I. Dee, F.R.S., for his keen interest in the work, and Dr. W. McFarlane and his assistants for providing many hours of beam time on the synchrotron.

CONTENTS.

Chapter I

Introduction

It is now quarter of a century since Yukawa proposed that a particle which we call the π- meson (pion) should exist and be responsible for the strong forces which act between nucleons. The basic Yukawa assumption was that apart from obvious differences of mass, charge, spin and coupling strength the π- meson played a role with respect to the nucleon which was analogous to that played by the photon with respect to the electron.

However, as experiments involving real π- mesons have become possible, it is clear that the quantitative explanation of observed cross sections for meson production and scattering is at least as important a task for the theory as the explanation of nuclear forces. Indeed it has been from such experiments involving free π- mesons, that their fundamental properties have been revealed. We now know that they have zero intrinsic spin and exhibit odd parity relative to the nucleon. A good discussion of these and other properties has been given by Bethe and de Hoffmann (1955).

Meson production has been accomplished by two principal techniques. These are by nucleon - nucleon and photon - nucleon collisions. The former technique involves two nucleons rather than one and is fundamentally more complicated than photoproduction or for that matter meson - nucleon scattering.

The first observations of the creation of charged pions in nuclear collisons of photons were made at Berkeley by McMillan et. al. (1949) when a carbon target was irradiated with a bremsstrahlung beam of maximum energy 335 MeV. Shortly afterwards Steinberger and Bishop (1950) investigated charged pion photoproduction from protons. It is natural to expect that the production of mesons from single nucleons would yield the most information about the nature of mesons and their coupling to nucleons. In general, a study of π- meson production from complex nuclei yields more information about nuclear structure than about the elementary Yukawa interaction.

We may represent the above two types of reactions by the following:

(i) From free nucleons

$$\gamma + P \rightarrow \pi^{+} + n \qquad (1)$$

$$\gamma + n \rightarrow \pi^{-} + P \qquad (2)$$

(ii) From complex nuclei - bound final state

$$\gamma + B_Z^A \longrightarrow \pi^+ + C_{Z-1}^A \qquad (3)$$

- continuum final state

$$\gamma + D_Z^A \longrightarrow \pi^+ E_{Z-1}^{A-1} + n \qquad (4)$$

with similar equations for π^- production.
In this Thesis, consideration will be given to photo-production up to photon energies of about 350 MeV. At energies not much higher than this, complications begin to set in due to the possibility of multiple meson production.

In the processes (1) to (4) the photons have always been obtained in the form of the bremsstrahlung radiation from an electron accelerator. Because the energy spectrum of bremsstrahlung radiation is continuous the energy of the photon responsible for a given event is not usually known. However, in the case of (i), being a two body process, the measurement of the angle and energy of one of the recoiling particles uniquely specifies the kinematics of the reaction, including the energy of the initiating gamma ray. In reaction (1) the recoiling particle chosen is invariably the charged pi-meson.

(a) Photoproduction of Pions from Hydrogen.

Since the pioneering experiments of Steinberger et. al. (1950) a great quantity of experimental data has accumulated. In general, for comparison with theory, the main characteristics of pion photoproduction are the shape and energy dependence of the angular distributions, and the energy dependence and absolute magnitude of the total cross sections.

The salient features of the experimental results appear to be threefold;

i) The total cross sections for both π^+ and π^0 photoproduction were found to exhibit a resonant behaviour at a photon energy near 300 MeV. This was shown to be due to a specially strong P - wave interaction in the pion - nucleon system (Bethe and de Hoffmann 1955).

ii) At threshold the π^+ production cross section increased proportionally to $(E_\gamma - E_o)^{\frac{1}{2}}$ where E_γ is the photon energy and E_0 is the threshold energy for the reaction. This together with the fact that the angular distribution was almost isotropic near threshold indicated that the pion was principally emitted as an S - wave.

iii) In contrast to the π^+ production at threshold, the π° cross section was found to increase as $(E_\gamma - E_\circ)^{3/2}$ indicating a predominant P - wave production of the neutral pion.

The theoretical work which has endeavoured to produce a complete description of the photoproduction of mesons has undergone three distinct phases of development in the years since 1949. Let us consider these phases in some detail.

Phase I

These early theoretical treatments can be subdivided into three perhaps slightly overlapping groups

1. Strong coupling (classical) theories.
2. Weak coupling (relativistic) theories.
3. Phenomenological theories.

The first two of these groups are now only of interest from a historical point of view. The characteristics of strong coupling theories are that the nucleons are treated non-relativistically, that they have a finite size, and that both nucleons and mesons are treated classically, (Brueckner and Case 1951, Watson 1952), (Brueckner and Watson 1952). Its fundamental weakness lies in the fact that the pion - nucleon coupling is not really strong enough for one to treat the virtual mesons as an unquantized classical field. However, qualitative agreement with the observed π^+ angular distribution and energy dependence is obtained. The point of view in the weak coupling approach is entirely opposite to that discussed above. Here it is assumed that in the Hamiltonian of the system, the part corresponding to the free particles is considered much larger than the term describing the interaction and that therefore this term can be considered a small perturbation in the Hamiltonian. The resulting mathematical method can be that of the usual perturbation calculation or that of the so called Tamm Dancoff method (Dancoff 1950). Unfortunately, while the meson nucleon coupling constant is too small for a strict strong coupling approach, it is too large for the weak coupling theory to be effective. Consequently the results are seldom in agreement with experiment.

The phenomenological approach in general, explores the consequences of the most basic laws in physics as applied to the specific situation in hand. These laws usually describe the symmetry properties in nature, such as coordinate inversions. In particular conservation of momentum, energy, isotopic spin, angular momentum and parity have been used by Feld (1953) in his excellent paper, and subsequently by Watson et al. (1956).

Since such an approach leads to generally valid conclusions, independent of specific meson theories, and is based only on the firmly established pseudoscalar nature of the pion, we reproduce what has become known as the "Feld scheme" in figure. 1 The angular distribution of the product pion is denoted by W (θ), where θ is the angle that the pion direction makes with the incident direction of the gamma ray. It is interesting to note that W (θ) depends only on j and ℓ_γ, where j is the total angular momentum of the system and ℓ_γ is the order of the radiation, but not on the angular momentum of the emitted pion ℓ_π or on the nature (i.e. electric or magnetic) of the multipole involved. The pion momentum dependance given in the last column is reliable only near threshold and will be compared with experimental results in the next chapter.

Phase II

The emphasis at this stage was on an approach to the Yukawa theory which has been developed almost entirely since 1954. Chew and Low developed their so called non-local or cut-off form of the Yukawa theory which has had outstanding success in describing low

TABLE I

γ Ray Absorbed	*Intermediate State*	*l of Meson*	l_j	$W(\theta)$	*π-Momentum Dependence*
Mag. dipole	$\frac{1}{2}+$	1	$P_{1/2}$	constant	p^3
Mag. dipole	$\frac{3}{2}+$	1	$P_{3/2}$	$2 + 3\sin^2\theta$	p^3
Elect. dipole	$\frac{1}{2}-$	0	$S_{1/2}$	constant	p
Elect. dipole	$\frac{3}{2}-$	2	$D_{3/2}$	$2 + 3\sin^2\theta$	p^5
Elect. quadrupole	$\frac{3}{2}+$	1	$P_{3/2}$	$1 + \cos^2\theta$	p^3
Elect. quadrupole	$\frac{5}{2}+$	3	$F_{5/2}$	$1 + 6\cos^2\theta - 5\cos^4\theta$	p^7

energy meson phenomena, including both photoproduction and scattering.

The difficulty in evaluating the local form of the Yukawa theory is that it leads to virtual nucleon anti-nucleon pairs which produce a fearful complication. The cut-off form of the theory circumvents this difficulty by introducing a non-locality to smear out the pion - nucleon interaction. This, of course, introduces a new parameter, the size of the interaction region. Thus the cut-off theory contains two parameters, namely the pion - nucleon coupling constant and the pion - nucleon "effective - range" of interaction. The assumption of a "radius" of the interaction region is related to a cut-off in momentum space (Wmax in units of meson mass) through a Fourier transform. Chew and Low have shown that the cut-off theory is highly successful in correlating photo-production with meson scattering if a value of $W_{max} \approx 6$ and f^2 (renormalized coupling constant) = 0.08 are employed. The cut-off theory is discussed by Chew (1957) in his excellent review article.

Phase III

In the last four years an entirely new approach to the whole problem of elementary particle interactions has developed with the application of dispersion relations. The first important contribution along these lines was due to Chew, Low, Goldberger and Nambu (1957) in their now famous paper.

In general, the new study started from an explicit form of the Yukawa scattering matrix, derived by Low (1955) and modified by Goldberger (1955), and has attempted to deduce certain functional properties of the scattering matrix. The motivation for this was the desire to generalize dispersion relations which have been known in electromagnetic theory for many years. It turned out that there was a plausible and essentially unique way in which they could be generalized and the result coincided with certain intuitive conjectures of Nambu.

However, at that time the rigorous derivation of the π- meson dispersion relations required assumptions about the underlying theory which had not been proved. The first proof of the analyticity of the dispersion relations in photoproduction of pions was given by Bremermann, Oehme and Taylor (1958) and Oehme and Taylor (1959) using the theory of functions of several complex variables. Independently, Bogoliubov (1959) was able to show, in a slightly different representation, the correctness of the dispersion relations in pion photoproduction. Simultaneously Lehmann (1959) using a quite different approach, namely an integral representation of the commutator bracket, was able to arrive at the same conclusions. It would seem that this last approach is the most elegant and simple treatment of the complex problem.

It would appear that all the information which the Yukawa approach contains is also contained in the dispersion equations when these are supplemented by unitarity. The condition of unitarity for photo-meson production amounts to the statement that if the production amplitude is decomposed according to total angular momentum, total isotopic spin and parity of the final state then each "eigen - amplitude" has a phase $e^{i\delta}$ where δ is the scattering phase shift for the state in question. It is then possible to project out dispersion relations for individual multipole amplitudes which depend only on a single variable W (the total energy in the barycentric system).

Using $f^2 = 0.08$, a camparison by Koester and Mills (1957) of the numerical results of the dispersion method for neutral pion production with the best available experimental data reveals extremely good agreement. It turns out that the π^+, π^0 mass difference is at least as important as some of the approximations in the numerical evaluation. A major extension of the theory would be required to handle the mass difference properly since a violation of charge independence is involved.

In the case of positively charged pion production Bernardini (1959) using $f^2 = 0.08$ has carried out a comparison of the numerical results of the dispersion method with the best available experimental information and found reasonable (within 20%) agreement with respect to absolute value of the cross section at 90° in C.M.S. from threshold up to the resonance energy. However, it was felt (Cini et. al. 1958) that there was a finite discrepancy between the threshold behaviour of the photoproduction amplitude of π^+ mesons from hydrogen and the experimental data. A better experimental determination of this quantity has been the main topic of this Thesis.

In conclusion we may adopt the view point of Gell-Mann (1955). Let us suppose the Yukawa theory to be defined through the conventional relativistic field formalism in exact analogy to quantum electrodynamics.

Then let the predictions of meson theory and electrodynamics be evaluated by the dispersion equation method. Up to now this method has not been applied to all possible problems but it seems plausible that eventually it will be. Gell-Mann then argues that from such a standpoint the two theories stand, fundamentally speaking, on an equal footing. The low energy limits of both have been experimentally confirmed, and ambiguities exist in both due to unknown high energy cross sections under dispersion integrals. In the case of meson theory the deviations from the zero energy limits set in much more rapidly. This circumstance, argues Gell-Mann, is of no fundamental significance. The final theory of elementary particles will have to predict the mass, spin, parity, etc., spectrum for all particles, and give a general method for calculating the various interactions between the particles.

b) Photoproduction of Charged Pions from Deuterium.

We have considered the basic theoretical approaches to a description of photoproduction of mesons from protons. Let us now turn our attention to the reaction

$$\gamma + n \rightarrow \pi^- + p \qquad (5)$$

All the theories which we have discussed indicate that π^- production from neutrons should be more prolific than π^+ production from protons. Breuckner and Goldberger (1949) were the first to show that there was a constructive interference between the contributions of the current of the meson and that of the recoil proton. In the positive meson production, the recoil particle is a neutron and consequently does not contribute in this way. Thus we could expect that

$$r = \frac{(\gamma + n \rightarrow \pi^- + p)}{(\gamma + p \rightarrow \pi^+ + n)} > 1 \qquad (6)$$

Clearly it is not possible to study the photoproduction of mesons from neutrons experimentally, since we have no free neutron targets available. The closest approach we have to a free neutron is the neutron in the deuterium nucleus. Therefore, a great deal of experimental and theoretical work has gone into the photoproduction of mesons from deuterium. The deuteron is a relatively simple structure of two nucleons and in fact more is known about this system than about almost any other nucleus. The kinematic considerations are simpler also, and the system left over after charged meson photoproduction is not a bound system and hence can be treated by relatively simple approximations. The effect of final state interactions is the same in both π^+ and π^- production from deuterium except for the Coulomb interaction in the case of π^+ production because there is only one charged particle present. For negative pion production, however, there are three charged particles in the final state, two protons and a pion. The other complication that arises is the loss of the one to one relationship between the energy of the in-coming photon and the energy of the meson produced. This results from the internal motion of the nucleons in the nucleus. Thus the angle and energy of a single reaction product in either of the reactions,

$$\gamma + d \rightarrow \pi^- + 2p \qquad (7)$$

$$\gamma + d \rightarrow \pi^+ + 2n \qquad (8)$$

does not uniquely define the energy of the incident photon responsible for the reaction.

As well as the study of the photoproduction of mesons, there are other reasons why meson photoproduction from deuterium is of interest. For example, such a study yields information about the dependence of photoproduction on the charge and spin of the nucleon. This has been discussed in detail by several authors, notably by Lax and Feshback (1951). The charge dependence is revealed in the ratio of the cross sections of negative to positive mesons, and the spin dependence in the ratio of positive mesons from protons and from deuterons.

Experimentally, the measured quantity is the ratio R where

$$R = \frac{(\gamma + d \rightarrow \pi^- + 2p)}{(\gamma + d \rightarrow \pi^+ + 2n)} \qquad (9)$$

Moravesik (1957) using the Chew Low cut-off theory has developed expressions describing the variation of R with meson angle of emission and gamma ray energy. Good agreement is obtained both between the theory and previous experimental work, and with results described in this Thesis.

Similar to the interest in charged pion production from hydrogen near threshold there is interest in the variation of R near threshold. First, there is the very well founded theoretical prediction of 1.3 (Chew et. al. 1957) for the value of the ratio r at threshold

$$r_o = \left\{ \frac{(\gamma + n \rightarrow \pi^- + p)}{(\gamma + p \rightarrow \pi^+ + n)} \right\}_{\text{threshold}} \qquad (10)$$

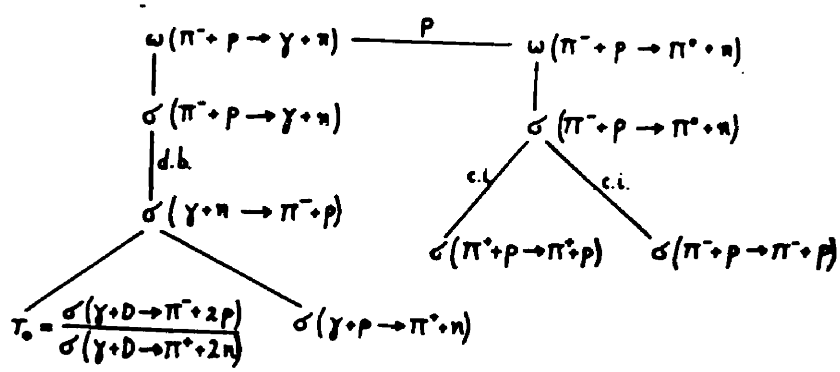

Figure 2. Diagramatic representation of the connection between pion scattering, absorption and photoproduction.

The relationship between the measured ratio, R, and the ratio for free nucleons, r, has been most recently discussed by Baldin (1958). Secondly very general arguments using charge independence and detailed balance can be used to inter-relate the threshold values in pion physics. Figure 2 shows the connections between the Panofsky ratio and the positive energy S - wave cross sections for pion - proton scattering and pion photoproduction. This topic will be discussed in more detail later as the threshold values in pion physics form the main content of this Thesis.

Chapter 11

Review of Published Work.

This is a review of previous measurements in the field of low energy pion physics, and also includes a brief description of the present studies.

a) π^+ Production from Hydrogen.

The early measurements of charged pion production from hydrogen were obtained with bremsstrahlung beams of maximum energies about 300 MeV. The mesons detected, had energies in the range 40 to 130 MeV, and were emitted at angles between 30° and 150° in the laboratory system. Both nuclear plates and counter telescopes (with and without magnetic analysis) were used in conjunction with the following types of targets.

i) Subtraction technique (for example polythene (CH_2) - carbon (C)) as used by Lebow et al. (1953), Goldschmidt et al. (1953), Luckey et al. (1953), Jenkins et al. (1954).

ii) Cooled high pressure gas target as used by White et al. (1952)(1953).

The statistical accuracy of this early work was not very good as can be seen from figures 3,4 & 5 , where the

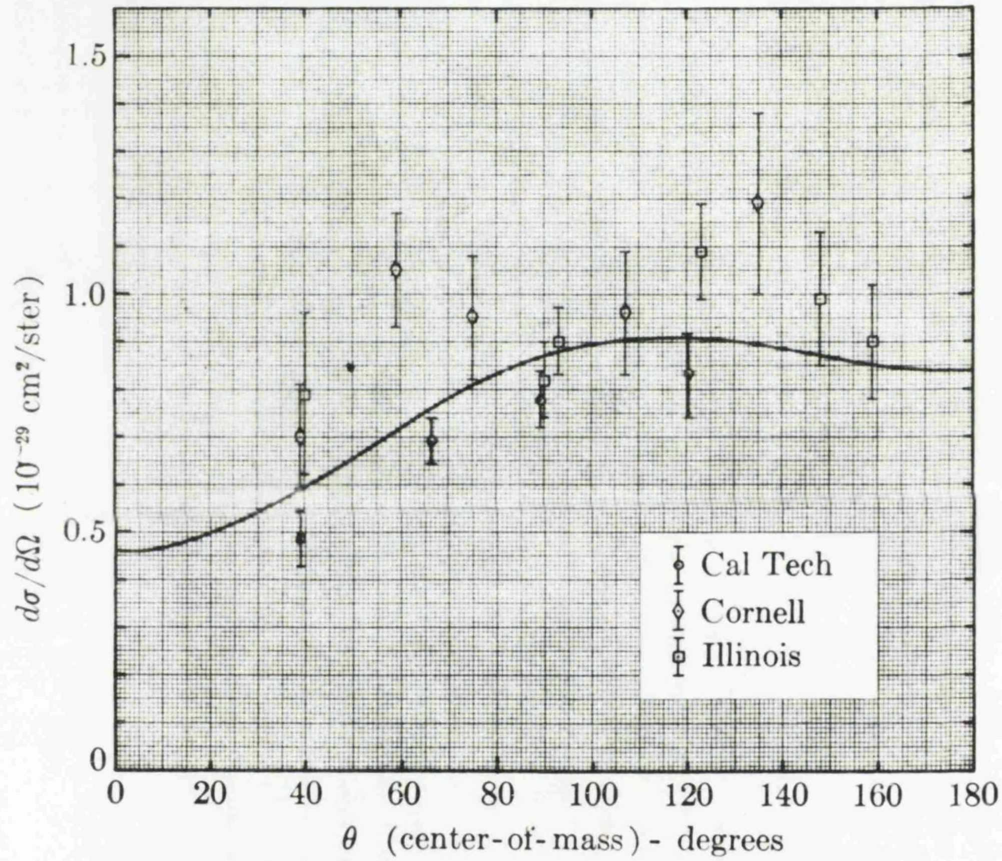

Fig. 3. π^+ photoproduction from hydrogen at 200 Mev. The Cornell data are those of Luckey (1954); the Illinois data those of Bernardini and Goldwasser (Bernardini 1954a, c); and the Cal Tech data those of Walker et al (1954).

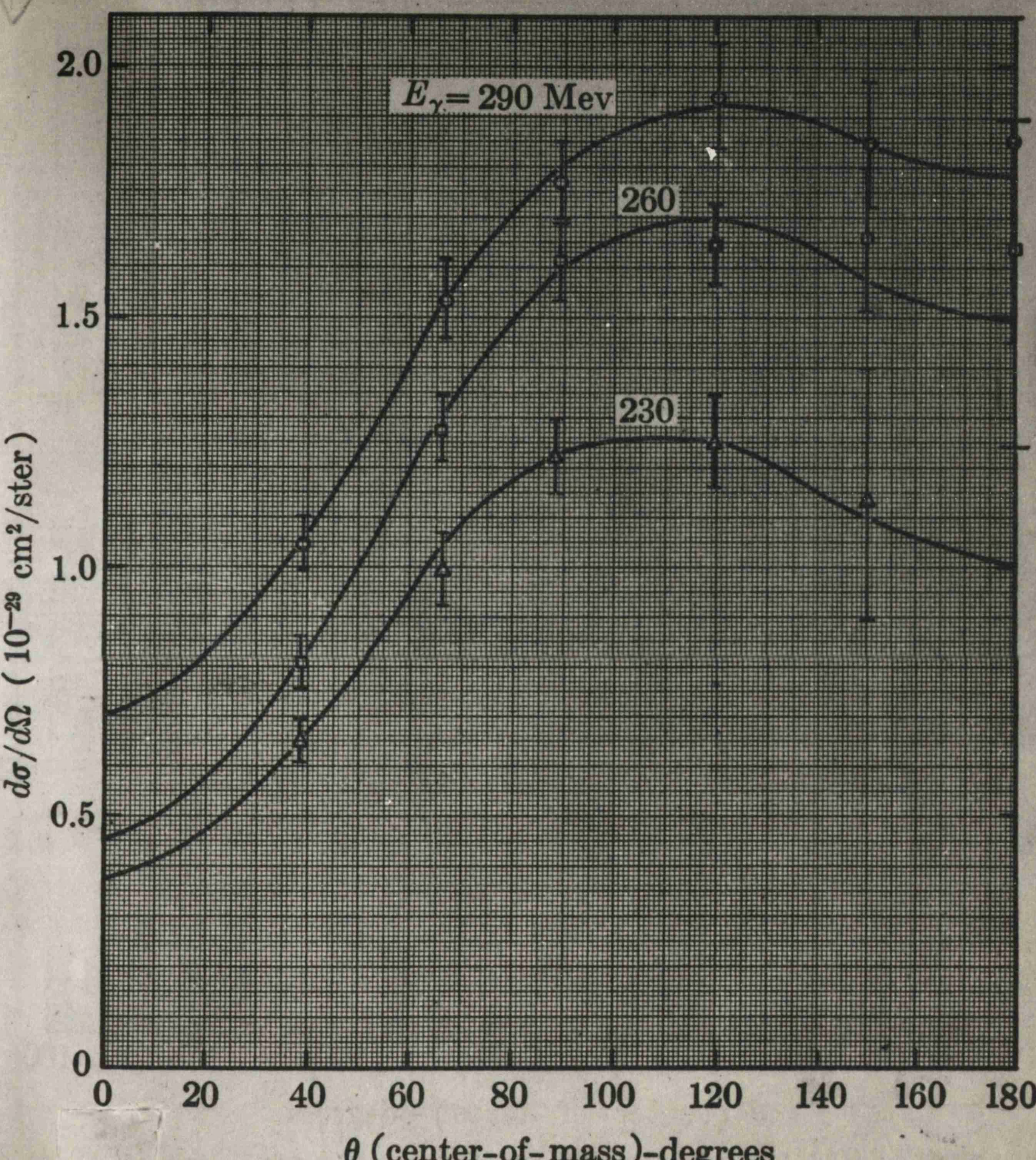

Fig. 4 —π^+ photoproduction from hydrogen from 230 to 290 Mev. The experimental points are magnet data due to Walker et al (1954). The solid curves are fits to the experimental data.

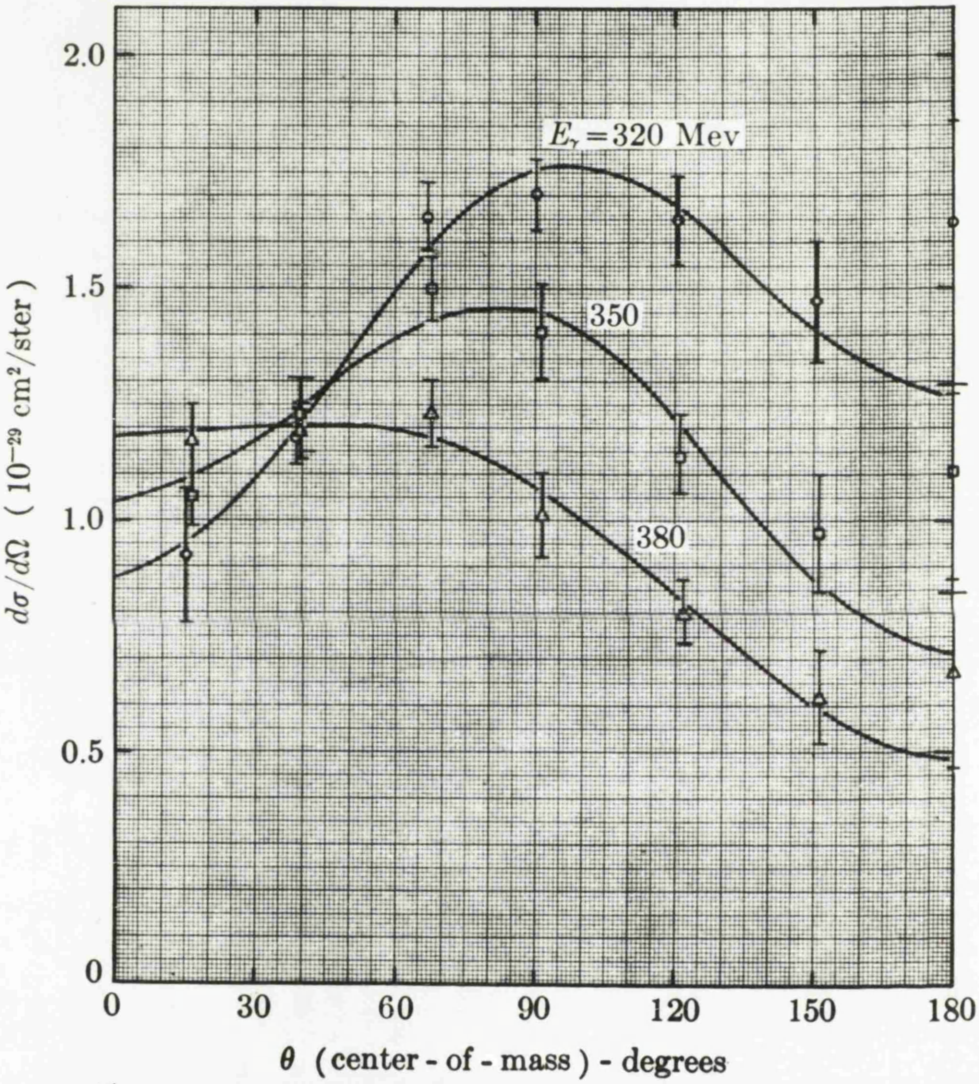

Fig. 5. π^+ photoproduction from hydrogen from 320 to 380 Mev. The experimental points are magnet data due to Walker et al (1954). The solid curves are fits to the experimental data.

angular distribution of π^+ mesons photoproduced from hydrogen is shown as a function of gamma ray energy. On eof the major disadvantages of this early work was the inability to compare reliably, the so called absolute cross sections between various laboratories. This was due to the difficulty experienced in monitoring correctly the gamma ray beams which were used. Only quite recently has a really reliable intercalibration of monitors between laboratories, been accomplished (Loeffler et al. 1959). Thus the results of experiments up until around 1955 were only able to discern the crudest features of the photoproduction reaction. The following conclusions were drawn by Bethe and de Hoffmann (1955) from the early work;

a) The resonance exhibited at 300 MeV by the total cross section and variation of angular distribution could be described satisfactorily by a strong P - wave pion-nucleon interaction.

b) From the threshold behaviour of the cross section and angular distribution it could be inferred that the pion was produced in an S - state at low energies.

This early work really gave the first indication that a resonance existed in the pion - nucleon interaction. Subsequently the same resonance was excited in studies of pion - nucleon scattering. If the resonance is attributed to a P - wave interaction between the pion and nucleon, it can be shown that a good description of the experimental results could be obtained (Chew 1954, 1956). Since then, however, an era of much more refined measurements has existed. The era was heralded in by the now classical experiment by Beneventano et al. (1956) on the production of charged pions from hydrogen near threshold. The statistical accuracy ($\lesssim$ 4%) their results was in general greater than any previous photoproduction experiment with hydrogen. Figure 6 shows their measurements of the angular distribution of π^+ mesons between 170 and 220 MeV of photon. When their results for the angular distributions are analysed in the form

$$\frac{d\sigma}{d\Omega} = W\left\{ a_0 + a_1 \cos\theta + a_2 \cos^2\theta \right\} \qquad (11)$$

where W is a kinematical factor and is in fact given by

$$W = \frac{3\,\omega}{(1 + \frac{\mu}{M})^2} \qquad (12)$$

where $\mathfrak{p}$ and W are the c.m.s. momentum and energy of the emitted pion, and θ is the meson angle of emission in the centre of mass system, they found a_o to be independent of energy. This is shown in figure 7 . Thus to a good approximation, we may say that Benevantano et al. found that the differential cross section for π^+ production increased linearly with momentum from threshold up to about 220 MeV of gamma ray. From the Feld scheme in figure 1 we can see that this implies that the meson is emitted in an S - state relative to the proton.

The variation of a_1 and a_2 was found and is plotted in figure 8 . The solid curves shown, were theoretical attempts to describe the results. As the variation of a_o with energy appeared to be negligible their extrapolated value for a_o at threshold was 14.8 x 10^{-30} cm^2/sterad. The experimental technique which had been adopted for this experiment was a liquid hydrogen target and nuclear pellicles embedded in a sea of emulsion as meson detectors. Their final publication, Beneventano et al. (1956) gives a review of their results, experimental technique, corrections to results and the method of analysis. The scanning efficiency was reported to be around 99% and never below 97%. All

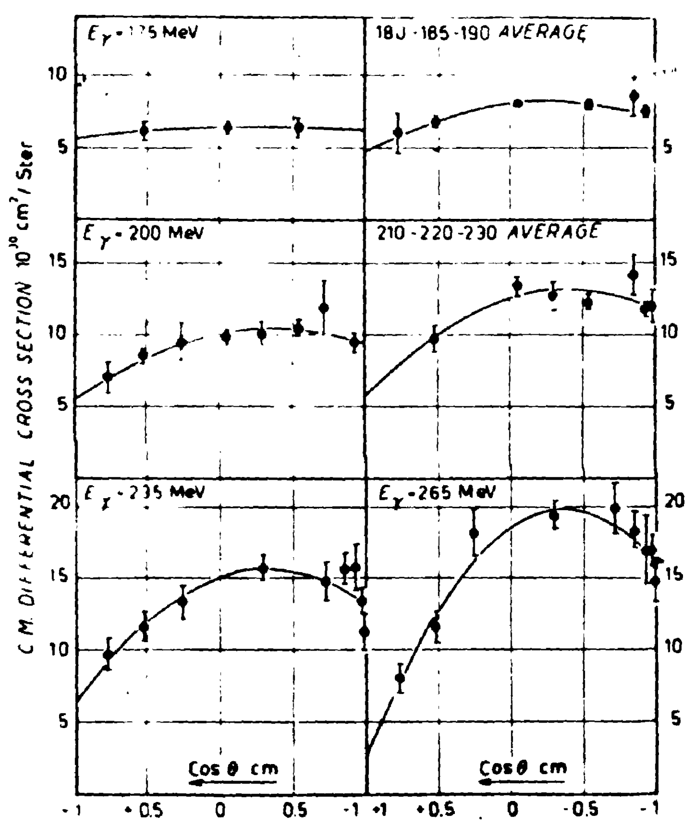

C.M. DIFFERENTIAL CROSS SECTION 10^{-30} cm²/Ster
MeV
18J -185-190 AVERAGE
Eγ - 200 MeV
210 -220-230 AVERAGE
MeV
Eγ -265 MeV
Cos θ cm
Cos θ cm

FIG. 6.

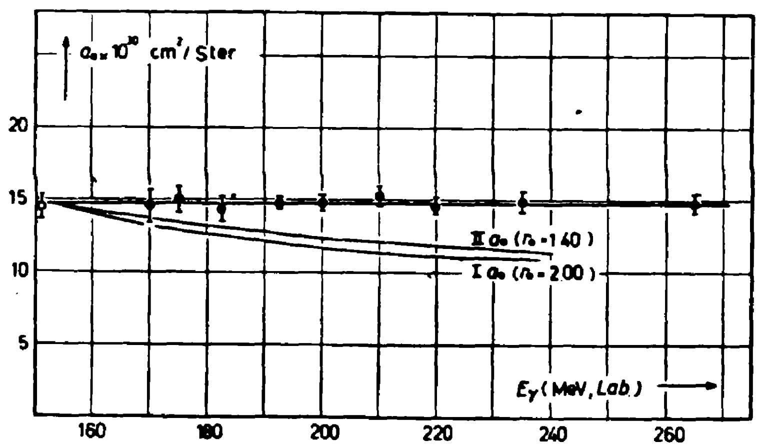
$a_0 \times 10^{30}$ cm^2/ Ster
20
15
10
5
II a_0 (r_0 = 1.40)
I a_0 (r_0 = 2.00)
E_γ (MeV, Lab.)
160
180
200
220
240
260

FIG. 7.

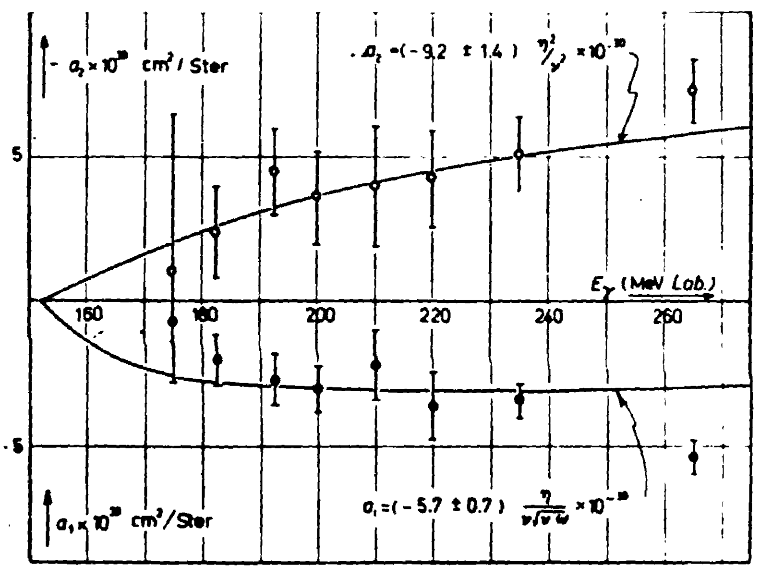

Fig. 8. Plots of the coefficients, a_1 and a_2

obvious corrections were taken into account and included decay in flight, nuclear interaction of the pions before coming to rest, background from target walls and edge effects of the pellicles. It is difficult to offer any criticism of this experiment as the results exhibited considerable self consistency. Also reported in the Beneventano (1956) paper is the result of an experiment performed by Leiss Penner and Robinson of the National Bureau of Standards (N.B.S.). The technique they used was most in genious.

They irradiated a liquid hydrogen target with a bremsstrahlung beam which had a time duration of $2\,\mu$ sec. Then with the use of a scintillation counter telescope they detected the positron from the decay.

$$\pi^+ \xrightarrow[\tau_1]{} \mu^+ \xrightarrow[\tau_2]{} e^+$$

$$\tau_1 \approx 2 \times 10^{-8} \text{ sec}$$

$$\tau_2 \approx 2 \times 10^{-6} \text{ sec}$$

By varying the maximum energy of the bremsstrahlung beam they were able to observe the activation cross section for π^+ production at 154 MeV of gamma ray. Several points deserve mention in this technique.

To obtain an absolute cross section they required to know the exact shape of the energy spectrum in the neighbourhood of the bremsstrahlung end point. This is neither an easy thing to calculate not to find experimentally. Secondly the efficiency of the telescope for detection of the positron must be know. Because the positrons have a continuous energy spectrum, and also can annhilate in flight the overall efficiency can be less than 50%. Thus a systematic error in the assessment of the efficiency of the telescope produces a much larger error in the absolute cross section. Their first result is shown in the form of an open circle in figure 7 where good agreement is obtained with the extrapolation due to Beneventano. The Leiss et al. result was subsequently retracted, underwent revision due to neglected correction factors in the telescope efficiency and was republished about 25% higher than the original result (Bernardini 1959).

Since 1956, three other groups, Adamovic et. al. (1959), Carlson - Lee et al. (1959) and Barbaro et al. (1959), using nuclear emulsions as detectors and liquid hydrogen targets habe repeated the experiment and in general obtained internal consistency but rather systematically disagree with the original Beneventano results.

This is shown in figure 9 where the coefficient a_o, as defined previously, is plotted against gamma ray energy. Included in this figure are the results of Lewis and Azuma (1959) who used a scintillation counter and delayed coincidence system in conjunction with a subtraction technique (CH_2 - C). It is seen that the Lewis and Azuma results are in reasonable agreement with those due to Beneventano et al. The curves shown in figure 9 are the predictions of the dispersion relations under different assumptions for the recoil terms $N^{(-)}$ which can not at present be evaluated accurately due to lack of knowledge of the small P - wave phase shifts.

In conclusion, a summary of the main points of the above review can be made as follows.

1) There appear to be two "schools" of results a) Beneventano et al. and Lewis et al., who appear to agree as to absolute value and energy independence of a_o.
b) Adamovic et al., Carlson Lee et al., Barbaro et al. and Leiss et al., whose combined results at low energy indicate a value of a_o around 25% higher than school a).

2) Monitoring uncertainties of gamma beams in different laboratories have long been a source of difficulty in intercomparison of absolute cross sections. The question

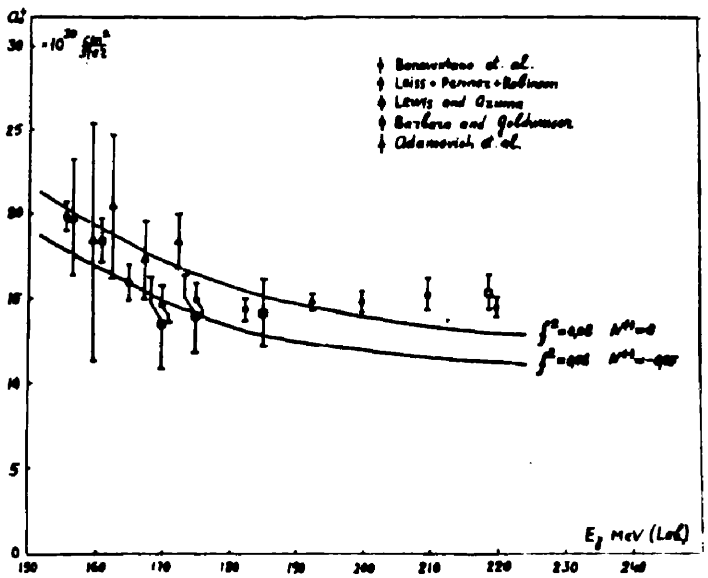

Figure 9. . Photoproduction of charged pions from hydrogen at 90^{0} in c.m. Plotted is the square of the matrix element against gamma energy. The curves are the predictions of the of the dispersion relations.

arises, is the above difference of 25% due to some systematic error, or does it reflect a true energy variation?

3) No single experiment shows the variation of a_0, as a function of energy, which is predicted by the dispersion relations. In particular the statistically significant Beneventano results show a marked energy independence.

In view of the above discrepancies and uncertainties it is clear that there is a need for a single experimental determination of the variation of a_0 from 200 MeV down to as close to threshold as possible, to show whether or not the energy dependence predicted by the dispersion relations is correct or otherwise. This was one of the reasons why an investigation of the photoproduction of charged pions from hydrogen at low pion energies was undertaken.

Recently several observations have been made at sufficiently small angles that the pion current contribution, in the dispersion relations (and also in some of the older theories), has been identified explicitly. For example Malmberg and Robinson (1958) at 225 MeV and Knapp et al. at 275 MeV incident photon energy, have performed detailed angular distributions. Knapp et al., have shown that detailed information on the small P - wave phase shifts of the pion nucleon interaction may be obtained in this manner.

Taylor et al. (1960) at Stanford have photoproduced mesons with plane polarized bremsstrahlung and have shown that this is a sensitive test of the dispersion relations with which good agreement is obtained.

The conclusion to all this work would seem to be that the dispersion predictions appear to describe the photoproduction mechanism rather satisfactorily.

b) π^-/π^+ Ratio from Deuterium.

The early measurements of the ratio of negative to positive pions photoproduced from deuterium gave a value close to unity, and independent of pion energy. These results were obtained using bremsstrahlung beams of maximum energies around 300 MeV. The most statistically significant results have been obtained at the Californian Institute of Technology by Sands et al. (1954) and at Illinois by Beneventano et al. (1956). The technique used in the former case was a high pressure gas target in conjunction with a magnet and counter telescope. In the latter case, Beneventano used the experimental set up described in the hydrogen experiment. The results are shown in figures 10,11,12&13.

It is seen that a reasonably complete and self consistent set of results has been obtained. However, the following point is worthy of notice. The Cal. Tech. and Illinois experiments were performed with the maximum energy of the bremsstrahlung at 500 MeV and 300 MeV respectively. Due to the availability of higher energy quanta for producing pions, it is possible for a high energy pion, at creation, which is scattered in the nucleus and is detected as a low energy pion. The general result of such processes would be to make the observed π^-/π^+ ratio less steeply dependent on the pion energy. This effect would be expected to be more pronounced in the Cal. Tech. results than the Illinois, however, the magnitude of such an effect on the ratio is difficult to estimate. To investigate whether such an effect was at all serious, it was decided to obtain some π^-/π^+ ratios from deuterium with a bremsstrahlung maximum energy of 240 MeV.

There has been considerable interest in the ratio from deuterium in the neighbourhood of threshold as discussed in Chapter 1. Figure 14 shows the present position from the experimental point of view. At these low pion energies the Coulomb interaction in

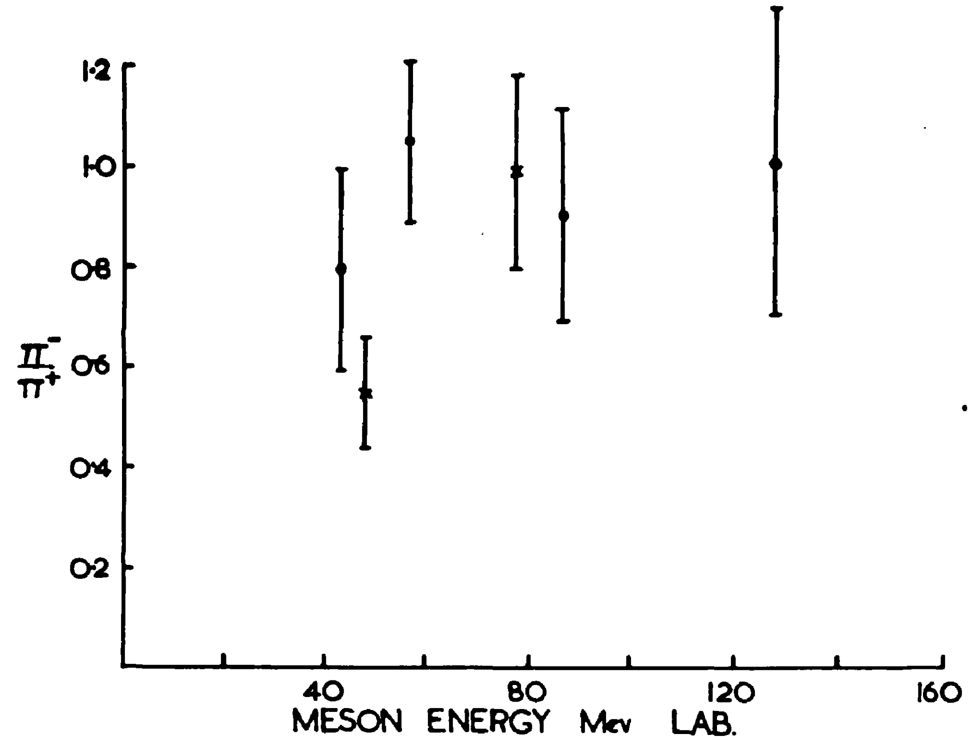

Figure 10. 45°
• White et al (1952), × Jenkins et al (1954).

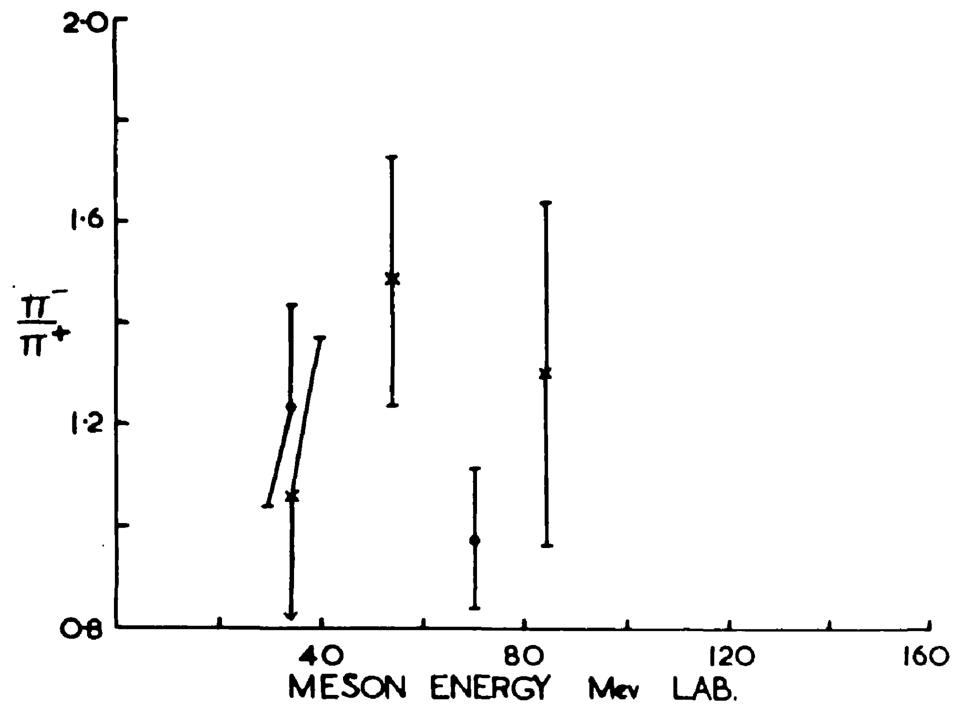

Figure 11. 90°
• White et al (1952), × Jenkins et al (1954).

π^-/π^+ ratio from deuterium as a function of meson energy, angles measured in the laboratory system.

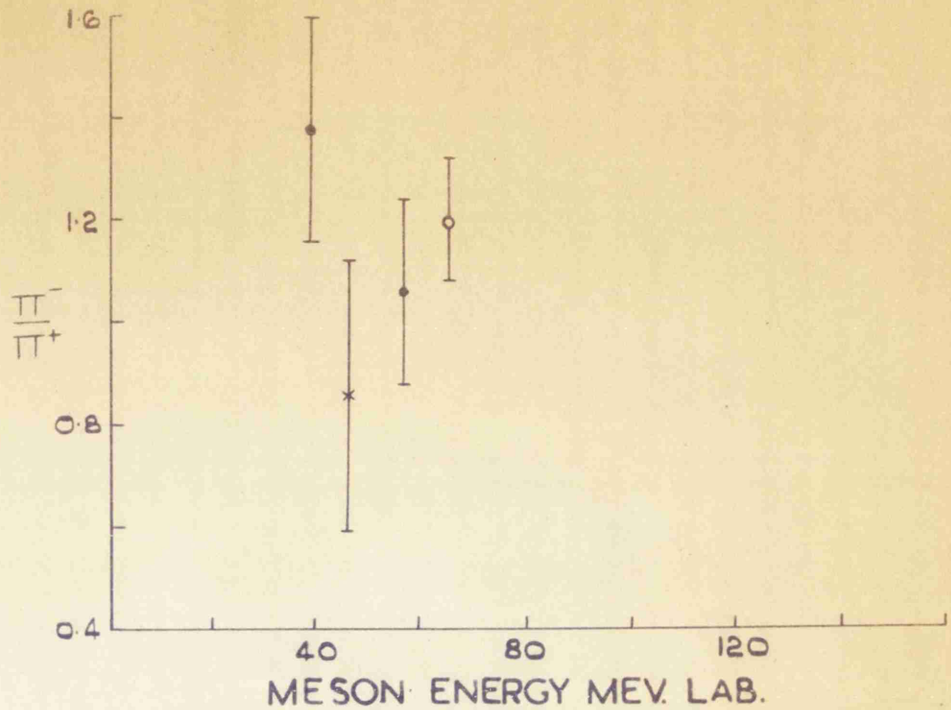

Figure 12.

• 135° White et al (1952), x 180° Jenkins et al (1954), ○ 135° Littauer and Walker (1952).

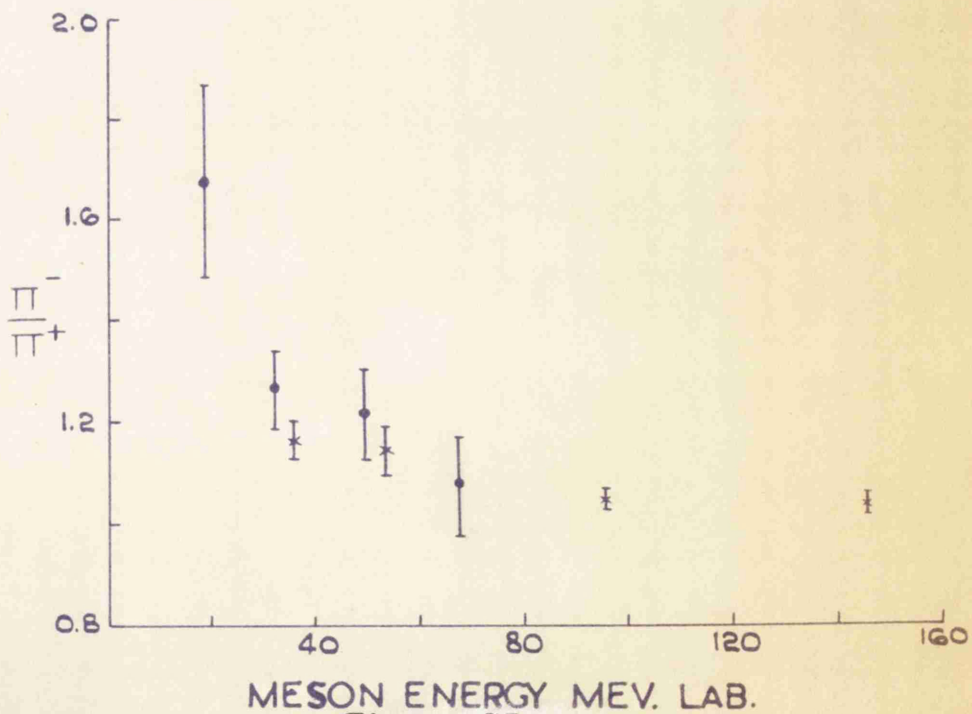

Figure 13.

x 29° Sands et al (1954),

• 45° Beneventano et al (1956).

π^-/π^+ ratio from deuterium as a function of meson energy, angles measured in the laboratory system.

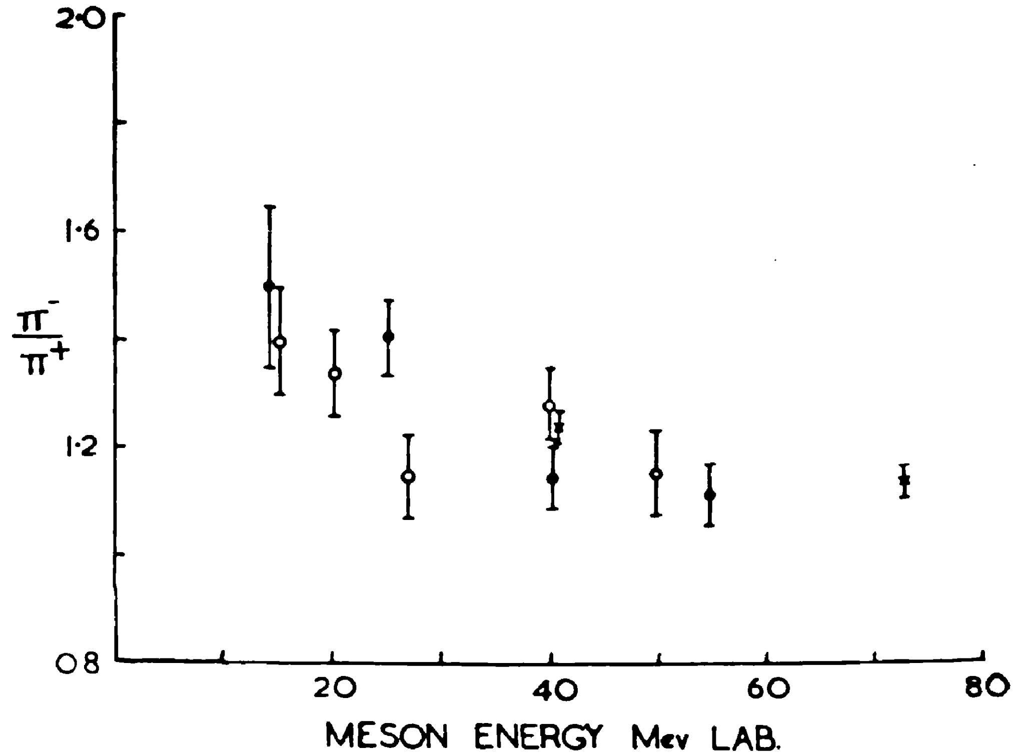

Figure 14.
× 73° Sands et al (1954),
• 75° Beneventano et al (1956),
○ 75° Hogg et al. (1958).

π^-/π^+ ratio from deuterium as a function of meson energy, angles measured in the laboratory system.

the final state is important. This effect has been considered in detail by Baldin (1958). When the Baldin corrections are applied to the experimental data a value for production from free nucleons is obtained in good agreement with dispersion predictions (Hogg 1958)

$$r_o = \frac{\gamma + n \rightarrow \pi^+ + p}{\gamma + p \rightarrow \pi^+ + n} = 1.3 \pm 0.1 \quad (13)$$

It is interesting to notice that the two techniques which have been most frequently used are the nuclear emulsion technique, Beneventano et al. (1956), Carlson Lee et al. (1959), Karlamov et al. (1959), Adamovic et al. (1959), and the magnetic spectrometer in association with a counter telescope Sands et al. (1954), and Hogg et al. (1959). The emulstion technique has the advantage that the positive and negative pions are recorded simultaneously but has the disadvantage that a large scanning time is required to obtain adequate statistics. The method of magnetic analysis is not limited in this way, but has the disadvantage that the positive and negative pions cannot be counted at the same time. The technique developed for the present work overcomes this difficulty.

c) Panofsky Ratio and the S-wave Scattering Lengths.

Panofsky et al. (1951) have observed that when a meson is captured from a Bohr orbit in hydrogen (i.e., when the π^- has little kinetic energy and is in a bound state) then about half the time a gamma ray is emitted, whereas the other half of the time a π^o is emitted. More precisely they have observed that

$$P = \frac{W(\pi^- + p \rightarrow \pi^o + n)}{W(\pi^- + p \rightarrow \gamma + p)} = 0.94 \pm 0.20 \qquad (14)$$

In the case of radiative capture the gamma ray is monoenergetic of 130 MeV, whereas in the charge exchange case the decay gammas have a distribution of energies centered on 70 MeV. This is due to the Doppler shift produced by the motion of the π^o meson. The experiment was performed by allowing π^- mesons, produced in the Berkeley 184 inch cyclotron, to come to rest in a cooled high pressure hydrogen target and observing the resultant energy distribution of the gamma rays by means of a conventional pair spectrometer. Although the energy resolution of the apparatus was good, the drawback of low detection efficiency, inherent in pair spectrometer work, produced a result of rather poor statistical accuracy.

Since the original experiment of Panofsky et al. many other groups have repeated the measurement with more intense pion beams. At Liverpool, two groups carried out the experiment using complementary techniques. Cassels et al. (1957) used a total absorption Cerenkov counter to measure the spectrum of gamma radiation from the absorption of negative pions in a liquid hydrogen target. In this case the efficiency of detection was high but the energy resolution was poor. The result obtained by this group was $P = 1.5 \pm 0.15$. Keuhner et al. (1956), using a 180^{o} focussing pair spectrometer and a liquid hydrogen target, obtained the value $P = 1.60 \pm 0.17$.

At Chicago Fischer et al. (1958) using a technique more or less identical to that used by Cassels et al., obtained a value of $P = 1.87 \pm 0.10$, which is more than 20% higher than the Cassels result. It would seem that a systematic error existed in at least one of these two experiments. It has been pointed out, principally by Cassels, that such an error most probably lay in the collimation arrangement used in the Chicago experiment, however, no definite proof of this can be given.

More recently the Panofsky ratio has been measured with great accuracy at Nevis (Columbia) by Koller and Sachs, the result being $P = 1.46 \pm 0.1$. This agrees very well with the Liverpool results, puts considerable doubt upon the first Panofsky value and contradicts that of Fischer et al.

Finally two measurements have been completed in the last few months and have yielded results which are in agreement within their quoted uncertainties of about 3 or 4%. They are due to Merrison et al. (1960) at Cern who obtained 1.59 ± 0.06 and Samieson (1960) who used a bubble chamber and obtained a value of $P = 1.62 \pm 0.06$. The weighted mean of all these results is 1.60 ± 0.035. We shall take the value of the Panofsky Ratio P to be given by $P = 1.60 \pm 0.04$

Let us now turn to a consideration of low energy meson nucleon scattering. It is possible to analyse the scattering of mesons from protons in terms of the isotopic and angular momentum states involved (Bethe and de Hoffmann 1955). For very low energies where S - wave scattering is dominant, only two parameters need to be considered, namely α_1, which is the phase shift, corresponding to the isotopic spin state I = $\frac{1}{2}$, and α_3 that for I = $\frac{3}{2}$. The total cross sections corresponding to the three possible reactions may be written down as:

$$\begin{aligned} \sigma(\pi^+,\pi^+) &= 4\pi \lambda_c^2 \; a_3^2 \\ \sigma(\pi^-,\pi^-) &= \frac{4\pi}{9} \lambda_c^2 \; (a_3 + 2a_1)^2 \qquad (16) \\ \sigma(\pi^-,\pi^0) &= \frac{8\pi}{9} \frac{V_0}{V_-} \lambda_c^2 \; (a_1 - a_3)^2 \end{aligned}$$

where λ_c is the pion Compton wave length,

a is the scattering length i.e., $a = \frac{\alpha}{q}$ where

α is the phase shift,

q is defined as the pion momentum, in units of μc in the centre of mass frame,

V_0 is the velocity of the outgoing π^0 and

V_- is the velocity of the incoming π^-.

Clearly a determination of any two of the total cross sections yields solutions for the two scattering lengths a_1 and a_3.

There have been many experimental determinations of these cross sections (for references prior to 1956 see Orear (1956)). Orear performed a least squares determination of reported data for all low energy pion-nucleon scattering. This analysis was based on the assumption that the S - wave scattering lengths showed a linear dependence on the c.m.s. pion momentum. His results were

$$\begin{aligned} a_1 &= 0.167 \pm 0.012 \\ a_3 &= 0.105 \pm 0.010 \end{aligned} \tag{17}$$

The situation of the charge exchange scattering amplitude ($a_1 - a_3$) has improved however due to contributions from Nagle et al. (1957), Wooten (1959), Fischer et al. (1959) and Barnes et al. (1958). These results together with others were summarized by Hamilton et al. (1960) and yielded

$$(a_1 - a_3) = 0.245 \tag{18}$$

at zero energy in the c.m.s.

As has already been mentioned, it is possible to construct a relationship between the various threshold processes, that is photoproduction, scattering and capture of pions. An argument of this type was first used by Brueckner et al. (1951). The only assumptions required in such an argument are that charge independence of nuclear forces and detailed balance are both valid concepts. A diagramatic representation of the general link up in low energy pion physics is shown in figure 2 . The quantitative relationship may be expressed as (Hogg 1958)

$$P = 6.70 \; 10^{-28} \times \left\{ \frac{(a_1 - a_3)^2}{r_0 \times a_0} \right\}_{W = 1} \qquad (19)$$

where W is the pion energy in the c.m.s. and the constant factor has been derived mainly from kinematical relationships and can only introduce a negligible source of error. As the right hand side of (19) has to be evaluated at zero pion energy in the c.m.s. some method of extrapolation is required. This can be seen when it is remembered that a_0, $(a_1 - a_3)$ and r_0 are measured at finite positive pion energies while the Panofsky Ratio P is measured at small negative pion energies. The various extrapolation procedures which have been suggested will be described later.

If we assume for the moment the following values,

$$P = 1.60$$

$$(a_1 - a_3) = 0.25$$

$$r_o = 1.3$$

then calculation using (19) yields

$$a_o \simeq 20 \times 10^{-30} \text{ cm}^2/\text{sterad.}$$

This value of a_o should be compared with the extrapolated value in figure 9 where it is seen that a value of 20 is in apparent agreement with some of the data.

Hence, it is concluded that it is possible to obtain agreement between the negative energy result of the Panofsky ratio measured from capture data and that predicted from positive energy results of pion scattering and photoproduction. There are two points however which are worth emphasising. These are, first, that the experimental results on a_o show internal inconsistency as has already been discussed and the above mentioned agreement is obtained in contradiction to the best experimental results on a_o by Beneventano et al. (1956) who obtained $a_o = 14.8$. Secondly it is clear that better experimental evidence is required in this interesting low energy region of photoproduction to provide unambiguous evidence for the correctness of the energy dependence predicted by the dispersion relations and also for better evidence for the "required" value of $a_o = 20 \times 10^{-30}$ cm^2/sterad. It was for these reasons that an investigation of the photoproduction of pions from hydrogen at low energies was undertaken.

d) Present Investigations.

The hydrogen and deuterium experiments were carried out using liquid targets, and the charged pions were detected in a scintillation counter telescope.

In the hydrogen experiment a 1 cm. thick flat walled liquid target was exposed to the 320 MeV bremsstrahlung beam from the Glasgow electron synchrotron. Pions, in the energy range 7 to 48 MeV, were detected at a mean laboratory angle of 50 degrees to the photon beam. The telescope consisted of four scintillation counters. Particles which stopped in the second counter were defined by a $12\bar{3}$ coincidence - anticoincidence. Mesons were separated from electrons and protons by means of their $\frac{dE}{dx}$ and E pulse heights from counters 1 and 2.

Similarly particles which stopped in the third counter were defined by a $123\overline{4}$ coincidence - anticoincidence and mesons were separated out by the pulse heights from counters 2 and 3. Thus two well defined energy intervals of pions were studied simultaneously, and with the use of absorbers of carbon and copper placed between the target and the telescope, pions of higher energy were studied. This enabled the variation of the cross section to be studied in the range 200 down to 160 MeV of gamma ray. If the energy dependence of a_0 was described properly by the dispersion approach then there would be $\sim$ 20% variation of a_0 in this energy interval. Previous experimental determinations of a_0 below 200 MeV of gamma ray were unable to show this energy dependence. This was primarily due to the inability of previous techniques to cover a wide enough energy interval. In this way the present technique was superior to previous methods.

In the deuterium investigation the scintillation counter distinguished mesons from other particles by pulse height analysis. The characteristic π^+ meson decay scheme was used to separate the two types of charged meson. Thus both π^+ and π^- mesons were detected simultaneously. This represents a considerable advantage over previous electronic systems which usually involved magnetic selection of one type of charged pion at a time.

Chapter III

Description of Meson Detector System

(a) Introduction.

The detection and identification of fast charged particles emitted from nuclear reactions is a frequent problem in nuclear physics. It is often necessary to identify particles of a particular mass among a flux of various other particles. This requires, in general, that any technique should consist of a simultaneous measurement of at least two dynamical quantities which have a different dependence on the masses of the particles.

In investigations on the production of pions from nuclei by photons it is necessary to identify pions among a large background of electrons and protons. It is also necessary to have separate identification of the positive and negative pions. For this purpose the techniques which have been most frequently employed are nuclear emulsions, magnetic analysis in association with counters, and scintillation counter telescopes.

(i) Nuclear Plates.

Both π^+ and π^- mesons may be detected simultaneously using nuclear photographic emulsions, each type of charged pion being distinguished by its track and track ending. It is found that more than 99% of all π^+ mesons exhibit a decay scheme

$$\pi^+ \rightarrow \mu^+ + \nu$$
$$\mu^+ \rightarrow e^+ + \nu + \tilde{\nu}$$

Such a decay scheme is easily identifiable in a nuclear emulsion. On the other hand π^- mesons, when they come to rest, are quickly captured by a nucleus and release their rest mass energy in the form of high energy nuclear fragments. Thus when a π^- meson comes to rest, there results a n pronged star where n = 0, 1, 2, 3 etc. A difficulty of this technique is therefore the identification of one pronged events, that is whether a given event is a $\pi^+ \rightarrow \mu^+$ decay or a π^- star with only one visible track. Such events, however, can be analysed in terms of previously established results of the prong frequency of π^- mesons in emulsions, Cheston et. al. (1950), De Sabata et. al. (1953), Beneventano et. al. (1954), and Demeur et. al. (1956). It would seem however that there is serious disagreement (about 15%) between several of these authors. Thus it would appear that until better experimental work is performed on the prong frequency of π^- stars in emulsions, the possibility of a systematic error in π^- to π^+ ratios must be recognised.

(ii) Magnetic Analysis:

A magnetic spectrometer in association with a counter telescope which measures either the energy loss, or range, or time of flight of the particles to be detected, can be used to identify both π^+ and π^- mesons.

In contrast to the lengthy procedure of scanning emulsions, the method of magnetic analysis produces results relatively quickly. There are, however, certain disadvantages of this technique not least of which are selection of one energy interval at a time, acceptance usually of a small solid angle and the detection of only one type of charged pion at a time.

(iii) Scintillation Counter Telescope.

Following the original work of Jakobson et. al. (1951) many workers have detected π^+ mesons by means of their decay scheme

$$\pi^+ \xrightarrow[\tau_1]{} \mu^+ \xrightarrow[\tau_2]{} e^+$$

where $\tau_1 = 2.56 \times 10^{-8}$ secs. and $\tau_2 = 2.22 \times 10^{-6}$ secs. (Crowe 1957). This technique can also be applied to detect π^- mesons, but in this case only those pions which decay in flight can be counted (Motz et. al. 1955). Such a method has a very low detection efficiency and has not been used to any extent.

A counter telescope system, which can be used to count both π^+ and π^- mesons simultaneously in a well defined solid angle and energy interval, has been developed for the present work on π^- to π^+ ratios.

(b) General Method

It can be shown (Wolfe et. al. 1955 and Keck et. al. 1952) that to a good approximation

$$\frac{dE}{dx} \propto \frac{M^{0.45} Z^{1.1}}{R^{0.45}}$$

in the usual notation. Thus for singly charged particles with the same range R, a measure of the specific ionization $\frac{dE}{dx}$ distinguishes particles of different mass. This implies that for mesons, protons and deuterons of the same residual range the $\frac{dE}{dx}$ are in the ratio of 0.4 : 1 : 1.3 respectively. This applies to mesons whether they are positively or negatively charged. To make use of this fact three counters were used; the first one to measure $\frac{dE}{dx}$, the second in which to stop particles and measure the resulting pulse heights E and the third to act as an anticoincidence counter. An automatic plot of $\frac{dE}{dx}$ against E was performed for every particle which stopped in the second counter. The resolution was sufficient to give with negligible uncertainty the total number of π^+ and π^- measons which stopped in the second counter.

To distinguish between π^+ and π^- mesons which stopped in the second counter, use was made of the characteristic decay properties of the π^+ meson. The π^+ decays into a μ^+ meson of kinetic energy 4.1 MeV with a half life of 18$m\mu$sec. A delayed coincidence technique for the $\pi^+ \rightarrow \mu^+$ decay has been used by several experimenters and is described in detail by Imhof et. al. (1958). A similar system for detecting the $\pi^+ \rightarrow \mu^+$ decay, with an efficiency of about 50%, has been developed in the present work. In order to determine the efficiency of the delayed coincidence system for detecting the μ^+ it is necessary to use hydrogen as a target from which only π^+ mesons can be photoproduced.

In the general case when there are π^+ and π^- mesons present the knowledge of the efficiency of the delayed coincidence system together with the number of delayed coincidences recorded yields the number of π^+ mesons which stop the second counter. Subtraction of this number from the total number of mesons yields the number of π^- mesons. Thus a simultaneous measurement on both types of charged pion can be performed.

(c) Description Of Counter Telescope.

The telescope consisted of three plastic scintillators (N.E. Type 101) connected by perspex light guides to R.C.A. 6810 A photomultipliers. Scintillators 1, 2 and 3 were .25", 0.75" and .5" thick and 3", 3" and 4" in diameter respectively. Between counters 1 and 2 there was a perspex absorber 0.25" thick. Figure 15 shows the telescope and the associated fast electronics, which was situated close to the counters.

Particles which stop in counter 2 register a $12\bar{3}$ coincidence anticoincidence in a Bell type coincidence circuit which has a resolving time of 20 $m\mu$ sec. When such an event occurs it is necessary to measure the pulse heights C1 and C2 from the collectors of photomultipliers 1 and 2. This is accomplished by means of the display unit to be described later.

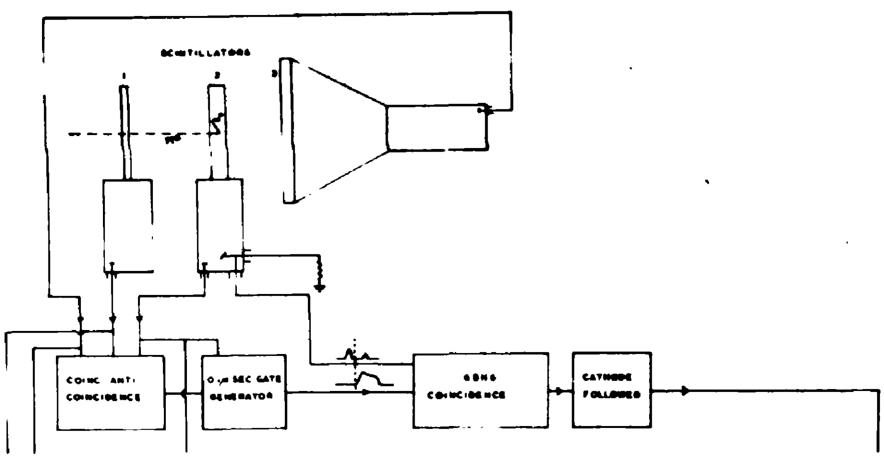

Fig. 15. The Scintillation Counter Telescope and associated fast electronics.

delayed coincidence system together with the number of delayed coincidences recorded yields the number of π^+ mesons which stop the second counter. Subtraction of this number from the total number of mesons yields the number of π^- mesons. Thus a simultaneous measurement on both types of charged pion can be performed.

(c) Description Of Counter Telescope.

The telescope consisted of three plastic scintillators (N.E. Type 101) connected by perspex light guides to R.C.A. 6810 A photomultipliers. Scintillators 1, 2 and 3 were .25", 0.75" and .5" thick and 3", 3" and 4" in diameter respectively. Between counters 1 and 2 there was a perspex absorber 0.25" thick. Figure 15 shows the telescope and the associated fast electronics, which was situated close to the counters.

Particles which stop in counter 2 register a $12\bar{3}$ coincidence anticoincidence in a Bell type coincidence circuit which has a resolving time of 20 $m\mu$ sec. When such an event occurs it is necessary to measure the pulse heights C1 and C2 from the collectors of photomultipliers 1 and 2. This is accomplished by means of the display unit to be described later.

We shall now consider the sequence of pulses for a $\pi^+ \rightarrow \mu^+$ decay in counter 2. A $12\bar{3}$ event, which may be a π^+ stopping in 2 was made to operate a trigger which produced a gate pulse 80$m\mu$sec long and rise time about 15$m\mu$ sec. In order to have a faster rise time and to minimise jitter this pulse was mixed with the limited pulse on the anode of a limiter fed by the collector of photomultiplier 2. This resulted in a gating pulse which had a rise time of about 8$m\mu$ sec to 3 volts high and lasted for nearly 100$m\mu$sec. The gate pulse was applied to one grid of 6BN6 valve. The output pulse from the last dynode of photomultiplier 2 was fed directly on to the other control grid of the 6BN6. A 27" length of 200 ohm cable was used as a clipping line on this dynode. This line was terminated with an 80 ohm resistor to minimise overshoot (Madey 1955). With this arrangement the total width of the pulse was about 15$m\mu$sec. The object of this was to keep the π^+ and μ^+ pulses as distinct as possible. The timing of the pulses on the grids of the 6BN6 was arranged so that the dynode pulse occurred first and the gate pulse was applied to the other grid 15$m\mu$sec later. As the half life for the $\pi^+ \rightarrow \mu^+$ decay is 18$m\mu$sec. it is clear that something like 50% of $\pi^+ \rightarrow \mu^+$ decays will be recorded as delayed coincidences. The anode pulse of the 6BN6 was integrated by the stray capacity of the anode. It was found that optimum response was obtained using -3 volts bias on both grids of the 6BN6.

The operation of the delayed coincidence circuits ($12\bar{3}\ \pi^+$) could be checked by measurements using the 2.6 MeV gamma ray of ThC^{11}. This was achieved by introducing sufficient 200 ohm delay cable for the dynode pulse to arrive at the grid of the 6BN6 sometime within the gate pulse. The maximum pulse height from ThC^{11} is slightly less than the equivalent light output of the 4.1 MeV meson. Thus operation on the maximum pulses of the ThC^{11} gamma ray spectrum was considered adequate for the delayed coincidence system. This was achieved by adjusting the E.H.T. voltage on photomultiplier 2 until the delayed coincidence was just functioning. The E.H.T. voltage on counter 1 was adjusted until the gain was suitable for the display unit to be described.

(d) Description of Display Unit.

The information from the telescope and its associated fast electronics was fed through 70 ohm cables to the display unit. This information consisted of the pulse heights from the collectors of photomultipliers 1 and 2 (C1 and C2) and the pulses from the fast coincidence circuit ($12\bar{3}$) and the delayed coincidence circuit ($12\bar{3}\,\pi^+$). The object of the display unit is to record the above pulses in such a manner as to require a minimum of subsequent analysis.

A block diagram of the electronics is shown in figure 16. A pulse signifying a $12\bar{3}$ event was used to trigger a blocking oscillator which produced a 10V pulse 100$m\mu$sec long. This pulse was used to open gates through which the collector pulses C1 and C2 passed to lengthening circuits, which produced 2 μ sec long flat-topped pulses of amplitudes proportional to the amplitudes of the C1 and C2 pulses. The lengthened pulses were fed to two paraphase amplifiers whose outputs were connected to the X and Y plates respectively of a cathode ray tude (Mullard Type DB 13/2). Simultaneously the cathode of the C.R.T. was pulsed 40 volts negative for 2μsec. This produced a spot on the C.R.T. whose coordinates were proportional to the pulse heights C1 and C2 from counters 1 and 2. A second C.R.T. whose X and Y plates were connected in parallel with the first was only brightened up when there was a delayed coincidence in counter 2. This was achieved by using the $12\bar{3}\,\pi^+$ pulse to trigger a

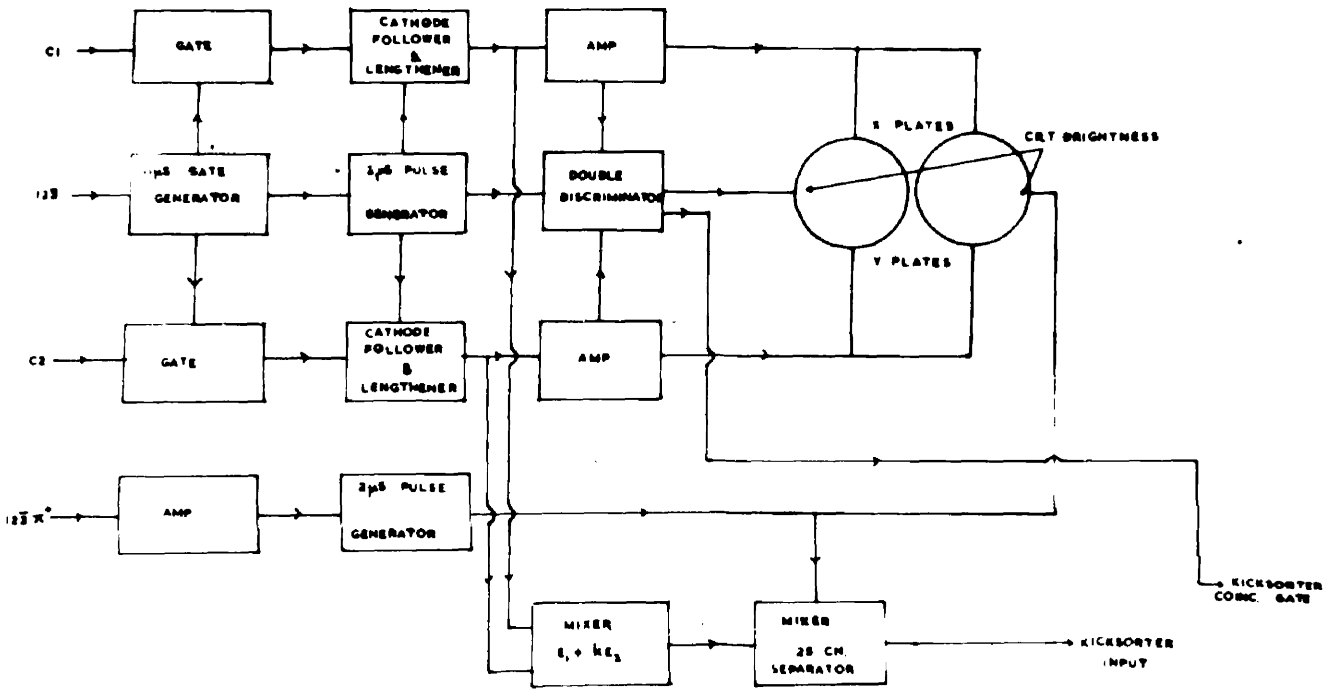

Fig. 16. A block diagram of the electronics in the display unit which records the pulse heights produced in counters 1 and 2 for all particles which stop in the second counter.

2μ sec pulse generator whose 40 volts negative output pulse was fed to the cathode of the second C.R.T. The two C.R.T.'s were photographed simultaneously.

Typical spot pictures are shown in figure 17 in which the "ordinary" and "delayed coincidence" pictures have been superimposed, the latter being shown by large spots. The three different groups of spots from left to right correspond to electrons, mesons and protons. The number of spots due to electrons is very large and only the outline of the electron region is shown. These pictures were obtained using liquid hydrogen as a target, from which only π^+ mesons can be photoproduced. It is seen that about 50% of the mesons have been detected as delayed coincidences. Protons which have produced large pulses in the second counter have produced "self delayed coincidences" due to the tail of the dynode pulse entering the delayed coincidence gate. Provided the pulse height level for the production of "self delayed coincidences" was higher than the top of the meson region in figure then no ambiguities could occur. Figure 17 is the result of a 15 minute run with a 3 cm liquid hydrogen target exposed to a 240 MeV bremsstrahlung beam, and with the telescope about 12" away from the centre of the target.

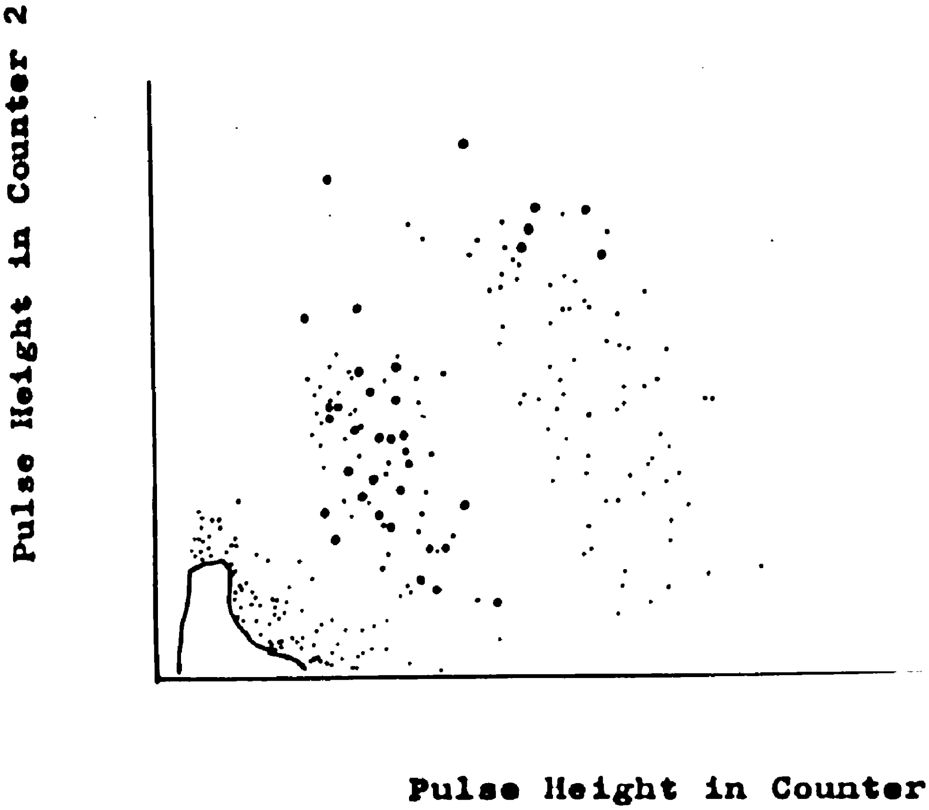

Fig. 17. A spot picture as photographed on the display unit. The target used was hydrogen from which only π^+ mesons may be produced. See text for explanation of large spots.

When a target other than hydrogen is exposed to the gamma ray beam, π^- as well as π^+ mesons are produced. Figure 18 shows the result of a 15 minute run using a 3 cm. deuterium target. The region between the mesons and protons is now occupied by a few spots. This is due to π^- mesons which stopped in the second counter and produced stars of high energy charged particles, thus increasing the pulse height from counter 2. Although the separation between mesons and protons is not quite so clearly defined as in the case of hydrogen, it is possible to obtain the total number of mesons with good accuracy from an analysis of the spot density. To reduce the probability of fast charged product particles from π^- stars entering the anti-coincidence counter and thus causing a veto, the anti-coincidence counter was situated as far away as possible from the second counter without producing a loss of anti-coincidence efficiency.

Although analysis of the results was normally performed by counting the spots from the photographs, it is useful in a long experiment to have some means of quickly checking the overall operation of the apparatus. Use was made of a multichannel pulse height analyser for this purpose.

The meson and proton groups on the normal 123 C.R.T.

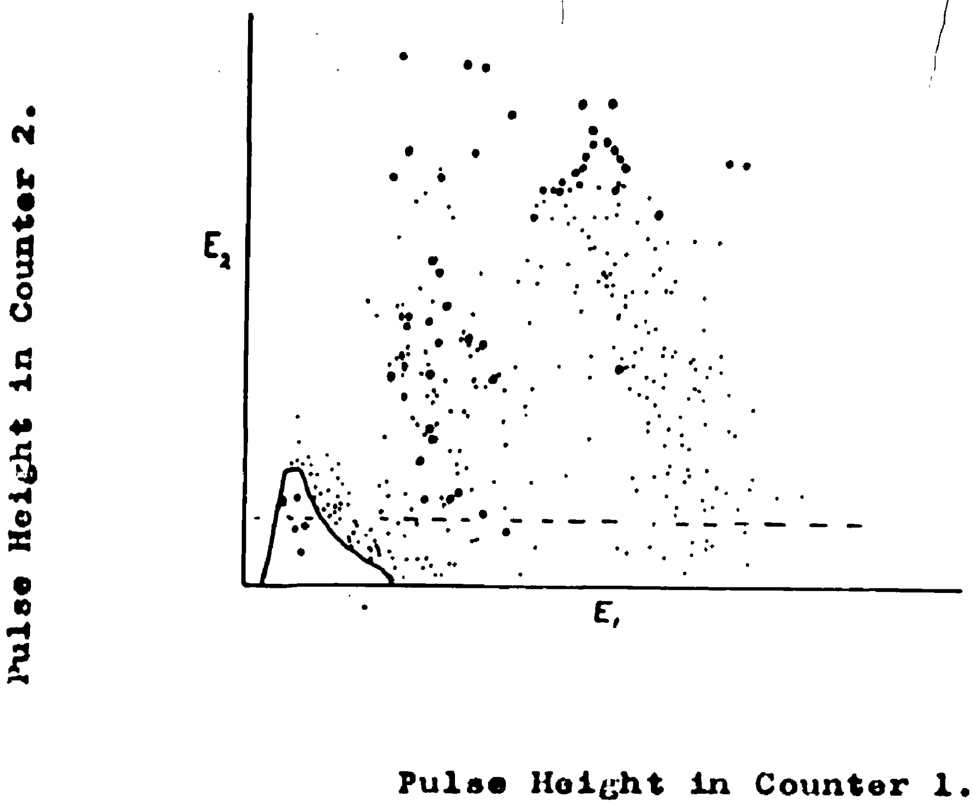

Fig. 18. A spot picture taken with deuterium as a target from which both π^+ and π^- mesons can be produced. See text for explanation of large spots.

display are approximately parallel straight lines. Hence if the pulses proportional to E_1 and E_2 are added to form a pulse of height $P = E_1 + kE_2$, the spectrum of the pulses P shows well defined peaks corresponding to mesons and protons when the constant k is correctly adjusted. In figure 19 such a spectrum, obtained with a liquid hydrogen target, is shown in the first 35 channels.

In order to display the events associated with a delayed coincidence separately a step pulse of standard height, equivalent to 35 channels on the kicksorter, was added to the corresponding P pulse. The peaks corresponding to π^+ mesons and "self delayed" high energy protons can be seen in channels 40 to 60 in figure 19 .

From the point of view of the dead time of the kicksorter it was desirable to prevent the majority of the large number of electrons from being counted by the kicksorter. This was achieved by gating the kicksorter by the output of a double discriminator which was fed by the E_1 and E_2 pulses.

It is seen that the kicksorter display fulfils the requirement of giving an instantaneous assessment of the results and an overall check on the operation of the apparatus at all times.

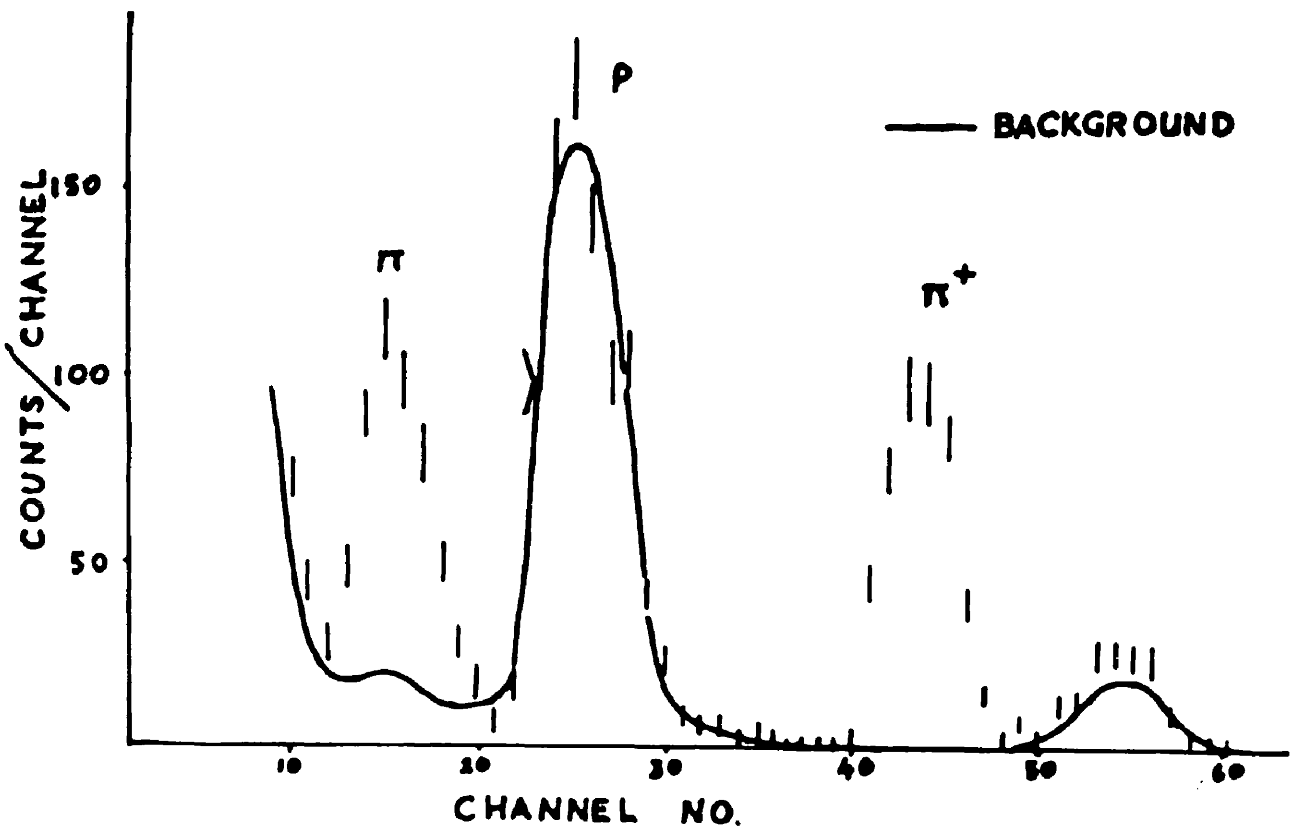

Kicksorter Channel Number

Fig. 19. Spectrum obtained on kicksorter using a liquid hydrogen target. The solid curve shows the spectrum obtained with the target empty. The two groups corresponding to π mesons are well resolved. The upper group contains mesons for which delayed coincidences have been recorded.

(e) Tests with Carbon and Polythene Targets:

Because of the facilities with which solid targets (as distinct from liquid hydrogen for example) could be obtained, carbon and polythene were used in the preliminary tests of the apparatus.

A 1 cm. thick slab of pure graphite was placed in the 240 MeV photon beam from the Glasgow synchrotron. The axis of the telescope was placed at 112° to the beam direction. To reduce the singles counting rate, due to general room background, a thick wall of lead was erected on three sides of the telescope. On the side facing the target, there was placed a lead collimator which had a hole of 2.5" diameter and whose centre was on the axis of the telescope. Under these conditions the telescope functioned satisfactorily.

Pions of energy 15 - 25 MeV were detected. In order to extend the region of investigation to higher pion energies,absorbers of various thicknesses were placed in front of the telescope. A typical spectrum on the kicksorter is shown in figure 20, which indicates the resolution obtainable with the use of a carbon target. From curves such as this the numbers of mesons ($\pi^{+}+\pi^{-}$) within the various energy intervals were estimated.

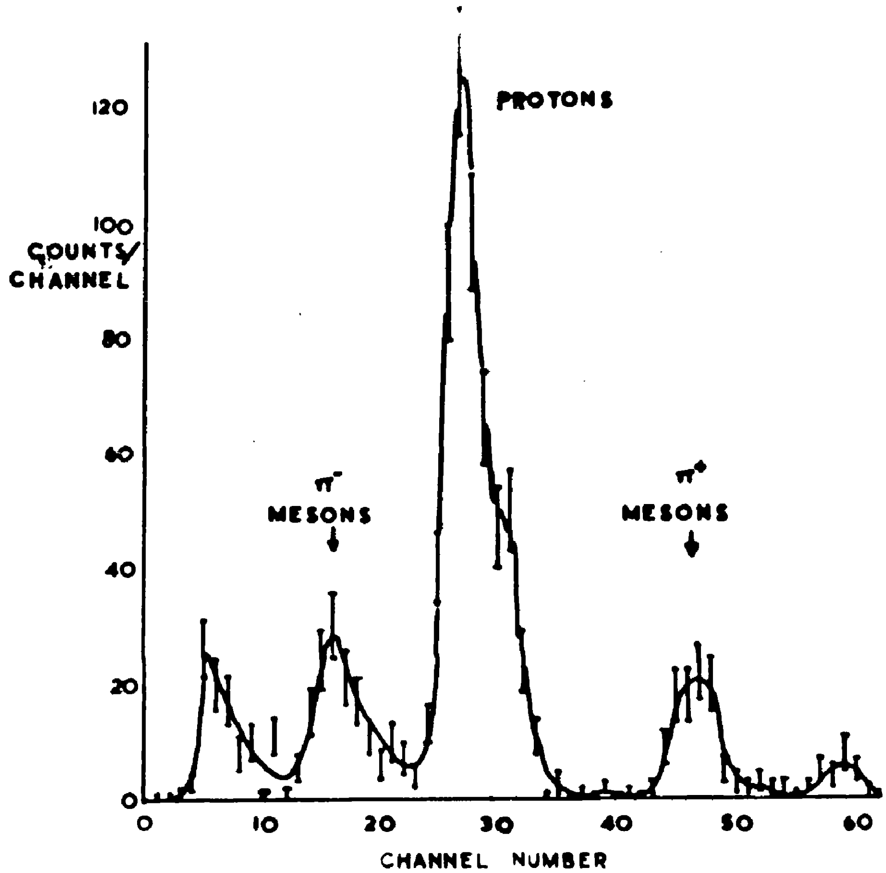

Figure 20. . Typical spectrum on Kicksorter showing resolution of the apparatus.

The observed energy spectrum of the pions was found to be of the form shown in the figure 21. No corrections, such as decay in flight, multiple scattering, etc., have been applied to the data shown. Curve I is the shape that would be expected from photoproduction from a free nucleon, namely hydrogen. This curve was calculated assuming the results of Beneventano (1956) for the variation of cross section with energy of the reaction

$$\gamma + P \longrightarrow \pi^+ + n$$

and also a Schiff thin target bremsstrahlung spectrum for the gamma ray beam. Curve II was obtained from I by folding in a typical Chew Goldberger momentum distribution to describe the motion of the nucleons within a carbon nucleus. Both curves are normalized to the experimental results at a pion energy of 32 MeV. It is seen that an energy dependence, in reasonable approximation to the experimental result, is obtained.

A run with polythene (CH_2) was performed at the same angle and under identical conditions to the carbon run. The thickness of the polythene was such that it had the same stopping power for mesons as the carbon target. Runs using the various absorbers were performed just as with the carbon target.

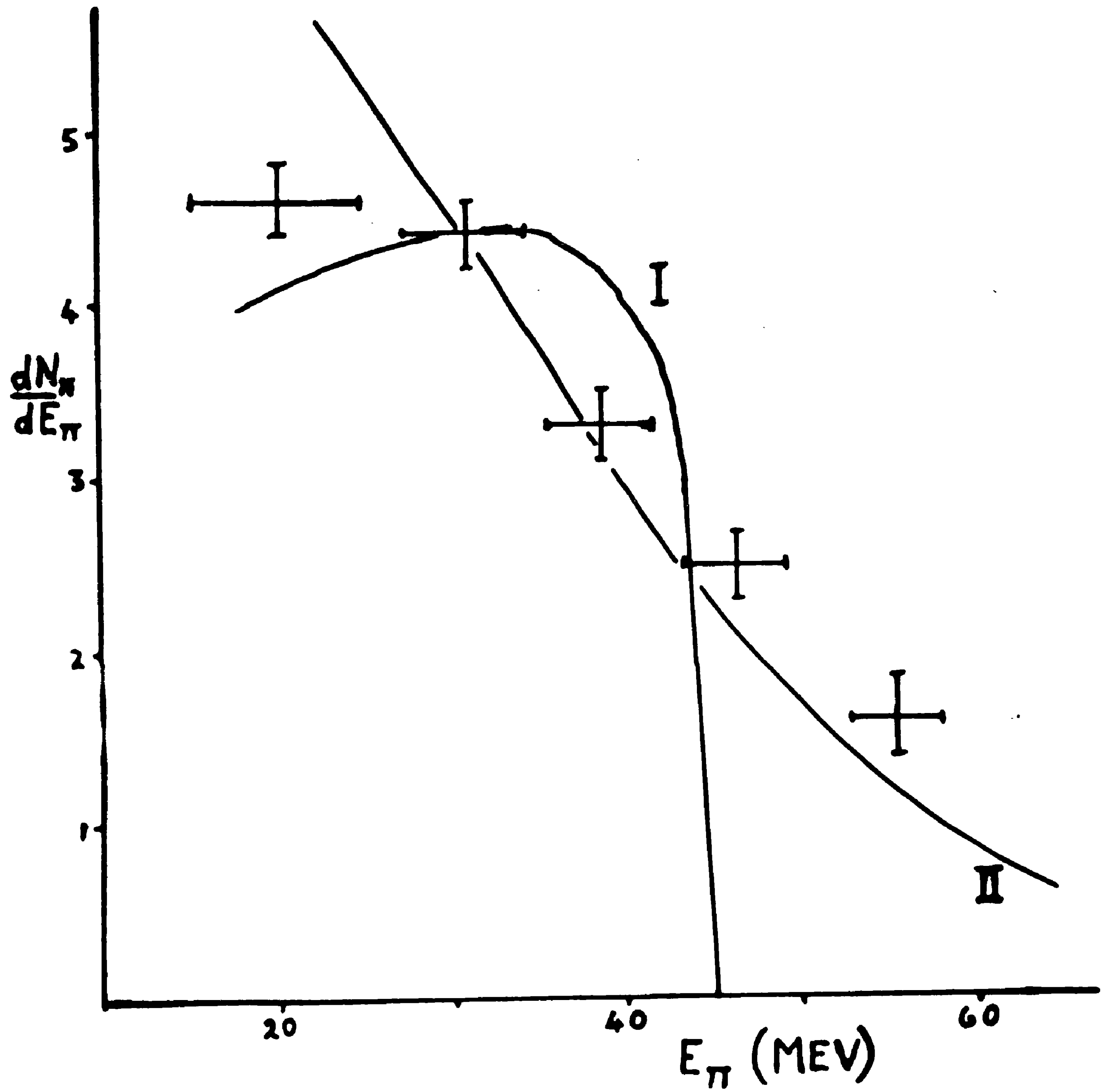

FIGURE 21.

The number of mesons in each energy interval was normalized to the same photon flux and also to the number of carbon atoms per square centimetre in the carbon target. A subtraction was then performed (CH_2 - C) so that the resulting numbers of mesons must have been photoproduced from hydrogen. It was found that about 50% of those mesons had been detected in association with a delayed coincidence. Thus we may say that the detection system for the $\pi^+ \rightarrow \mu^+$ decay was 50% efficient. Turning again to the carbon runs, this efficiency figure was used along with the actual number of delayed coincidences obtained, thereby yielding the total number of π^+ mesons photoproduced from carbon. Subtraction of the number of π^+ mesons from the total number of mesons gave the number of π^- mesons. The π^- to π^+ ratio was then calculated for each energy interval that was studied and the result is shown in figure 22 . The weighted mean of these ratios is 1.28 ± 0.10 over the range 15 - 59 MeV. Previous measurements on carbon in this angular and energy region were performed by Littauer (1952) who obtained 1.28 ± 0.12. The precise agreement is clearly very fortunate considering the attendant

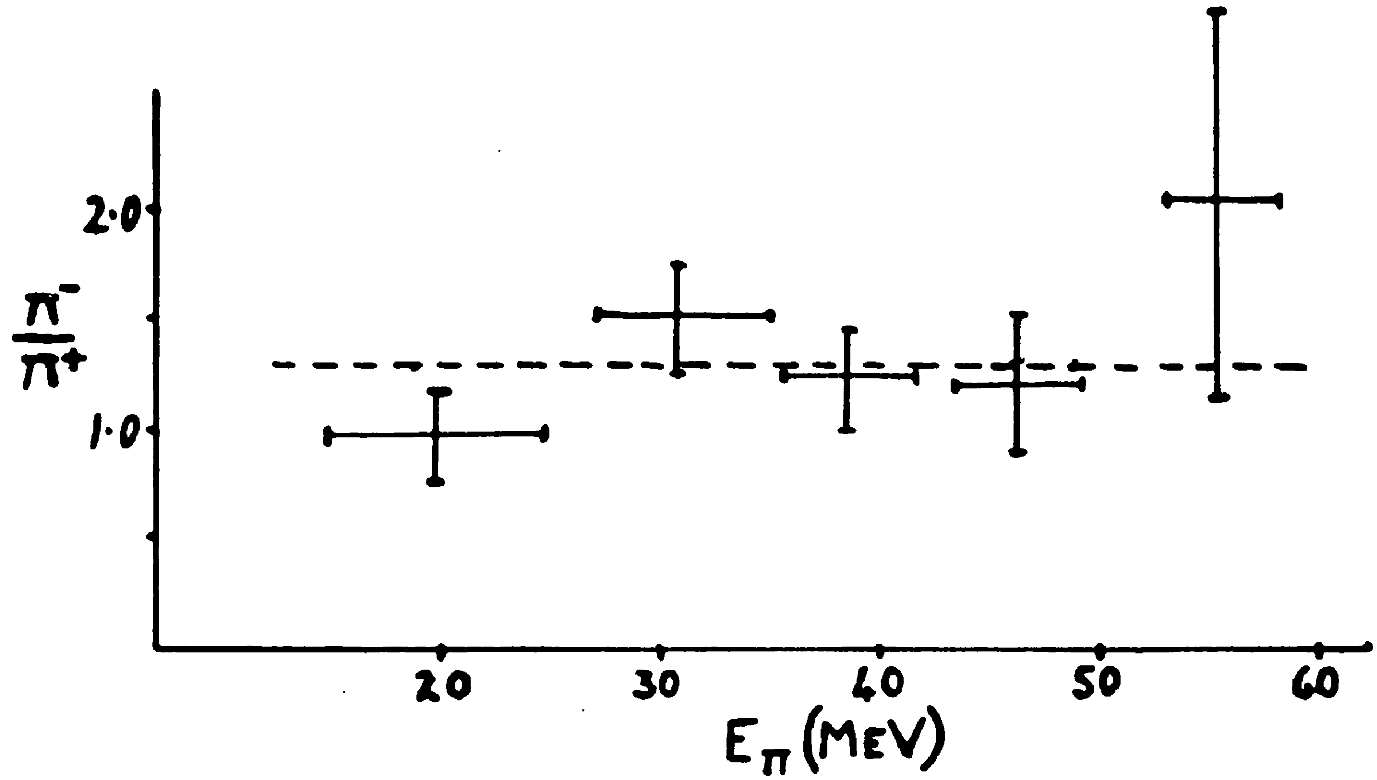

FIGURE 22.

uncertainties. It should be noted that this work was analysed from the kicksorter spectra in preference to the actual spot pictures. Although this procedure is not quite so accurate as the spot picture analysis it is extremely fast and convenient.

From this work it was possible to feel reasonably confident as to the following points:

(i) over a period of one week the overall electronic system appeared to be sufficiently stable,

(ii) oonditions of pulse "pile up" had not occurred at a beam intensity and width of 10^9 equivalent quanta per minute and 200 μsec. respectively in association with a "thicker" target than would be used in the deuterium experiment,

(iii) reasonable π^- to π^+ ratios had been obtained with the use of carbon as a target.

In conclusion, from the evidence presented here, it was plain that the detection technique for mesons would operate satisfactorily when liquid deuterium was used, since its behaviour was known under more severe background conditions than would be encountered with the use of liquid deuterium.

Chapter IV

The Photoproduction of Charged Pions From Deuterium.

(a) Experimental Details.

In the work to be described the source of photons was the bremsstrahlung beam from the Glasgow electron synchrotron. A description of this accelerator has been given by McFarlane et. al. (1955). Recent developments have enabled the peak energy of the machine to be raised from 340 MeV to 450 MeV. However, this facility was not used in the present work.

The photon beam is produced by the action of the accelerated electron beam striking a tungsten target which is a wire of 1/16 inch diameter, placed normal to the median plane of the synchrotron. The bremsstrahlung beam is emitted within a narrow cone in the forward direction with respect to the electron beam and passes out of the vacuum chamber through a thin window in the ceramic wall of the doughnut. At this stage the angular intensity distribution of the gamma beam has a width at half maximum of about 10 mille radians.

An aperture in the wall of the synchrotron chamber allows the gamma beam to pass into a separate experimental area. The nearest point to the machine at which experiments can be conveniently carried out is about six metres from the tungsten target, at which position the diameter of the beam is about two inches. For most experimental arrangements, it is desirable to have a smaller and better defined cross section of gamma beam. To achieve this a collimation system was devised by Atkinson et. al. (1957) which reduces the angular divergence of the beam to about five mille radians and a diameter just over one inch at the point six metres from the target. The collimator and beam tube are shown in figure 23 .

The liquid deuterium target was situated two metres from the exit port of the pair spectrometer. For half of this distance, the beam was enclosed in a three inch diameter tube, so that the beam was in vacuum from the collimator to within one metre of the liquid target. Further shielding was achieved by placing a six inch thick steel screen between the pair spectrometer and the deuterium target, the beam tube passing through a hole in this screen.

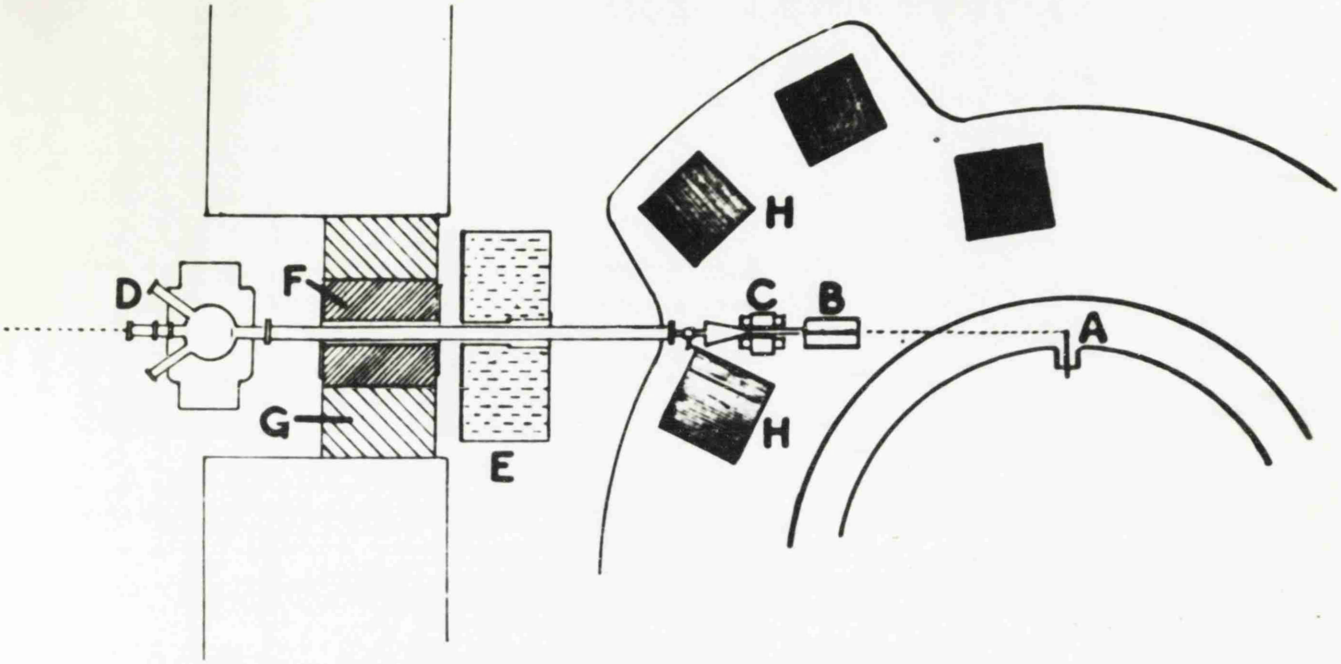

Figure 23.
Collimator and beam tube.
A - synchrotron target, B - collimator, C - scrubbing magnet, D - pair spectrometer, E - water tank, F-lead shielding, G - barytes loaded concrete, H - part of magnet yoke.

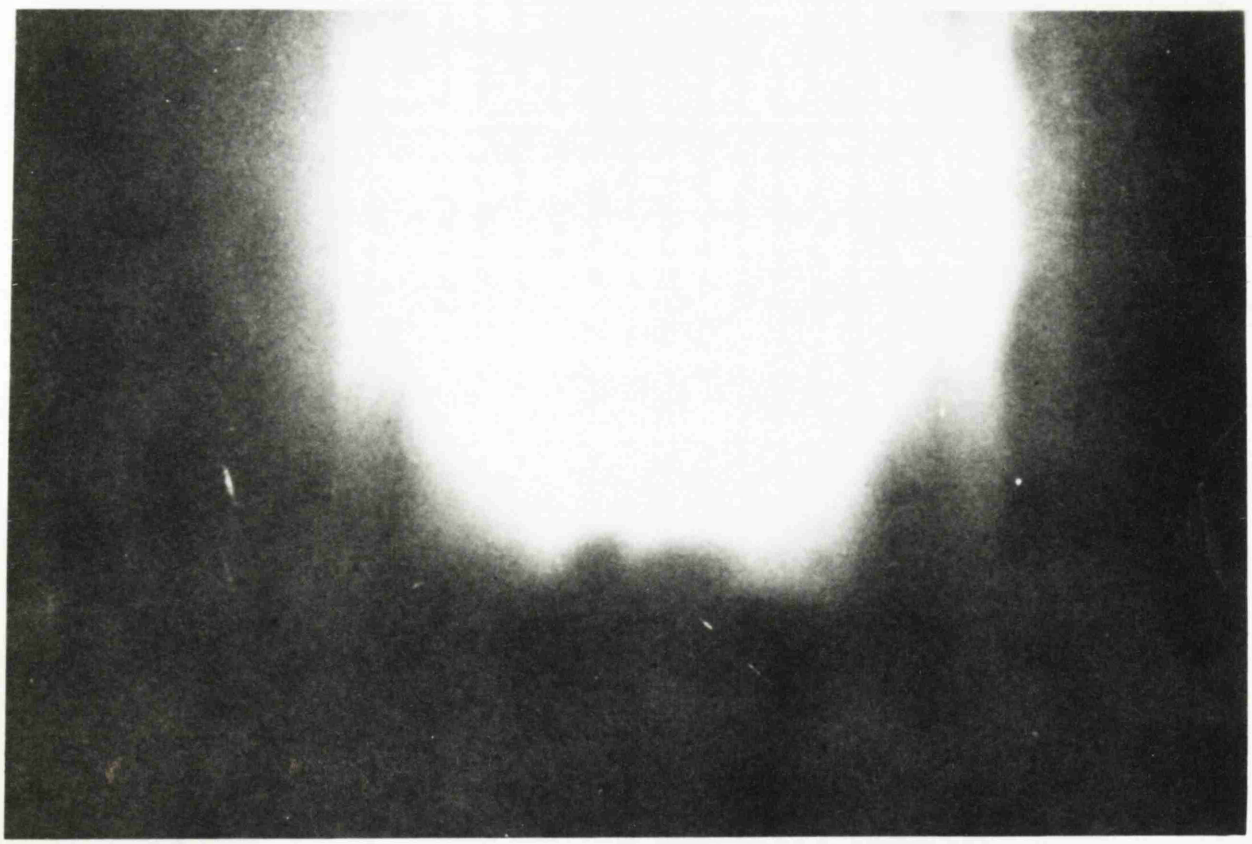

Figure 24.
Taken from an X-ray film ; showing the position of the photon beam in the target.
(Enlarged by a factor of 5/3)

For reasons which have been outlined in the previous chapter, the maximum energy of the bremsstrahlung beam required was 240 MeV. The machine was operated at a repetition rate of five pulses per second. The bremsstrahlung beam intensity was monitored by a Cornell thick walled ionization chamber (Wilson 1952) which was placed at the back of the experimental area, about twelve metres from the pair spectrometer. The maximum energy of the bremsstrahlung was known to 1%, from field measurements at the stable orbit position of the circulating electrons.

(ii) Liquid Deuterium Target.

The liquid deuterium target used in this investigation was constructed by Dr. W. Hogg of this laboratory and has been described elsewhere (Hogg 1958). A brief description will be given here of the target construction.

The target was essentially a thin walled vessel, containing the liquefied target gas in thermal contact with liquid hydrogen. This assembly was placed in a large metal double walled Dewar, the middle wall being a radiation shield at liquid nitrogen temperature (77^{o}K). The target chamber itself was a copper cylinder, of wall thickness 0.001 inch and of diameter 1.5 inches. Above the target chamber and connected to it by a thin walled capillary tube was the deuterium reservoir, which had a volume greater than the target chamber. The purpose of the deuterium reservoir was to enable background counting rates to be measured from the empty target chamber while there was still liquid deuterium in the system. The deuterium reservoir was in thermal contact with the base plate of the hydrogen reservoir. Resistance type level indicators were used to show when the target was full and empty.

(b) Experimental Procedure and Analysis of Results.

The purpose of the present investigation was two fold; first to supply more experimental evidence for the Moravcsik theory of the π^- to π^+ ratio from deuterium, and secondly, to see whether the low end point energy of 240 MeV for the bremsstrahlung beam produced any systematic difference between the present results and those obtained previously with end point energies greater than 300 MeV. The present results were obtained in a period of two weeks of machine time.

The position of the 1.5 inch diameter liquid deuterium target was about eight metres from the synchrotron target. At this distance the collimated beam diameter was 1.25 inches. This can be seen from figure 24, which is an electron scattering photograph used for the alignement of the liquid target in the photon beam. Pions emitted at a mean angle of 125 degrees to the photon beam direction were detected by the scintillation counter telescope. The solid angle subtended by the second scintillator at the target was 0.045 steradians. The arrangement of the apparatus is shown in figure 25. It was necessary to shield the telescope from background radiation produced from the target assembly and from air in the path of the beam. This was done by erecting a lead screen on three sides of the counters.

The telescope detected pions of energy 15 - 25 MeV. To extend the region of investigation to more energetic pions, absorbers of various thicknesses were placed between the telescope and the target. Three distinct measurements were made for each energy interval of pion. These were the pion counting rate with the target full of deuterium, hydrogen and then the target empty. The data were obtained in a series of runs of varying length, but usually of the order of an hour. Before the start of a run, the voltages on the counters and biases in the electronics were all checked.

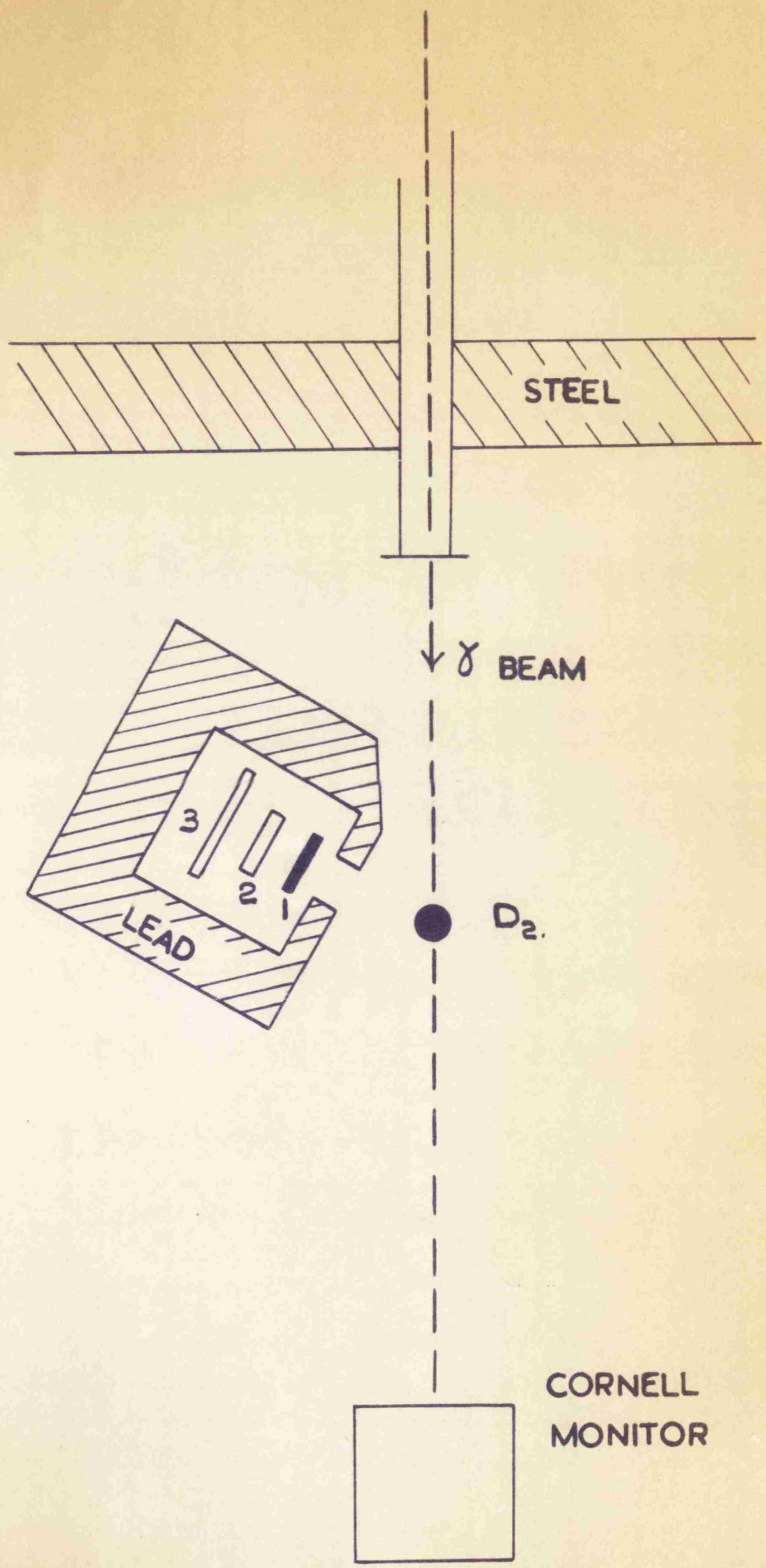

FIGURE. 25

beam diameter was 1.25 inches. This can be seen from figure 24, which is an electron scattering photograph used for the alignement of the liquid target in the photon beam. Pions emitted at a mean angle of 125 degrees to the photon beam direction were detected by the scintillation counter telescope. The solid angle subtended by the second scintillator at the target was 0.045 steradians. The arrangement of the apparatus is shown in figure 25. It was necessary to shield the telescope from background radiation produced from the target assembly and from air in the path of the beam. This was done by erecting a lead screen on three sides of the counters.

The telescope detected pions of energy 15 - 25 MeV. To extend the region of investigation to more energetic pions, absorbers of various thicknesses were placed between the telescope and the target. Three distinct measurements were made for each energy interval of pion. These were the pion counting rate with the target full of deuterium, hydrogen and then the target empty. The data were obtained in a series of runs of varying length, but usually of the order of an hour. Before the start of a run, the voltages on the counters and biases in the electronics were all checked.

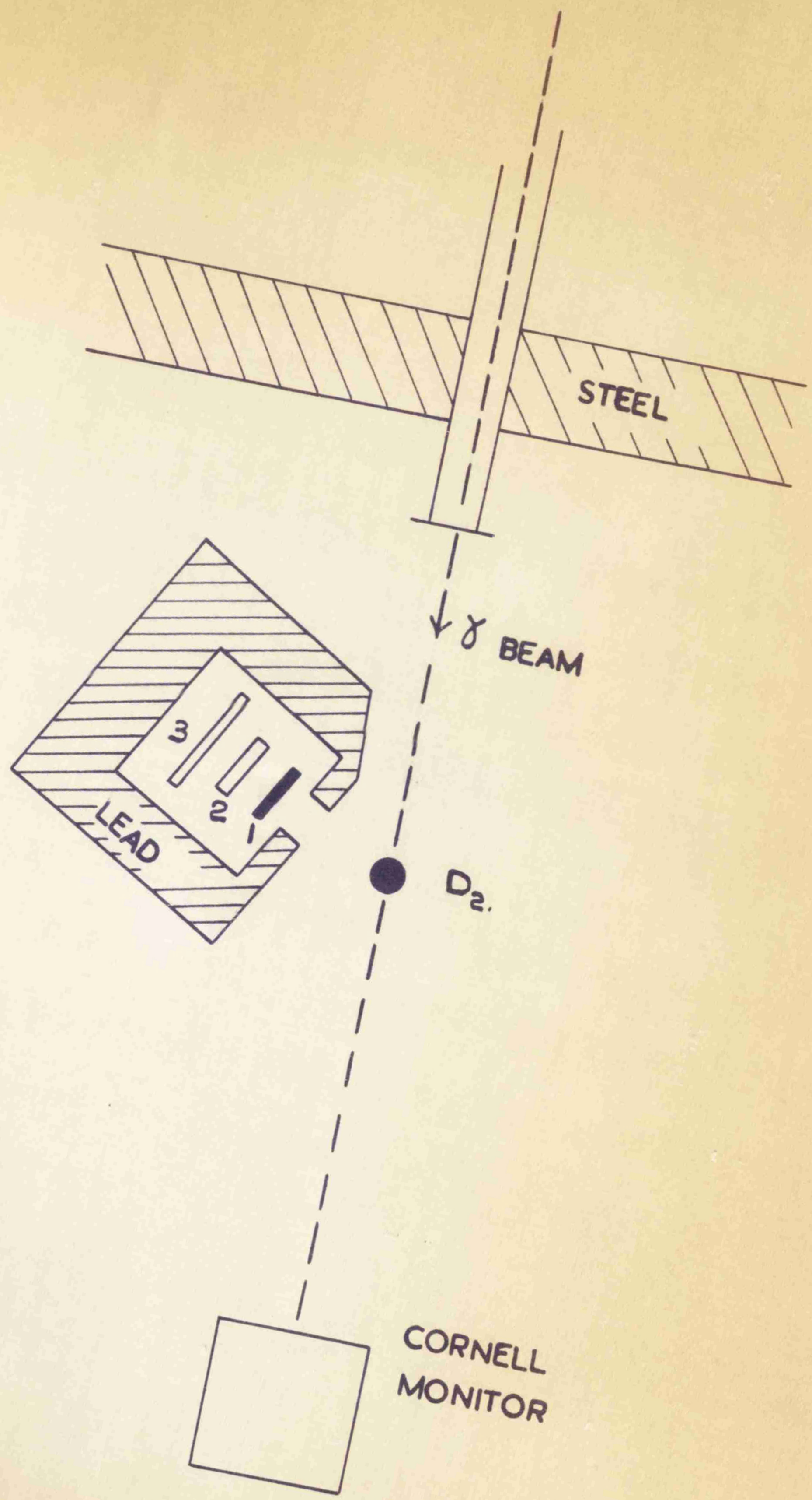

FIGURE. 25

Typical spot pictures obtained using hydrogen and deuterium in the target are shown in figures 17 and 18 . The resolution is seen to be reasonably good. The meson counting rate with the target empty was of the order of 10% that when the target was full of deuterium. For continuous monitoring during the course of a run the kicksorter served to catch any electronic troubles quickly. A typical spectrum obtained on the kicksorter using the hydrogen target is shown in figure 19 .

The spot pictures were analysed in the following manner. In the hydrogen runs there was rarely any doubt about whether a spot was due to a meson or some other particle as can be seen from figure 17 . The region of π^+ mesons is delineated by the area where delayed coincidences occurred. The number of delayed coincidences and the total number of π mesons were obtained from counting the spots. The data is shown in Table 2 . From the runs with the deuterium target the spot pictures were not quite so well defined as can be seen in figure 18 . The region between the normal meson band and the proton band is now occupied by a few spots. The identity of these spots was thought to be π^- mesons which stopped in the second

Table 2. Hydrogen Data

1	2	3	4	5	6	7	8	9	10	11
22.5 5.1	200	477.6	631	1.32 0.056	0.94 0.068	491	1.028 0.047	0.988 0.051	0.953 0.085	0.955 0.065
32.6 3.9	218	424.9	417	0.98 0.05	0.74 0.062	345	0.813 0.043	0.733 0.048	0.957 0.100	

1) Energy interval of pion (MeV)
2) Mean γ -ray energy (MeV)
3) Total number of integrator units where one integrator = 10^8 equivalent quanta
4) Total number of pions (without delayed coincidence) observed with target full of hydrogen
5) Number of pions per integrator unit
6) 5) corrected for background (empty target) N_1
7) Total number of pions (with delayed coincidence) observed with target full of hydrogen
8) Number of pions per integrator unit
9) 8) corrected for background (empty target) N_2
10) N_1/N_2
11) Mean value of N_1/N_2 say. ϵ.

scintillator and released at least one charged product in the resulting star. This process is known to occur in a very short time ($\sim 10^{-12}$ secs. Whiteman 1950) and thus the apparent energy in the second counter is increased, thereby moving the spot up into the previously vacant region. An analysis of the spot density across this region gave a good estimate of the number of mesons which were unidentifiable under the proton band. Thus the number of delayed coincidences were recorded and also the total number of mesons were obtained from the deuterium runs. A similar analysis was performed on the spot pictures taken on the background runs. The data obtained in this way is shown in Table 3 .

As can be seen only two pion energy intervals were studied within the allocated machine time when hydrogen was used in the target. The ratios of "undelayed" to "delayed" events were in good agreement between the two intervals and a mean value ϵ was obtained. This value was used in the following way. Let N_1 be the total pion counting rate from deuterium and N_2 be the counting rate for delayed coincidences from deuterium.

Table 3. Deuterium Data

1	2	3	4	5	6	7	8	9	10	11	12	13
22.7 5.0	200	921.3	3385	3.68 0.066	3.30 0.076	864	0.938 0.032	0.898 0.038	2.44 0.10	1.75 0.09	1.39 0.11	1.45 0.11
32.7 3.9	218	890.2	2081	2.41 0.054	2.17 0.065	607	0.683 0.028	0.643 0.035	1.55 0.09	1.26 0.07	1.23 0.12	1.27 0.12
40.5 3.4	233	219.6	316	1.44 0.085	1.26 0.12	80	0.364 0.041	0.344 0.045	0.93 0.12	0.67 0.09	1.39 0.25	1.43 0.25
48.3 3.1	-	124	87	0.70 0.08	0.55 0.11	17	0.137 0.033	0.127 0.035	0.43 0.11	0.25 0.07	1.71 0.71	1.83 0.71

1) --9) as for hydrogen data.

10) Number of π^- mesons = $N_1 - \epsilon N_2$

11) Number of π^+ mesons = $(1 + \epsilon)N_2$

12) Ratio of π^-/π^+.

13) 12) corrected for π^- star effect

Then we have;

counting rate of π^- from deuterium = $N_1 - \epsilon\ N_2$

counting rate of π^+ from deuterium = $(1 + \epsilon)\ N_2$

$$\text{Whence the ratio } \frac{\pi^-}{\pi^+} = \frac{N_1 - \epsilon\ N_2}{(1 + \epsilon)\ N_2}$$

The calculation of this quantity is shown in Table 3 . The errors which are quoted on the π^-/π^+ ratios have been obtained by finding the uncertainty produced in the ratio by the statistical standard deviation on each of the independent variables involved and then compounding these errors. A final small correction was applied to the π^-/π^+ ratios. This arises from the fact that a π^- meson produces a star when it comes to rest in the second scintillator. There is the possibility that one of the charged product particles from the star enters the third scintillator thereby reducing the efficiency of a $12\bar{3}$ coincidence anticoincidence event to be recorded. From the best available data on the star process in carbon (Lederman 1955) and an accurate knowledge of the geometry of the counters the probability for this process to happen was calculated and found to be about $4 \pm 1\%$. This correction was applied and the final results for the π^-/π^+ ratios are shown in the last column of Table 3 .

Other corrections were considered, such as a possible difference in the mean free paths for π^- and π^+ mesons in the carbon absorbers. However, it was felt that there was not sufficient experimental evidence to show such a difference. Decay in flight of the pions applies symmetrically to both π^- and π^+ mesons so that it cancels out in the ratios. It was also found that the counting losses of the display unit were negligible.

Due to the loss of energy of the pions in the liquid target and other materials, before they reached the telescope, it was necessary to calculate the energy of the pions at creation. The pion energies shown in Table 3 are those at creation within the target. If free nucleon kinematics are assumed then it is possible to assign a mean gamma ray energy to each pion energy interval. This has been done in column two of the Table 3 .

(c) Discussion of Results.

It is interesting to note that the π^-/π^+ ratio obtained in the highest energy interval is beyond the kinematic limit of 43.7 MeV for pion production at 125°

from a free nucleon by 240 MeV bremsstrahlung gamma rays. Mesons are only produced in this energy region because of the finite momentum of the nucleons within the deuterium nucleus.

The angular variation of the π^-/π^+ ratio from deuterium as a function of energy has been discussed in some detail by Moravcsik (1957). Figures 26 and 27 are reproduced from Moravcsik's paper with the addition of the present data in the form of open circles from the three lowest energy runs. The point in figure 27 is the weighted mean of the data from 218 - 233 MeV. It will be seen that the agreement with previous data is good. The dashed and solid curves represent two versions of the Moravcsik theory which he calls the "adjusted" and "unadjusted" versions respectively. The three lines in each case correspond to the upper and lower limits of the predictions given by various approximations.

The unadjusted version is basically an evaluation of the Low (1956) theory of photoproduction by using the experimental pion nucleon scattering phase shifts. An attempt was also made to include some recoil corrections but it was found that the effect of these corrections was small. The differential cross section

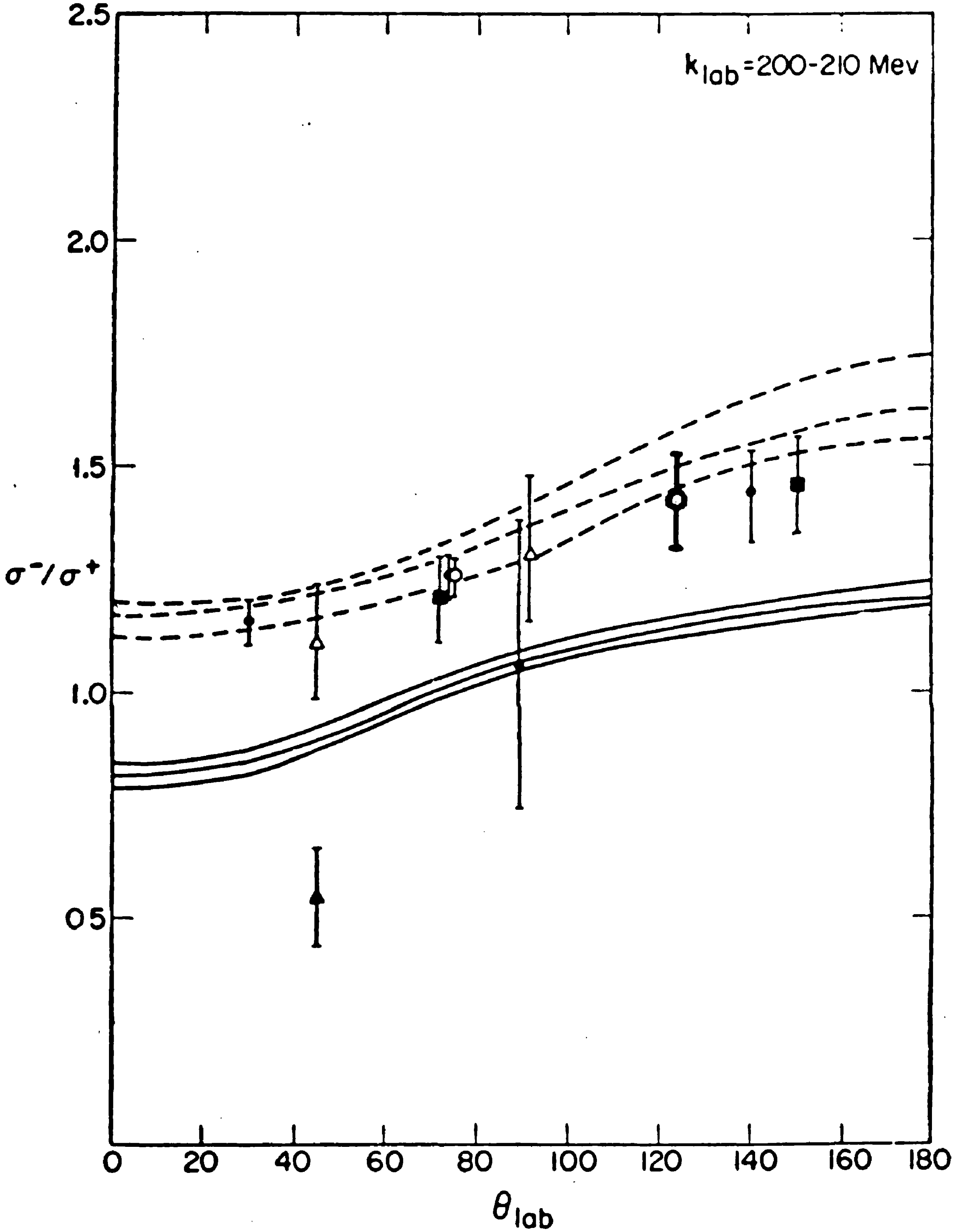

Figure 26. Ratio of π^- to π^+ mesons photo-produced from deuterium as a function of laboratory angle. The present data is indicated by open circles.

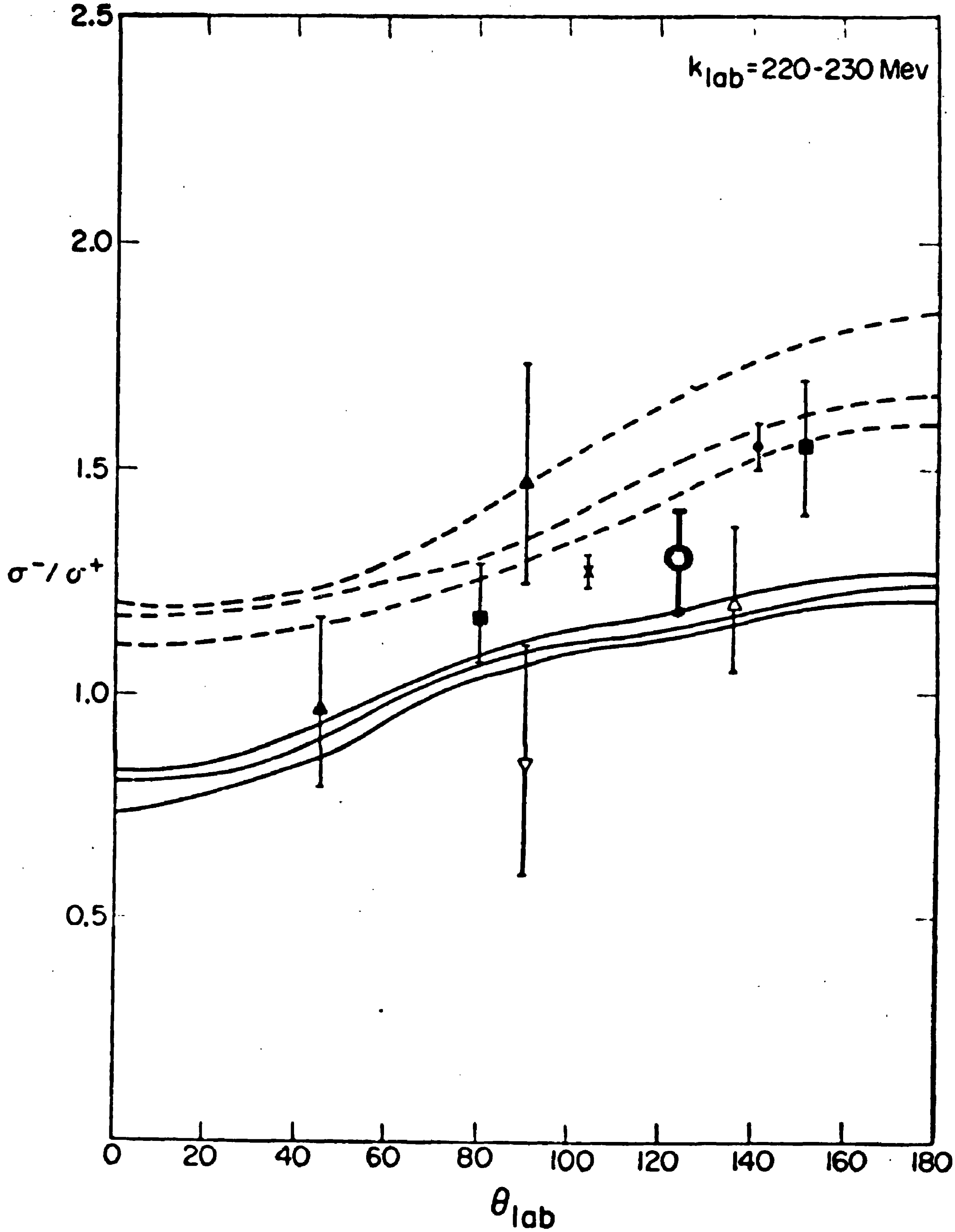

Figure 27. . Ratio of π^- to π^+ mesons photo-produced from deuterium as a function of laboratory angle. The present data is indicated by open circles.

for charged meson production including recoil was shown to be of the form

$$\frac{d\sigma}{d\Omega} = \frac{2f^2e^2}{\mu^2}\frac{q}{k}\left(1+\frac{k}{M}\right)^{-1}\left(1-\frac{q}{M+q_0+q^2/2M}\right)|m^{\pm}|^2 \qquad (20)$$

where $e^2 = 1/137$, f^2 is the renormalized pion nucleon coupling constant, μ is the pion rest mass, M is the necleon rest mass, q_0 is the meson energy and $m^{\pm}$ is the matrix element for charged pion production. Although the prediction of (20) using the known π - p scattering phase shifts gives reasonable agreement with the experimental results on π^+ production from hydrogen it gives unity for the π^-/π^+ ratio from deuterium near threshold. This fact is in disagreement with all experimental evidence.

To overcome this failure the procedure adopted in the adjusted version of the theory was to calculate the coefficient of the S - wave term of the matrix element using perturbation theory. The resulting coefficient is

$$\left(1 + \frac{k}{2M}\right)\left(1 + \frac{k}{M}\right)^{-1}$$

for positive pions and

$$\left(1 + \frac{k}{2M}\right)$$

for negative pions.

The justification for this is basically that the dispersion theoretical treatment shows that the perturbation result should be correct at low energies. In passing it is worth pointing out that a difficulty experienced with the dispersion technique is the very complicated numerical evaluation of the integrals involved and this has not been done adequately to date for the π^-/π^+ ratio. Thus the adjusted version of the theory uses a combination of a perturbation S - wave and higher angular momentum contributions of the Low type. As is to be expected this form of the theory produces little change in the shape of the angular distribution as compared to the previous unadjusted version.

At low energies ($\lesssim$ 200 MeV of gamma ray) the S - wave contribution is dominated and the unadjusted theory is not to be trusted. This is evident from figure 26 which shows poor agreement between experiment and theory. However, good agreement is obtained with the adjusted version of the theory. At higher energies the experimental data favour the region between the two versions of the theory as is becoming evident in figure 27 . This trend is continued at higher energies until the experimental data is well described by the unadjusted theory.

The conclusion that can be reached from the present work is that agreement has been obtained with previous experimental data and has added further evidence for the general Moravcsik interpretation of the Low theory of photoproduction. Finally it should be noted that as all the previous data was taken with bremsstrahlung maximum energies of 300 - 500 MeV, the present results provide a satisfactory confirmation that the previous results were not appreciably affected by contributions from gamma rays of energy much higher than that appropriate to the free nucleon case.

Chapter V

The Photoproduction of Charged Pions from Hydrogen.

(a) Experimental Details.

The object of the present investigation was to find the variation of the absolute differential cross section for the photoproduction of π^+ mesons at 90° in the centre of mass system (C.M.S.) as a function of energy between 160 and 200 MeV of gamma ray. In this work, therefore, an accurate knowledge of the energy spectrum of the gamma ray beam in the region 160 - 200 MeV was necessary. Due to the fact that the shape of the energy spectrum of the bremsstrahlung beam was rather uncertain near the maximum energy, the synchrotron was operated at 320 MeV.

The liquid target used in this investigation was constructed by Mr. D. Miller of this laboratory and is described by Bellamy et. al. (1960). The target chamber was a 1 cm. thick flat walled slice, constructed with 0.001 inch mylar walls. The cryostat was similar to that used in the deuterium experiment. It was possible to place the liquid target about seven metres from the synchrotron target, at which position the diameter of the gamma beam was just greater than one inch. Alignement of the target relative to the beam was performed with the aid of electron scattering photographs. To reach the liquid target the gamma beam passed through only one inch of air before entering the vacuum box of the target. The normal to the liquid hydrogen slice was set at 45 $\pm$ 0.3 degrees to the photon beam. The arrangement of the apparatus is shown in figure 28 . Due to the kinematics of the reaction, for a given minimum energy of meson detectable, a lower energy of gamma ray is reached as the angle of emission of the detected meson is decreased. For this reason the axis of the counter telescope was placed at 50 $\pm$ 0.5 degrees relative to the photon beam. At 160 MeV of gamma ray this is quite close to 90 degrees in the c.m.s. and the correction for the small difference was made in the final analysis. As can be seen in figure 28 , four scintillation counters are shown. The reason for this will now be explained.

With the previous three counter arrangement the minimum energy of pion detectable was about 15 MeV. At 50 degrees in the laboratory this corresponds to about 170 MeV of gamma ray. To reach lower gamma ray energies a thin plastic scintillation counter was placed

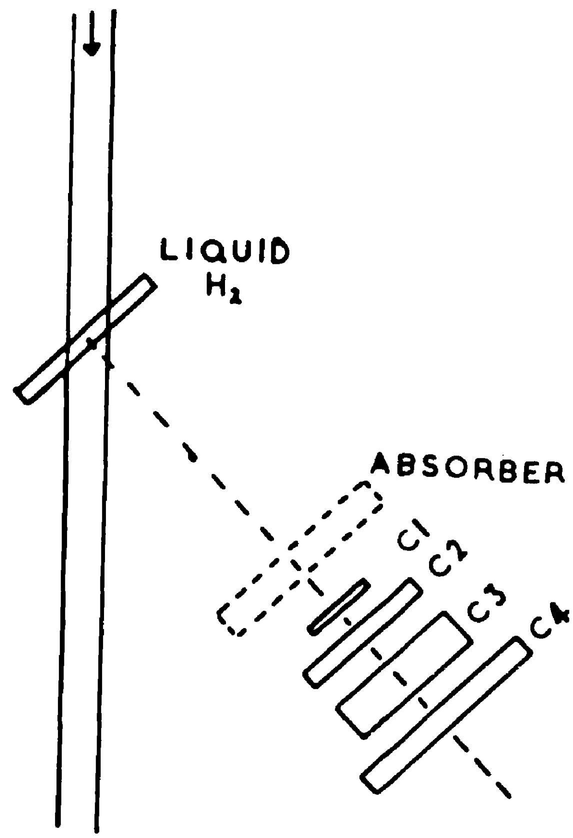

Figure 28. Schematic representation of counter telescope and hydrogen target, through which the gamma beam was allowed to pass.

in front of the previous front counter and a dE/dx and E analysis was performed for these two counters in the same manner as described previously. A fast coincidence circuit was now operated either as a $12\bar{3}$ or a $123\bar{4}$ coincidence anticoincidence depending on whether the particle stopped in the second or third counters. The resolving times of these circuits were 20 nanoseconds. When a $12\bar{3}$ event occurred, a gate was opened to detect a delayed coincidence from the second counter just as described before for $\pi^+ \rightarrow \mu^+$ decays in the third counter. Thus two energy intervals of pions were studied simultaneously.

All the information was now displayed as spots on four cathode ray tubes which were photographed by one camera on 60 m.m. film. These four displays correspond to events of the type $12\bar{3}$, $12\bar{3}\,\pi^+$, $123\bar{4}$, and $123\bar{4}\,\pi^+$. For continuous monitoring the kicksorter was used in the following manner. The first 25 channels were used to display the $12\bar{3}$ formation and the $12\bar{3}\ \pi^+$ events were displayed in channels 26 - 50. The second 50 channels were used in a similar way for the $123\bar{4}$ system.

The dimensions of the additional counter were 0.1 inches thick and 2.0 inches diameter. This counter defined the solid angle of acceptance of the telescope and as the distance between the centre of the target and the front of the counter was 14.3 inches the solid angle was 0.0154 steradians. The distances between the counters from front to back of the telescope were 1.23, 1.18 and 0.78 inches.

(b) Experimental Procedure and Analysis of Results.

The counter telescope having been carefully aligned, was shielded from stray radiation by lead screening on all sides. Even although this precaution was taken, it was found that time background produced a few spots in the region of the spot pictures of the $12\bar{3}$ system, which should have been occupied only by spots due to mesons. To overcome this, the display unit was gated by a 2 m.sec. pulse from the synchrotron which completely overlapped the time during which the bremsstrahlung beam was produced. Under these conditions the time background was reduced by a factor of a hundred, to a negligible contribution.

The present results were obtained in a period of one month of machine time. During most of this time, the output of the machine was about 5×10^8 equivalent quanta as measured by the Cornell thick walled ionization chamber. The ranges of pion energies which were detected by the telescope were 6 - 13 MeV and 14 - 25 MeV and with the use of absorbers of carbon and copper (4.44 gm./cm^2 and 8.74 gm./cm^2 respectively) pions of higher energy were studied.

The data were obtained in a series of runs of about one hour each. Before the start of a run the absorber at the front of the telescope was changed, the level of liquid hydrogen in the target was checked, biases in the electronics were checked and film of the previous run was developed. During the course of the experiment the target was emptied twice and series of runs on background counting rates were performed.

Figure 29 shows the spot pictures of a typical run with no absorber in front of the telescope. In the diagram, (a), (b), (c) and (d) represent the $12\bar{3}$, $12\bar{3}\ \pi^+$, $123\bar{4}$ and $123\bar{4}\ \pi^+$ displays respectively. They are, of course, similar to the spot pictures illustrated in a previous chapter. In the $12\bar{3}$ picture, the large number of protons is mainly from the reaction of π^0 production, which releases a low energy recoil proton. Also, it can be seen that the Landau spread in pulse height for electrons passing through counter one, has produced a few spots well over towards the meson group.

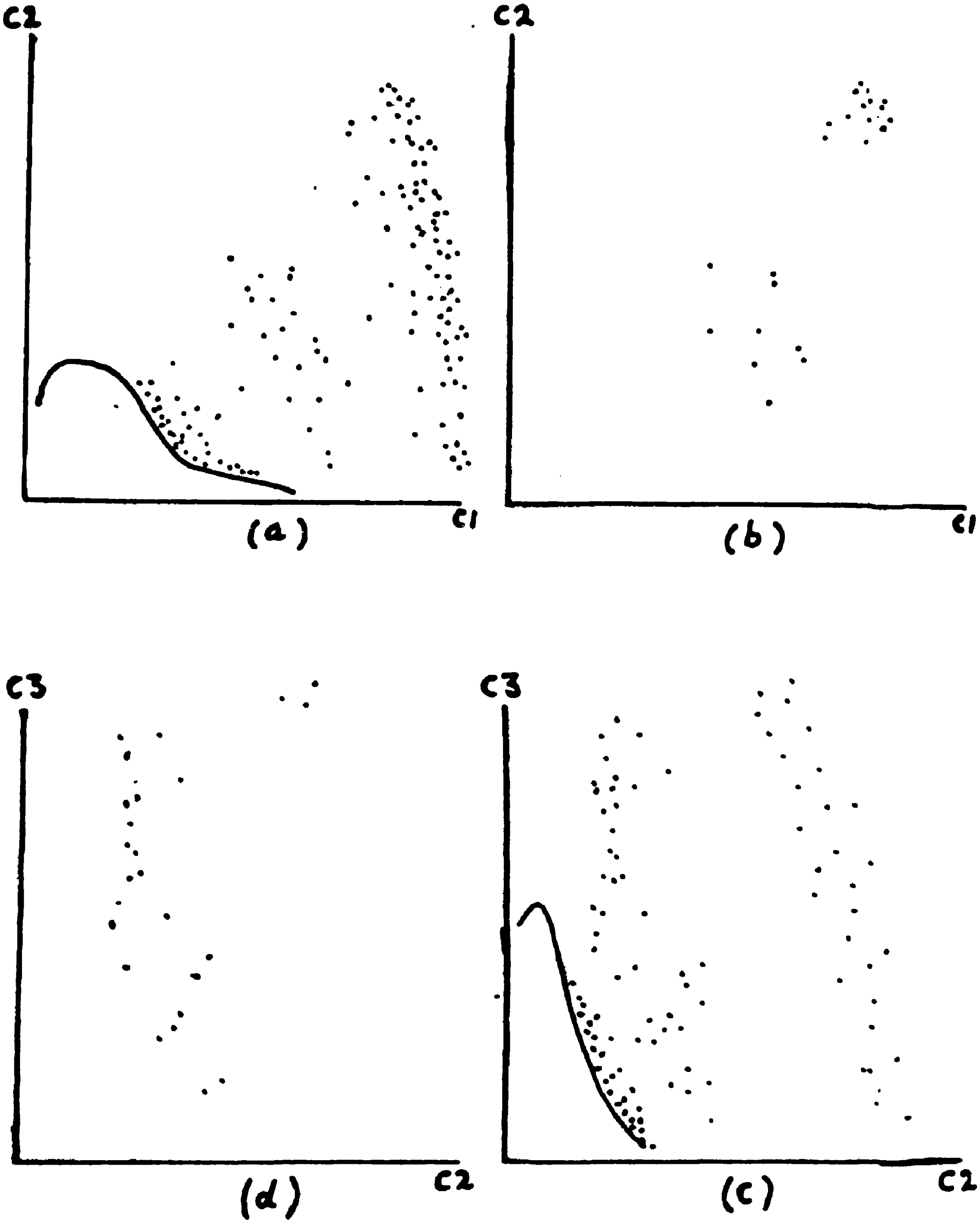

FIGURE 29.

The spot pictures were projected and the distribution of spots corresponding to delayed coincidences was recorded. Lines were drawn down the centres of these distributions and also at equally spaced distances on either side. Similarly the entire distribution was divided by a set of horizontal lines so that the region formed a matrix of small boxes. Each box was labelled by calling the horizontal divisions from 1 to 20 and the vertical divisions from A to R. All the experimental data was then recorded in the form of the number of spots, for both delayed and undelayed events, observed in each box. About 5,000 mesons were recorded in this way. Horizontal and vertical distributions were then drawn for all the energy intervals of detected pions. From these curves the numbers of mesons in each energy interval were estimated.

It was found that little ambiguity arose for any of these intervals except for the lowest energy one. In this case the general distinction between electrons mesons and photons was not sufficiently good to make a reliable estimate of the number of mesons. Therefore two criteria were demanded; first that the spot be within the general meson region and secondly that there should have been an associated delayed coincidence.

The number of such events was found and also the similar numbers in the same system when absorbers were used. This gave a relative measure of the counting rate of pions which stopped in the same range interval (the second scintillator), but which had different energy intervals at creation.

All the data is shown in Table 4 . Column six shows the observed counting rate for pions from the empty target after normalising to the number of equivalent quanta which were used in the corresponding target full runs. The nett number of pions per integrator "sweep" were corrected for the following effects:

(1) Dead time of the display unit.

The dead time of the display unit was measured and found to be 5 μ sec. in both the $12\bar{3}$ and $123\bar{4}$ systems. This dead time occurred in the blocking oscillator circuits. From a knowledge of the counting rates of four scalars of known dead times, two of which measured the counting rates of the blocking oscillators, and the other two measured the counting rates of the triggering pulses to the blocking oscillators, accurate allowance was made for counting losses. As can be seen from column 9, a 6% correction was applied to the lowest

Table 4. Hydrogen Experimental Data

	1	2	3	4	5	6	7	8	9
	162.0	3674	231	19.7	211.3	0.0574 0.0046	0.0612 0.0050	0.0612 0.0050	0.0750 0.0060
$12\bar{3}$	184.0	2672	74	11.2	62.8	0.0235 0.0038	0.0235 0.0038	0.0246 0.0040	0.0272 0.0045
	194.5	3104	98	10.0	79.0	0.0255 0.0035	0.0255 0.0035	0.0344 0.0050	0.0375 0.0055
	171.5	3557	1865	509	1356	0.380 0.020	0.380 0.020	0.380 0.020	0.380 0.020
$123\bar{4}$	191.0	2107	584	97.6	486.4	0.230 0.013	0.230 0.013	0.239 0.013	0.239 0.013
	200.6	2178	563	150.5	412.5	0.194 0.014	0.194 0.014	0.231 0.014	0.231 0.014

1) Mean γ -ray energy (MeV).
2) Total number of integrator units where one unit = 5.85×10^8 e.q.
3) Total number of pions observed with target full.
4) Total number of pions observed with target empty.
5) Nett number of pions.
6) Nett number of pions per integrator.
7) 6) corrected for dead time of display unit.
8) 7) corrected for multiple scattering and nuclear absorption
9) 8) corrected for decay in flight.

energy interval for this effect. It is interesting to note in passing that for every meson recorded in the lowest energy interval there were 20,000 electrons within the same energy band.

(2) Multiple scattering and nuclear absorption.

From the known geometry of the counter telescope and the absorber dimensions it was possible to obtain with good accuracy the losses due to multiple scattering in the absorbers. In this connection the graphical results of Sternheimer (1954) were most useful. With the aid of the data of Stork (1953) and Martin (1952) estimates were made of the losses due to nuclear absorption and large angle scatters of the mesons in the absorbers. In general the multiple scattering losses were found to be greater than those due to absorption. Column 10 shows the pion counting rate after correction for these losses.

(3) Meson decay in flight.

In the case of the $12\overline{3}$ system where only delayed coincidence events are recorded, a relatively easy calculation, involving the "proper" flight times and known lifetime of the pion, yields the appropriate corrections. However, in the case of the $123\overline{4}$ system a formidable calculation presents itself. The difficulty arises from the fact that the resolution of the detection system is not sufficient to discriminate a π-meson from a μ-meson. Thus although a π-meson, within the energy interval of detection, may decay in flight and the resulting μ-meson escape detection, it is possible for a π-meson outwith the energy interval of detection to decay such that the resulting μ-meson is detected by the telescope. The complexity of the effect can now be visualized. A complete analysis of the problem was carried out making reasonable assumptions about the energy and angular dependence of the photoproduced pions and using the exact decay kinematics of the pion. A three fold integral expression was obtained and evaluated numerically. The results showed that no correction should be applied to the observed data. This implied that with the particular geometry employed the losses were exactly balanced by μ-meson gains from pions which would not otherwise have been detected. The relative uncertainty of this correction factor on one energy interval of pion compared to another was thought to be small and $\sim 1\%$. An absolute uncertainty in the correction of $\pm$ 2% was estimated.

We wish now to obtain the differential cross sections corresponding to the corrected counting rates in Table 4 . The counting rate, N, of photoproduced pions may be written as

$$N = \frac{d\sigma}{d\Omega} \; n_t \; \frac{dn(k)}{dk} \; \Delta k \; \Delta\Omega \qquad (21)$$

where $\frac{dn(k)}{dk} \Delta k$ is the number of photons of mean energy k within the interval Δk, $\Delta\Omega$ is the solid angle subtended by the detection system at the target, $\frac{d\sigma}{d\Omega}$ is the differential laboratory cross section, and n_t is the number of target nuclei per square centimetre.

We may express (21) as

$$N = \frac{d\sigma^*}{d\Omega} \; \frac{d\cos\theta^*}{d\cos\theta} \; n_t \; \frac{dn(k)}{dk} \Delta E \; \frac{dk}{dE} \Delta\Omega \; (22)$$

where we have transformed the cross section into the c.m.s., and E is the laboratory kinetic energy of the pion. Since the reaction is a two body process $\frac{dk}{dE}$ and $\frac{d\cos\theta^*}{d\cos\theta}$ are uniquely defined functions of energy. Tables of these functions have been computed by Malmberg It was found, however, that the rest mass of the pion which was used by these authors in their computations was 1% in error according to recent experimental data (Crowe 1957). This produces errors of several per cent in values of the required functions not far above threshold. Values for the functions were computed therefore, using the most recent data on the pion rest mass.

An extensive work by Leiss and Penner (1958) contains tables of $\frac{dn}{dk}(k)$ as a function of k and in particular for a bremsstrahlung maximum energy of 320 MeV. These tables were used in the evaluation of the absolute photoproduction cross sections. However, to provide an additional check on this data, an experimental determination of the energy spectrum of the bremsstrahlung beam from the synchrotron was performed and will be described in the next chapter. The total energy contained in the bremsstrahlung beam was monitored continuously by an exact copy of the Cornell thick walled ionization chamber. This chamber has been calibrated most accurately by Palfrey et. al. (1959). The number of "equivalent quanta", Q is defined as

$$Q\, k_{max} = \int_0^{k\,max} k \frac{dn}{dk}(k)\, dk$$

or Q = total energy in the beam divided by the maximum photon energy. Thus the monitor provides a measure of the number of equivalent quanta which have been used in any run.

In expression (22) Δ E refers to the energy interval of pion at creation. To obtain this an estimate must first be made of the energy interval of pion which is detected by the telescope. Consider mesons which stop in the third scintillator i.e. $123\overline{4}$ events. From the spot picture distributions a horizontal level was decided upon, above which the spots were added and attributed to represent the meson counting rate, The electron energy required to produce spots at this level was found with the use of radioactive sources. From this information the equivalent meson energy was obtained after suitable allowance for light saturation in the scintillator (McDiarmid 1957). The upper limit of the meson energy interval was estimated in a similar fashion from the electron energy required to produce enough energy in the fourth scintillator to operate the anti coincidence circuit. It was thought that the energy interval of pions detected by the $123\overline{4}$ system was known to 5%. With the use of the range - energy relationships of Rich and Madey (1955) it was possible to obtain the energy intervals of the pions, detected by the $123\overline{4}$ system, at creation within the liquid hydrogen target.

The differential cross section for the photo production of pions was calculated using (22). By this means three absolute differential cross sections at mean gamma ray energies of 171.5, 191.0 and 200.6 MeV were obtained using the $123\bar{4}$ data. The mean of the two counting rates observed in the two energy intervals in the $12\bar{3}$ system was taken and normalised to the now known cross section at the appropriate gamma ray energy (obtained from interpolation of the results from the $123\bar{4}$ system). This normalisation served to give an absolute differential cross section at 162 MeV of gamma ray for the lowest energy interval. Table 5 shows the cross sections obtained in the above manner. The errors quoted in Table 5 are the statistical standard deviations compounded with the relative uncertainties of the correction factors which were applied to the pion counting rates in the different energy intervals. This procedure was adopted to show clearly the observed trend with energy of the differential cross section. The absolute values must be taken with a larger uncertainty to take into account the errors present in the determination of the solid angle of detection, the maximum photon energy, the calibration of the beam intensity monitor and absolute errors in the corrections

Table 5. Hydrogen Experiment Results.

1	2	3	4	5	6
162	71	5.93 0.83	5.99 0.85	0.272	22.1 3.1
171.5	66	6.92 0.74	7.30 0.77	0.392	18.7 1.9
191	64	8.03 0.43	9.14 0.46	0.595	15.3 0.9
200.6	63.5	9.03 0.55	10.51 0.60	0.682	15.3 1.0

1) Mean gamma ray energy.

2) Centre of mass system angle at which pion was emitted.

3) Differential cross sections for π^+ production.

4) 3) transformed to 90 degrees in c.m.s.

5) Values of kinematical factor, W.

6) a_0 coefficient obtained from 4) and 5).

made to the counting rates. One might estimate these as follows:

Solid angle of detection	3%
Energy interval of detection	5%
Maximum photon energy	1%
Calibration of beam monitor	4%
Uncertainties in the corrections	3%

Thus the absolute values of the cross sections are uncertain by a further 8%.

To make a comparison of the results obtained in this experiment with the predictions of dispersion relations and also previous experimental results, the cross sections at the c.m.s. angles shown in Table 5 must be transformed to 90^{o} in the c.m.s. This was performed using the experimentally determined coefficients a_o a_1 a_2 (solid curves of figures 7 & 8) of Beneventano et. al. (1956). The percentage change in the cross section between the present c.m.s. angles and 90^{o} c.m. was found to range from 1% at the lowest energy to 16% at 200.6 MeV of gamma ray.

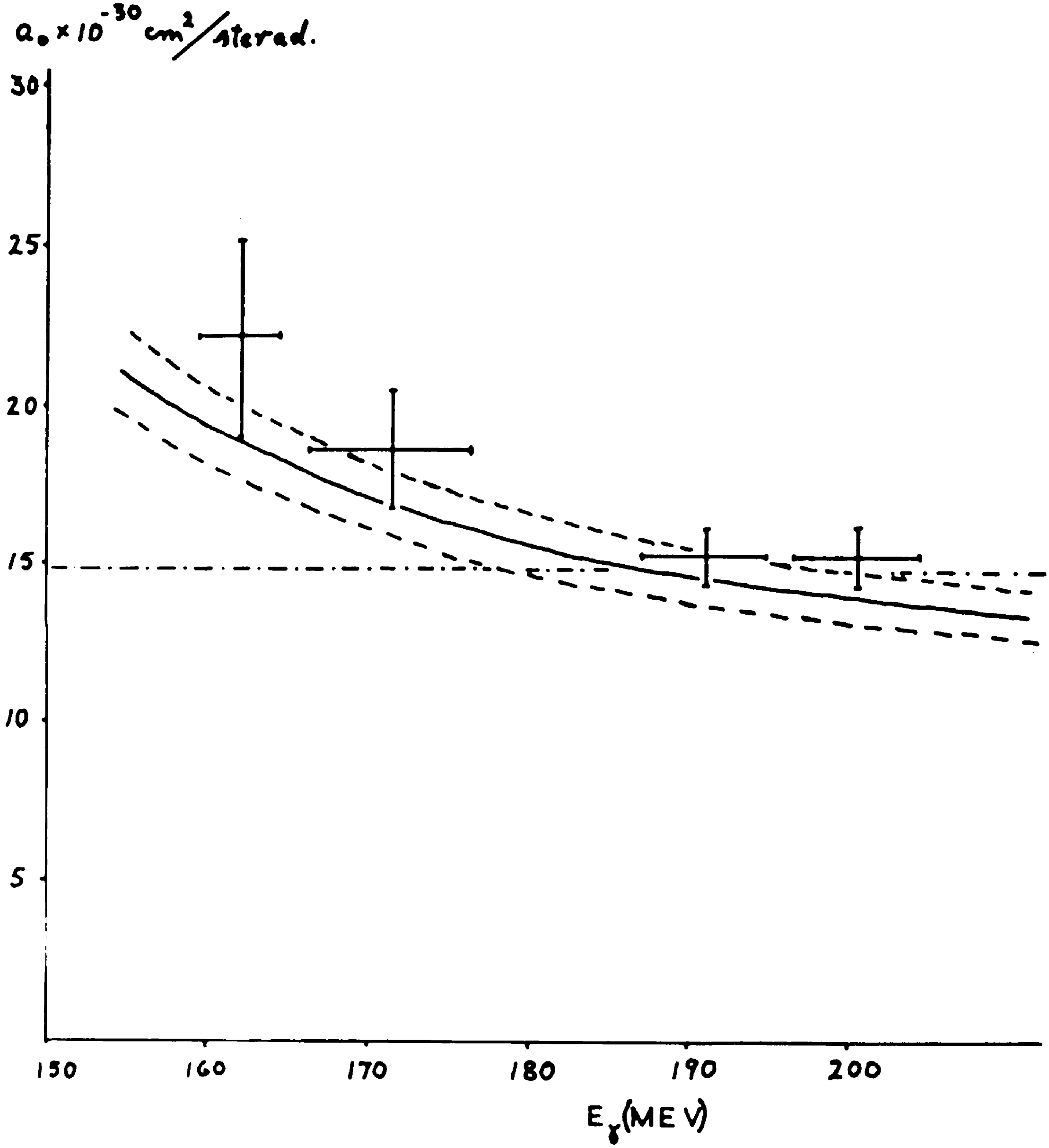

Figure 30. Photoprodection of charged pions from hydrogen at 90° in C.M.S. Plotted are the results of the present experiment. The curves are explained in the text.

The slight uncertainty in this process was compounded into the new cross sections. It should be remarked here that although the present results show a definite disagreement with the absolute values of the cross sections found by Beneventano et. al. (1956) at their lowest energy (170 MeV), the angular distribution correction which we have derived from their results is so small (~5%) at this energy, that no serious systematic error can result. The values thus found for the absolute differential cross sections at 90^{o} c.m.s. are shown in column four of Table 5 .

In order toobtain the square of the matrix element for the process (a_o) it is necessary to obtain the mean values of W (see Chapter 11) for each of the energy intervals of interest. Using the most accurate values of the pion rest mass (Crowe 1957), W was calculated as a function of energy. From a curve of W against E_γ the mean values of W over the appropriate energy intervals were obtained and are shown in column five of Table 5 . In the next column values of a_o are listed as obtained by division of columns four by five.

Figure 30 shows the values of a_o plotted as a function of gamma ray energy. The solid curve is the prediction of Chew et. al. (1957) who used the fixed momentum transfer dispersion relation and the dominance of the $(\frac{3}{2}, \frac{3}{2})$ pion nucleon interaction. In their numerical evaluation it has been assumed that $f^2 = 0.08$, where f^2 is the renormalized pion nucleon coupling constant, and that the $N^{(-)}$ term is zero (Bernardini 1959). The two dashed curves represent a 6% uncertainty both in the theoretical prediction and also in the absolute values of the experimental results.

It is clear that good agreement is obtained with the theoretical prediction, both with respect to absolute magnitude and also energy dependence of the square of the matrix element for the photoproduction of π^+ mesons from hydrogen at 90 degrees in the centre of mass system. It should be pointed out, that this is the first experimental evidence which, by itself, shows clearly the non linear behaviour of a_0 as threshold is approached.

Chapter Vl

Determination of the Energy Spectrum of the Bremsstrahlung Beam.

(a) Introduction.

The determination of photon cross sections from activation measurements using the bremsstrahlung from high energy accelerators is a well known technique in nuclear physics. In order to avoid systematic errors in the derived photon cross sections two things must be known about the gamma ray beam. These are a) an absolute measure of the total energy in the beam and b) an accurate knowledge of the bremsstrahlung spectrum.

i) Absolute Monitor.

To date the most widely used monitor for photon beams up to a peack energy of 500 MeV has been the ionization chamber developed at Cornell. A description of this chamber has been given in a Cornell University progress report (Wilson 1952). An exact copy of this chamber has been constructed at Glasgow and is used to monitor the 320 MeV gamma beam. The chamber is constructed with one inch copper walls, which thickness is such that the charge collected is largely due to ionization by electrons of a shower near the shower maximum for a large range of energies. Since the number of electrons at the shower maximum per incident photon is roughly proportional to the photon energy the charge collected is roughly proportional to the total energy in the beam. Thus to a rough approximation, the sensitivity of the chamber when expressed in units of MeV / coulomb is independent of photon energy. A number of workers (Dixon et. al. 1956, Loeffler et. al. 1959, Oakley et. al.1955) have reported calibrations of chambers of this design at energies in the range 50 - 500 MeV. Agreement has been obtained in the absolute response of the chamber to an accuracy of $\lesssim$ 5% and also in its dependence on photon energy.

ii) Shape of the Bremsstrahlung Spectrum.

In the Glasgow synchrotron the circulating electron beam is allowed to strike a 0.06 inch diameter tungsten wire. This corresponds to about one tenth of a radiation length. As the radio frequency power in the synchrotron is turned off slowly, the electron beam spirals inwards and begins to traverse the edge of the tungsten wire whose axis is vertical and at right angles to the electron beam direction. If an electron does not bremsstrahlung in its first traversal of the target it may do so at a later time as the normal ionization loss of the electron in the target is not sufficient to upset the electron orbit seriously. Thus the precise effective target thickness is not known as it depends critically on the number of "multiple traversals" of the target. The root mean square angle of multiple scattering of a 320 MeV electron in 0.06 inch of tungsten is greater than the characteristic angle of bremsstrahlung which is $m_e c^2/E = 1/640$ radians, i.e. $\gtrsim$ 1/10 degree. Thus the angular intensity of the emitted bremsstrahlung depends mainly on the multiple scattering of the electrons in the target. As is seen in figure 23 , a 0.25 inch lead collimator is placed 125 cm. away from the target and therefore selects only the bremsstrahlung in an angular interval of 1/500 radian. Thus the bremsstrahlung which passes through the collimator is predominently produced in the first few thousandths of an inch in the tungsten target. There have been various theoretical attempts (Sirlin 1957 and Hisdal) to calculate the spectral shape of the bremsstrahlung as afraction of target thickness and angle of emission of the bremsstrahlung. These calculations indicate that with the collimation used in the Glasgow synchrotron that the shape of the spectrum of gamma rays should be the same as that given by the Schiff "infinitely thin target" spectrum integrated over all angles to an accuracy of $\lesssim 3\%$ at all energies. To verify these calculations a high resolution pair spectrometer has been used to determine the energy spectrum of the bremsstrahlung beam.

b) The Pair Spectrometer.

The pair spectrometer consists essentially of the following parts:

i) Magnet, for deflection of the electron position pair;

ii) Converter, in which the incident gamma ray beam may produce an electron positron pair.

iii) Scintillation counters and associated electronics for the detection of the electron positron pair.

i) Description of the Magnet and Vacuum Box.

The electro-magnet is of conventional design and provides a field of up to 10,600 gauss. This field is sufficient to measure gamma ray energies up to 320 MeV. A magnet current of 100 Amps., is required and this is supplied by a D.C. generator. The current is controlled manually to an accuracy of 0.2%.

The vacuum chamber of the spectrometer consisted of a circular brass cylinder 12 inches in diameter and 3 inches long with circular end plates 0.5 inches thick, The gamma ray beam passed through two 2 inch diameter mylar covered port holes in the side of the brass cylinder. Similarly, electron positron pairs which are detected, emerged from the vacuum chamber via two 2 inch diameter mylar covered port holes symmetrically placed with respect to the beam axis.

A plan view of the magnet pole face is shown in figure 31 . The dispersion of the magnet is defined as

$$D = \frac{dx}{dp}$$

where dp is the difference in momentum of a particle which is distant dx perpendicular to the trajectory of a particle of momentum p. As indicated in figure 31 , r is the radius of curvature of the trajectory, ϕ is the angle of deflection, α is the angle that the trajectory makes with the normal to the magnet pole face, and ℓ is the distance of the counter from the edge of the pole face. It can be shown that, (Sona 1958)

$$D = \frac{1}{p}\left[r(1 - \cos\phi)(1 + \frac{\ell}{r}\tan\alpha) + \ell\sin\phi \right] \quad (23)$$

we have

$$r \approx 46 \text{ cms.}$$

$$\phi = 30^{\circ}$$

$$\ell \approx 65.2 \text{ cms.}$$

$$\alpha \approx 12^{\circ}$$

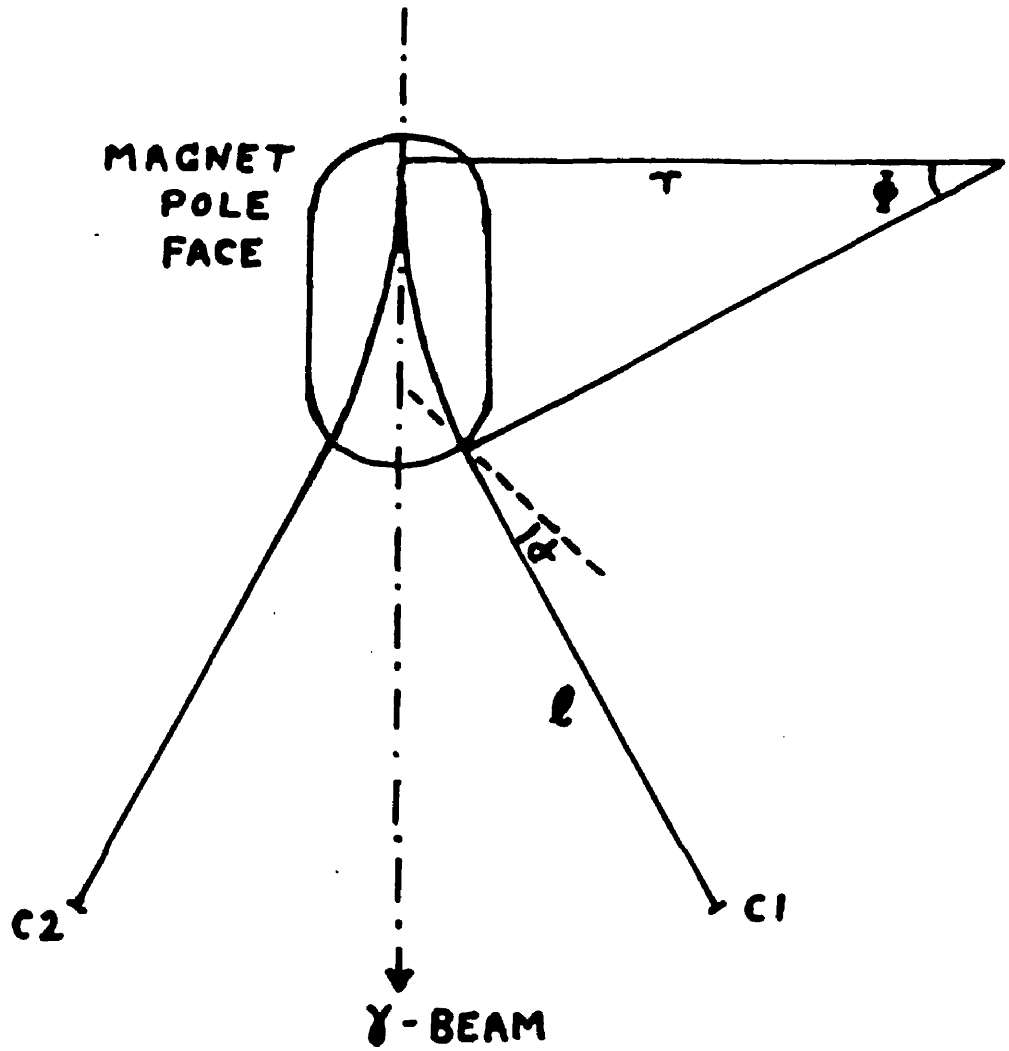

FIGURE 31. PLAN VIEW OF PAIR SPECTROMETER MAGNET.

and we obtain

$$\frac{1}{pD} = \frac{dp}{p} / dx = 2.55\% / \text{cm.}$$

The scintillation counters were 1.27 cms. wide so that the resulting resolution (R) was,

$$R = \frac{dp}{p} = 2.55 \times 1.27$$
$$= 3.24\%$$

This value for the resolution agreed within 5% with measurements performed with the floating wire technique (A. Cockroft - private communication).

The theoretical resolution may be affected by various other factors such as:

1) The finite angles between the photon and the electron and positron.
2) Radiation by the electron and positron in the converter.
3) Effect of the spreading out in time of the gamma ray beam on the average peak energy of the beam.
4) Edge effects of the scintillation counters.
5) Multiple scattering of the emergent particles in the converter.
6) Scattering into the detector system of particles which would otherwise not have been counted, for example from the vacuum box.

The first four of these effects were estimated and found to be individually unable to change the resolution by more than 1%. Effects 5) and 6) will be discussed later.

ii) Converter and Detection System.

The converter used was a 0.002 inch thick foil of aluminium, whose area was greater than that of the collimated gamma beam. There is no particular merit in the choice of aluminium as converter other than the fact that the Born approximation used in the theoretical interpretation is more valid for a material with a low atomic number. The thinnest foil consistent with reasonable counting rates tends to minimize the effects of multiple scattering of the particles in the converter.

Both positron and electron were deflected through 30 degrees and detected in scintillation counters which consisted of plastic scintillators, type N.E. 101, perspex lightguides and R.C.A. 6810 photo-multipliers. The dimensions of the scintillators were 3 inches high, 0.5 inches wide and 0.25 inches thick. Effects such as 1) and 5) of the previous section were minimized in the vertical plane by having the counters 3 inches high whereas the diameter of the gamma ray beam at the converter was only 1 inch. The width of the scintillators was chosen in conjunction with the dispersion of the magnet, so as to give an overall resolution of the order of 3% as described earlier. To minimize edge effects, such as electrons not traversing the full thickness of the scintillator, its thickness was kept as little as was consistent with providing enough light output for 100% efficiency in the operation of the coincidence circuits.

The phototubes were magnetically shielded by μ metal and soft iron cylinders. It was found to be convenient to mount the phototubes vertically and view the plastic scintillators from their 0.5 inch by 0.25 inch bases.

To record coincidences between the two counters a fast coincidence circuit, with a resolving time equal to 9 nanoseconds was used. The slow output of this unit operated a scalar. In operating a one channel pair spectrometer at fairly high resolution it is important that a simultaneous measurement of the random coincidence rate should be made. The reason for this is that the ratio of single counts in either of the counters to the true pair counting rate is approximately inversely proportional to the resolution. As a consequence, the random coincidence rate is not negligible. In this experiment the random coincidence rate was continually monitored by taking delayed coincidences between the electron counter and the positron counter. The coincidence unit used was identical to the one used in measuring true coincidences. Typical random coincidence counting rates were of the order of 10% of the true coincidences.

(c) Experimental Procedure.

The general arrangement of the gamma ray beam and spectrometer has been described earlier. During the alloted time for the experiment, the synchrotron operated at about 7×10^8 equivalent quanta per minute.

With the use of electron scattering photographs the spectrometer was aligned relative to the gamma beam. A reasonable counting rate was obtained by adjusting the current in the magnet coils until pairs from 100 MeV quanta were being counted. The voltages on the two photomultipliers were adjusted until they gave approximately equal sized pulse heights from fast electrons. The coincidence rate was then measured as a function of the voltage on each of the counters. A well defined plateau was obtained in each case. The potentiometers were set so that the operating position was well on to the plateau.

Next, the variation of counting rate as a function of the relative delay in the transit times of the pulses from the two counters to the coincidence unit was measured. The coincidence resolving time, as given by the full width at half height of the resolving curve was found to be 9 nanoseconds. The real and random coincidence units were interchanged and it was verified that they had identical resolving times to within 1 nanosecond. The apparatus was then adjusted so that real and random coincidences were counted simultaneously with zero relative delay for pulses arriving at the real coincidence unit and 26 nanoseconds relative delay for pulses arriving at the random coincidence unit.

To investigate the effect of electron scattering in the vacuum chamber and subsequently being counted, a lead screen was erected around the chamber so that electrons which were detected, definitely came out of the mylar covered port holes in the chamber. When this was done it was found that the counting rate was reduced by about 50%, indicating that this could have been a serious source of error. There remained the possibility that appreciable numbers of electrons were scattering from the sides of the lead slits at the port holes. The coincidence rate from this source was found by placin g a thin slab of lead in the centre of one of the 2.5 inch wide slits in the lead screen. The purpose of this was to eliminate the true pair counting rate but still allow the scattered electron contribution to count. It was found that the coincidence rate was now 10% of the true rate and that variation of the thickness of the slab from 0.25 inches to 0.75 inches did not affect the figure of 10%. This gave considerable weight to the belief that the coincidence rate was now 90% due to electrons which left the vacuum chamber via the port holes and did not scatter before reaching the counters. The system was now considered to be ready to investigate the shape of the bremsstrahlung energy spectrum from the synchrotron.

A series of runs were made at a sequence of values of the magnetic field to cover the entire energy spectrum of the bremsstrahlung beam. The random coincidence rate was not greater than about 10% of the true rate except at very low ($<$ 100 MeV of gamma ray) energies. For the same values of magnetic field, the runs were repeated, but this time the lead slab was in the centre of one of the slits. The energy spectrum of this contribution was found to be quite flat. When the slab was placed in the centre of the other slit a very similar result was obtained. Finally the runs were repeated without the lead slab and also without the aluminium converter being in place in the vacuum chamber. This background counting rate amounted to about 1.5% of the true rate and was roughly independent of energy.

The whole procedure was repeated and it was verified that the results were reproducible.

d) Analysis and Results.

An ideal electron-positron pair spectrometer samples one region, Δk, of the gamma ray spectrum and gives a total number of counts proportional to the number of photons between k and $k + \Delta k$. The number of pairs counted, N, when the converter is bombarded with Q equivalent quanta will be given by

$$N = Q \; N_t \iint \Phi_+(k, E_+) \, . \; \Phi(k, k_o) \, dk dE_+$$

where N_t is the target thickness in atoms / cm^2.,
$\Phi_+(k, E_+)$ is the differential positron cross section,
$\Phi(k, k_o)$ is the bremsstrahlung spectrum.
Experimentally, one measures the number of pairs N per equivalent quantum. The variation of the differential

positron cross section $\Phi_+(k, E_+)$ as a function of photon energy was obtained after suitable interpolation from the curves given in Rossi's book on high energy physics. Thus it is possible to calculate the energy spectrum of the bremsstrahlung beam.

All the numberical data is presented in Table 6 . The figures in the last column have been obtained by dividing the nett coincidence counting rate by a number proportional to the pair cross section at each energy. Thus the numbers in the last column are proportional to the number of quanta in the resolution bin width around each energy. These results are shown plotted in figure 32 , where the ordinate scale is in the usual units such that

$$\int_0^{k_0} k . \Phi(k, k_0) \quad dk \quad = \quad k_0$$

The solid curve is the theoretical Schiff bremsstrahlung spectrum, calculated for a target of negligible thickness. This curve has been normalized to the experimental data at 200 MeV. The resolution of the spectrometer at 300 MeV is shown by the triangle whose base width is 3.2% i.e., 9.6 MeV at 300 MeV of gamma ray.

Table 6.

Experimental Data of Pair Spectrometer Experiment

(1)	(2)	(3)	(4)	(5)
20	10.0 ± 1.3	5.0 ± 1.0	5.0 ± 1.5	7.6 ± 2.0
44	30.1 ± 1.0	4.5 ± 1.0	25.6 ± 1.4	29.5 ± 1.6
88	40.0 ± 0.9	4.0 ± 0.5	36.0 ± 1.1	36.0 ± 1.1
113	42.0 ± 1.6	4.0 ± 1.0	38.0 ± 2.0	36.4 ± 2.0
162	39.5 ± 1.6	3.5 ± 1.0	36.0 ± 1.8	32.8 ± 1.6
207	39.0 ± 1.5	3.0 ± 1.0	36.0 ± 1.8	32.0 ± 1.6
255	38.8 ± 2.3	2.8 ± 0.8	36.0 ± 2.5	31.7 ± 2.1
269	37.0 ± 0.8	2.6 ± 0.8	34.4 ± 1.2	30.2 ± 1.0
281	35.2 ± 1.7	2.3 ± 0.8	33.2 ± 2.0	29.1 ± 1.8
301	34.6 ± 1.7	2.0 ± 0.5	32.6 ± 2.0	28.5 ± 1.8
311	30.0 ± 1.9	1.5 ± 0.5	28.5 ± 2.1	25.0 ± 1.9
318	16.2 ± 0.8	1.0 ± 0.5	15.2 ± 1.0	13.3 ± 0.9
323	1.0 ± 1.0	0	1.0 ± 1.0	0.9 ± 0.9

(1) Mean energy of gamma ray interval.

(2) Observed number of coincidences, normalised for photon flux, after subtraction of random coincidence background.

(3) Observed number of coincidences, normalised for photon flux, from a) scattered background with converter in place plus b) background with no converter present.

(4) Nett number of coincidences corrected forbackground.

(5) These numbers which were obtained from (4) as described in the text are proportional to the number of quanta contained in a given percentage bin width around each gamma ray energy.

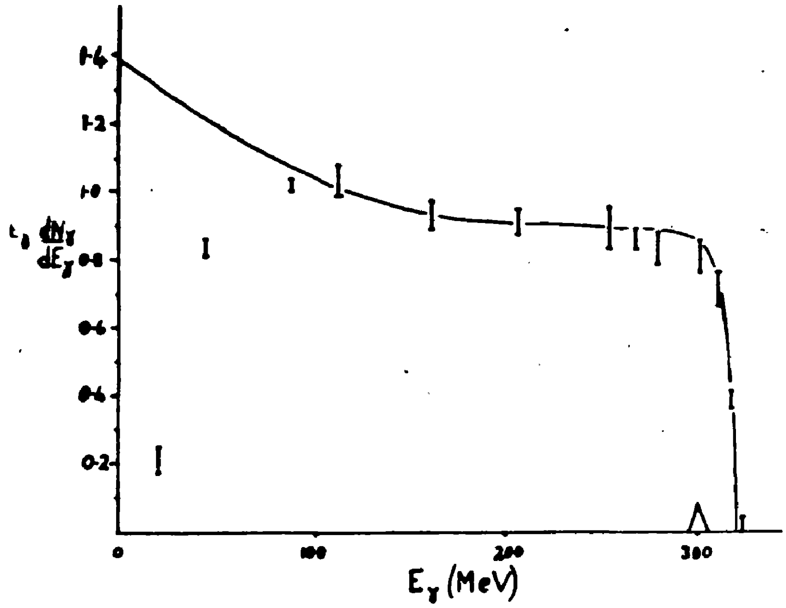

Figure 32. Bremsstrahlung spectrum. The experimental data is shown together with the resolution at 300 MeV. The curve is the Schiff "thin target" spectrum.

It can be seen that a good agreement exists between the curve and the experimental data from 100 MeV up to the end point energy. Below 100 MeV however, the multiple scattering of the electrons and positrons as they emerge from the aluminium converter enables them to pass above and below the scintillation counters. As the shape of the bremsstrahlung from meson threshold upwards was the thing of interest no detailed calculation on multiple scattering losses was performed. A rough calculation did show however that the above remarks are almost certainly true.

It has been shown that the bremsstrahlung radiation from the synchrotron has the same energy spectrum (to within 5%) as that predicted for a very thin radiator. Thus the conclusion is that the analysis of the photo-meson absolute cross sections has been conducted correctly, as it was based on the Schiff bremsstrahlung spectrum.

Chapter Vll

Conclusions

Low Energy Pion Phenomena

The experimental data in the field of low energy pion physics has at the present time reached the satisfactory state of exhibiting self consistency and also being able to be described with good accuracy by dispersion theory.

Until 1958 however, the position was one of some confusion with discrepancies existing between the various experimental data amounting in some cases to 50%. It was to the credit of Cini et. al. (1958) who clarified the situation, and asserted that with the use of well justified extrapolation procedures, the data were in agreement. The main points in their argument were the following:

i) Following a suggestion by Bernardini (1955) the extrapolation of the π^+ photoproduction cross section to threshold was performed making due allowance for the retardation term in the photoproduction amplitude. The effect of this was to increase the threshold value of a_o to about $20 \times 10^{-30}\ cm^2 / $ sterad.

ii) It was suggested that the crossing symmetry, which the pion nucleon scattering relations exhibited, required a new plot for the S - wave scattering lengths. This led to the low value of $a_1 - a_3 = 0.24$. Using these newly obtained threshold values, a Panofsky ratio P = 1.5, and a threshold π^- / π^+ ratio of 1.3, reasonable agreement in the data were obtained when inserted into the general S - wave pion nucleon relationship (Hogg 1958):

$$P = 6.7 \times 10^{-28} \left\{ \frac{(a_1 - a_3)^2}{\tau_o \ a_o} \right\}_{w = 1} \qquad (19)$$

At the time that Cini et. al. performed their analysis the existing experimental data did not substantiate their arguments. However, since then more accurate experiments have been performed and also more detailed theoretical treatments, based on the original Cini ideas, have been published (Hamilton and Woolcock 1960). A brief discussion of the present position will now be given.

As described in Chapter 11 the Panofsky ratio seems to have settled down to a value of

$$P = 1.60 \pm 0.04$$

The results on π^+ photoproduction from hydrogen, presented in this Thesis, are consistent with the extrapolation to threshold predicted by the dispersion relations, with a threshold value of a_0^+ given by

$$a_0^+ = (20.2 \pm 1.5) \times 10^{-30} \text{ cm}^2/\text{sterad}$$

(Hamilton et. al . 1960). Recent work on the π^-/π^+ ratio from deuterium at low energies (Hogg 1958) have lead to a ratio at threshold of 1.33, after using the theoretical Coulomb correction factor of Baldin (1958). This implies that for the neutron

$$a_0^- = (26.9 \pm 2.0) \times 10^{-30} \text{ cm}^2/\text{sterad}.$$

The experimental results of Adamovic et. al. reported by Hamilton et. al. (1960) on π^- photoproduction from deuterium are in good agreement with this value of a_0^-.

When these values of P, a_0^+ and r_0 are inserted into (19) we obtain the cross section for charge exchange scattering,

$$a_1 - a_3 = 0.253 \pm 0.02$$

This has to be compared with various recent values of the scattering lengths deduced from low energy scattering by protons:

$a_1 - a_3$	$= 0.283 \pm 0.012$	Cern Conference (1958)
$a_1 - a_3$	$= 0.28$	Chiu, Lomon (1959)
$a_1 - a_3$	$= 0.320 \pm 0.006$	Barnes et. al. (1960)
$a_1 - a_3$	$= 0.24 \pm 0.02$	Cini et. al. (1958)
$a_1 - a_3$	$= 0.267 \pm 0.007$	Hamilton et.al.(1960)

The wide disagreement between these various workers is due to the different analytical procedures they have adopted to obtain the value of $a_1 - a_3$ at threshold from the same experimental data. This has been discussed in some detail by Hamilton et. al.(1960) whose analysis would appear to be the most trustworthy. These authors have in addition pointed out the necessity of applying small corrections to the scattering lengths to allow for Coulomb effects which have previously been ignored. They find that when these corrections have been applied a value of

$$a_1 - a_3 = 0.245 \pm 0.007$$

is obtained. This is the quantity which should be compared with value obtained from the photoproduction threshold data and the Panofsky ratio, namely

$$a_1 - a_3 = 0.253 \pm 0.02$$

All the low energy pion data are, therefore, in good agreement with one another.

It should be remembered that the entire analysis has been carried out within the framework of total istopic spin being regarded as a good quantum number. Clearly this is a good approximation, but final agreement to better than 5% should not be expected, Noyes (1956). To show up such a breakdown of the hypothesis of charge independence, it would be necessary to perform really high precision photoproduction and scattering experiments, possibly to an accuracy of 2% or better. At the present time such experiments seem remote. However, it is to be hoped that advances in techniques will provide the necessary tools to probe the finer details of the pion - nucleon interaction.

Appendix

a) Polarization of Free Relativistic Electrons.

Introduction.

The two component neutrins theory (Lee and Yang 1957, Salam 1957, Landau 1957) has up to the present, been very successful in accounting for experimental data concerning the weak interactions between fermions . Implicit in this theory, are the ideas that the neutrino and anti-neutrino are fully polarized parallel and anti-parallel with respect to their direction of motion, and that in all reactions the number of leptons minus the number of anti-leptons remains constant. An immediate consequence of this hypothesis is that in weak interactions the product fermions and anti-fermions should have different longitudonal polarizations. This has been confirmed in the case of the high energy electrons and positrons from the decay of unpolarized negative and positive muons (Culligun et al. 1958, Crowe et al. 1958). Similarly, recent work on nuclear B-decay (Goldhaber et al. 1958) has led to the same conclusions regarding the fermion polarizations in this process. In the case of strange particle decays even without the presence of neutrinos the same fermion anti-fermion polarization scheme seems to hold (Sakurai 1959).

All these facts, however, can be understood in terms of the Universal V - A Theory (Sakurai 1959). Ther has been a recent suggestion by Guggenheimer (private communication) that similar polarization phenomena should occur when fermions become extremely relativistic and that these effects should be independent of the strength of the interaction which has produced the particles.

To be more specific let us look at the Dirac equation describing the properties of a spin one half particle. In the usual notation we have,

$$(i\gamma_\mu p_\mu + m)\Psi = 0$$

We may decompose Ψ into two parts,

$$\Psi = \tfrac{1}{2}(1-\gamma_5)\Psi^{(R)} + \tfrac{1}{2}(1+\gamma_5)\Psi^{(L)}$$

where $\Psi^{(R)}$ can be regarded as a wave function for a right handed electron and similarly for $\Psi^{(L)}$. The solution for $\Psi^{(R)}$ becomes

$$\Psi^{(R)} \propto \begin{pmatrix} 1 \\ 0 \\ (E+m)^{-1} \\ 0 \end{pmatrix} \exp(ip_z z - iEt)$$

for an electron moving in the z direction.

As $m \rightarrow o$ and $p_z \rightarrow E$ we have

$$\tfrac{1}{2}(1+\gamma_5)\Psi^{(R)} \longrightarrow 0$$

$$\tfrac{1}{2}(1-\gamma_5)\Psi^{(R)} \longrightarrow \Psi^{(R)}$$

In other words, $\frac{1}{2}(1-\gamma_5)$ can be regarded as the projection operator for the right handed state as particles become relativistic. In normal Dirac theory clearly the two states are equally populated. Guggenheimer, however, proposes that only one of these states is picked out in nature. His conjecture rests upon the fact that in weak interactions, fermions and anti-fermions exhibt a natural left and right helicity respectively.

There are clearly certain important corollaries if the suggestion turned out to be correct. These are that at extreme relativistic energies, Invariance under

a) charge conjugation would be violated

b) Invariance under the parity operation would be violated

c) Special relativity would break down. (This can be seen by applying a Lorentz transformation to the "new" Dirac description of a fermion).

A large number of possible observable consequences of this hypothesis would therefore be possible. The most available relativistic fermions are of course electrons and we consider if any experiments which have been performed in the past, would show any of the effects a), b) or c). Consider for example, the electron scattering experiments at Stanford using an electron linear accelerator. It can be shown that the angular distributions of elastically scattered electrons from nuclei are independent of the state of longitudonal polarization of the electron beam. This applies equally well both to the electric and magnetic scattering amplitudes. The required condition to observe specific polarization phenomena in electron scattering is that the target nuclei must be ligned up and pointing in a particular direction. This type of experiment has been considered from the theoretical point of view by Newton (1956) who showed that information regarding the nuclear magnetic form factors could be obtained in this way. Unfortunately such experiments have not been performed. By a similar token any experiments on the multiple scattering of electrons do not give information on the state of longitudonal polarization of the electrons. The other type of experiment possible with high energy electron accelerators is to allow the electron beam to strike a target and produce a bremsstrahlung gamma ray beam. With a longitudonally polarized electron beam this would result in a circularly polarized gamma beam (McVoy and Dyson 1957). No experiment to date such as meson photoproduction or photodisintegration would have detected such a polarization.

In view of the apparent lack of experimental evidence against the Guggenheimer suggestion it was thought that an attempt should be made to provide justification or otherwise for the hypothesis.

i) Apparatus.

To detect longitudonal polarization of high energy ($\sim$ 50 MeV) electrons from muon decay, previous experimenters (Culligan et al., Crowe et al.) have made use of the fact that such polarization persists in the bremsstrahlung quanta produced by the electrons (McVoy and Dyson 1957). The polarization of the quanta can be detected by a comparison of their transmission through iron magnetized parallel or anti-parallel to their direction of motion. There is a difference in the transmission due to part of the Compton cross section being dependent on the relative directions of the spins of quantum and scattering electron (Gunst and Page 1953). Over the energy region with which we are concerned (10 MeV to 50 MeV) the difference in transmission through the 16 cm. thickness of iron used in the experiment, when the direction of magnetization is reversed, is expected to be 5% if the γ -radiation is fully polarized.

A beam of approximately monoenergetic electrons was produced by allowing the bremsstrahlung beam from the synchrotron to strike an aluminium target .015" thick placed at the converter position in the pair spectrometer. The magnetic field in the spectrometer was adjusted to allow 52 $\pm$ 3 MeV electrons to bend out through a slit in a lead screen. Figure 33 shows the general arrangement of the apparatus. The electrons produce bremsstrahlung in the lead radiator, 6 mm. thick, and this then passes through the 16 cm. long cylindrical core of the magnet to be detected in the 2" diameter Na. I crystal. Integrated pulses from the counter were taken to a gate which was opened for a period of 2 m sec during which time the synchrotron beam existed for about 1 m sec. The pulses which passed through the gate were then amplified and delay line shaped so that they were of 1 μ sec duration and approximately flat topped. These pulses were passed to

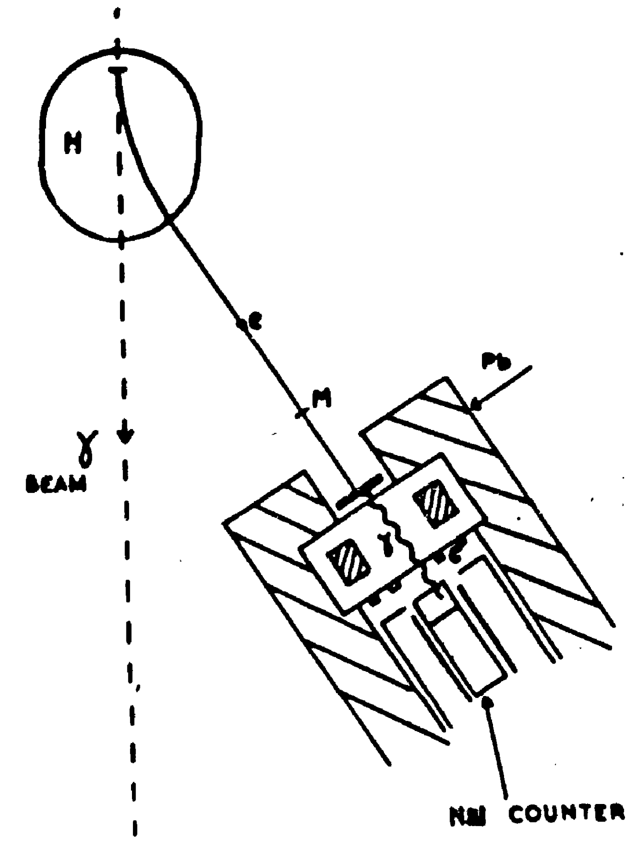

Figure 33. . General layout of apparatus for measuring polarization of relativistic electrons.

a 100 channel pulse height analyser.

Monitoring of the incident electron beam was carried out in two ways. First a small rectangular scintillation counter detected a fixed fraction of the total number of incident electrons. Secondly, the Cornell thick walled ionization chamber which actually monitored the bremsstrahlung beam but which effectively operated as a monitor for the incident flux of electrons as well. The results were calculated on the basis of each monitor and found to be identical.

One of the principle sources of possible systematic error in this investigation was direct magnetic effects on either of the counters. Both multipliers were shielded with soft iron and mu-metal and the field in the neighbourhood of the Na 1 counter could be minimized with compensating coils.

To check the counters for residual effects, pulses due to a radioactive source were taken from each counter in turn and passed to a pulse height analyser and recorded with the magnetic field of the polarization analyser first one way, then the other. In this way, it was shown that any change in pulse height was $< 1\%$. It was also verified that effects due to the spectrometer magnet were entirely negligible i.e., $\ll$ 1% . It will be shown later that the possible slight residual effect of the analyser cannot produce a systematic error in the final result.

The arrangement had been shown to be an analyser of circular polarization by the Liverpool group(to whom thanks are due for the kind gift of the magnet) by using the bremsstrahlung radiation from ^{90}Y -radiation, which is known to be highly polarized, (Goldhaber et al. 1957). The analyser was used in the present experiment with identical magnetization to that employed at Liverpool.

In order to establish the energy scale of the pulse height distribution from the Na I counter the analysing magnet was removed. Thus a beam of electrons of known and variable energy was allowed to strike the Na I counter. This was performed for electrons of energy 10 - 50 MeV. For energies less than about 25 MeV, peaks in the distributions could be discerned, but above this energy the resolution was poor.

Measurements and Results.

The spectrum of pulses from the sodium iodide counter was recorded for a given number of monitor counts with the analyser magnetic field first in one direction and then the other. There was an interval of about 5 minutes between reversals and each run lasted for about 15 minutes.

After about eight such reversals the magnetic field in the pair spectrometer was reversed thus providing a beam of positrons. The experiment was repeated exactly as for electrons for about eight runs.

The entire procedure was repeated three times with frequent checks on the gain of multipliers and overall electronic system.

To investigate background effects the 6 m.m. lead radiator was replaced by 10 cms. of lead which effectively allowed none of the shower products to enter the iron. It was found that the counting rate for pulses $>$ 10 MeV was less than 1% of the rate when the normal radiator was present. The principal constituent of this counting rate was time background due to cosmic rays. These background rates were subtracted from the normal counts with the 6 m.m. radiator present. The results were then analysed as follows. For the electrons the difference between the total spectra for the two directions of analyser magnetization was taken as a percentage of the mean. If we call this quantity $\delta_e(E)$ and the similar quantity for positrons $\delta_p(E)$ then

$$\delta = \frac{\delta_e(E) - \delta_p(E)}{2}$$

was obtained. The results should then be independent of any slight analyser magnetic effect on the sodium iodide counter as the effect would be opposite for electrons and positrons. The result is shown in figure 34 where all counts recorded in channels above the 10 MeV level have been grouped into one point. The error shown is the statistical standard deviation. Also shown for comparison in figure 34 are the results obtained by the Liverpool and Chicago groups for the polarization of electrons and positrons from muons using more or less identical apparatus. The broken curves are due to Culligan et al., and attempt to set limits between which the experimental points should lie if the electrons are fully polarized. The curve showing the greater effect was calculated on the assumption that the bremsstrahlung radiation also was fully polarized. The formula of Gunst and Page (1953) for the spin dependence of the Compton cross section as a function of energy was used, putting in the thickness of the iron and its

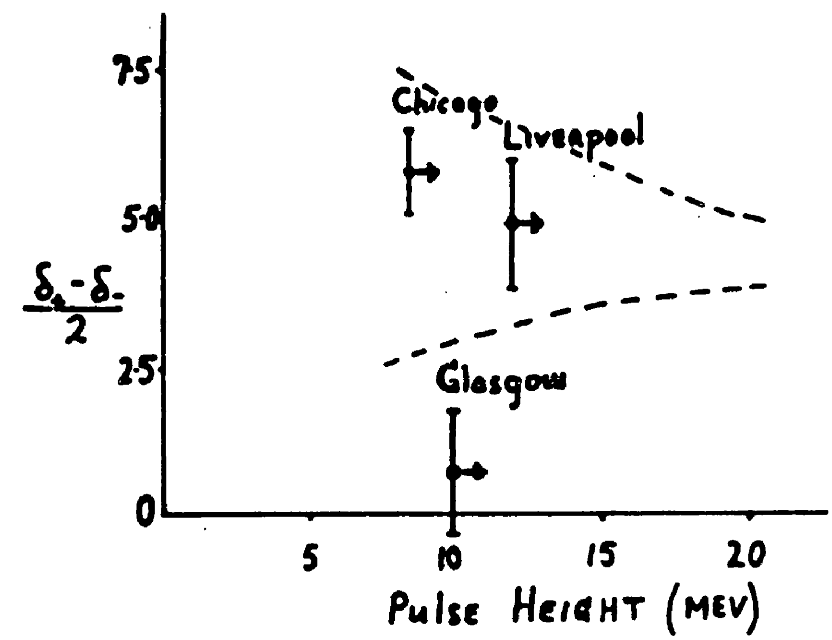

Figure 34. . Results of electron polarization experiment. The present experiment indicates very probably zero polarization. The curves are explained in the text.

degree of saturation. The curve showing the smaller effect was calculated by considering 50 MeV fully polarized electrons to be incident on the lead radiator and carrying through a Monte Carlo calculation on the showers produced, using the formulae given by Dyson (1957) for the polarization of the secondary quanta and electrons. The second case clearly applies directly to the present experiment. Two conclusions may therefore be reached:

1) The present result shows a distinct difference from the results with the 100% polarized β -spectrum from muon decay.
2) The present result is in better agreement with an assignment of zero polarization rather than 100% polarization by about two standard deviations. This constitutes a positive result of zero polarization with something like 90% certainty.

It may be said that reasonable experimental evidence has been obtained to show that the Guggenheimer hypothesis is very likely false.

b) A Possible Method of Obtaining High Energy Plane Polarized Gamma Rays.

The following is a brief description of a technique proposed by the author to the Working Committee of the National Institute who at the present time are investigating the possibilities of high energy electron accelerators.

Two methods have been used up till now in the production of plane polarized gamma rays. These are the use of a mono-crystal as a target in the electron beam and secondly the use of bremsstrahlung emitted at the 'natural' angle $\frac{mc^2}{E}$ radians where E is the energy of the incident electron beam. Both of these techniques suffer from quite serious disadvantages such as high tolerances on very small angles and an extremely thin radiator to minimize multiple scattering in the latter case. With the use of mono-crystals one can only expect something like 15% plane polarization up to about one third of the energy of the incident electrons.

This would clearly be a most uneconomic means of studying asymuthal assymetrics in the photoproduction of strange particles where it is costly enough to even reach the threshold of some of these reactions.

100% transverse polarization would be obtained. The spin continues to precess and after a further 75 μ secs will have returned to its original state.

Meanwhile the electrons have been continuously made to produce a bremsstrahlung beam whose state of plane polarization varies sinusoidally between $\pm$ 100% with a wavelength of 100 μ sec.

Thus what we have to provide is a longitudonally polarized electron beam in a suitable phase space for injection into the linac. The β -decay of nuclei represents a natural supply of longitudonally polarized electrons, but unfortunately with totally inadequate currents for any available source strength. There are several ways of producing polarized electrons and these are discussed in some detail by Tolhock (1956). The most suitable method turns out to be what could be called 'Single Mott Scattering'. In this method we consider a beam of about 1 amp of 200 kev electrons from an ordinary gun focussed to a spot at which point a thin ($\sim$1 mgm) tungsten target is placed. Those electrons which are scattered backwards (60% polarized to the plane of scattering) at about 120° are focussed and bent through an angle $\gtrsim$ 90° by means of two electrostatic

The proposed method is based upon the fact that when a transversely polarized electron produces a bremsstrahlung gamma ray a high degree of plane polarization of the gamma ray results.

It turns out that the very conditions required to produce a high energy beam of transversely polarized electrons are inherent in the properties of a linac storage ring combination. To explain further, let us assume that we can in some way inject into the linear accelerator a beam of longitudonally polarized electrons. Then these electrons will be accelerated to say 2 GeV and simultaneously retain their longitudonal polarization. However, when the electron beam enters the storage ring, the purpose of which is to keep the electron beam circulating in a given orbit, the electron spin direction precesses relative to the electron momentum. This is due to the "g" value of the electron not being exactly 2. It is in fact about one part in a thousand different from two and this produces a transverse polarization of the electron beam after 250 revolutions. As the time for the electrons to go round the storage ring once would be of the order of 0.1 μ sec then 25 μ secs after injection of the electron beam a deflectors thus aligning their spins along their momenta. Rough calculations have indicated that for 1 amp intial current it should be possible to obtain a current $\gtrsim$ 100 μ amp within the phase space requirements of a buncher of a linear accelerator. Although this is down by a factor of $\sim$ 100 on the normal linac peak currents it would result in a bremsstrahlung intensity comparable (within an order of magnitude) with that of GeV synchrotrons.

It is clear that such a technique has decided advantages over the other means for creating plane polarized gamma rays. For instance the gamma polariza-tion remains up to the incident energy of the electron.

It may be, that such a technique would provide useful information about the photoproduction properties and structure of the strange particles of modern physics.

Publications.

1. The Photoproduction of Charged Pions from Deuterium by J.G. Rutherglen and J.K. Walker. Submitted to the "Proceeding of the Physical Society".

2. A Scintillation Counter Telescope for the Detection of Charged Pions by J.G. Rutherglen and J.K. Walker. Submitted to "Nuclear Instruments".

References

Atkinson, J.R., McFarlane, W., Reid, J.M., and Swinbank, P., (1957), N.I., 1, 152.

Adamovic et al., (1959) see Bernardini, G., (1959)

Baldin, A., (1958) N.C., 8, 569

Barbaro, G., et al., (1959) see Bernardini G., (1959)

Barnes, S.W., et al., (1960) P.R., 117, 226.

Bellamy, E.H., Hogg, W.R., and Miller, D., (1960) N.I., 7, 293.

Beneventano, M., Bernardini, G., Carlson-Lee, D., Stoppini, G., & Tau,L.,(1956) N.C., 4, 323 & (1954) N.C., 12, 156.

Bernardini, G., (1955) N.C.S., 1, 104.

Bernardini, G., (1959) Rochester Conference Report.

Bethe, H.A., and de Hoffmann, F., (1955) "Mesons and Fields" Vol. 2, Row, Peterson & Co.

Bogoliubov, N.N., and Shirkov, (1959), "Elementary Particle Physics".

Bremermann, Oehme & Taylor (1958) P.R., 109, 2178.

Brueckner, K.A., & Case, K.M., (1951), P.R., 83, 1141

Brueckner, K.A., & Watson, K.M., (1952), P.R., 86, 923

Carlson-Lee et al. (1959) Rochester Conference Report.

Cassels, J.M., Fidecaro, G., Wetherell, A.M., and Wormald, J.R., (1957) Poc. Phys. Soc. A, 70, 405.

Cheston, W.B., & Goldfarb, L.J.B., (1950) P.R., 78, 683.

Chew, G.F., (1957) U.C.R.L. 1957 - 45

Chew, G.F., (1954), P.R., 94, 1748; (1954) P.R., 95, 1669.

Chew, G.F., & Low, F.E., (1956) P.R., 101, 1579.

Chew, G.F., Goldberger, M.L., Low, F.E., and Nambu, Y., (1957) P.R., 106, 1345.

Chiu, H., & Lomon, E., (1959) Ann. Phys., 6, 50.

Cini, M., Gatto, R., Goldwasser, E.L., Ruderman, M., (1958) N.C., 10, 242.

Crowe et al. (1958) P.R., 112, 2061.

Crowe, K.M., (1957) N.C., 5, 541.

Culligan, G., Frank, S.G.F., & Holt, J.R., (1958) Proc. Phys. Soc., 73, 169.

Dancoff, S.M., (1950) P.R., 78, 382.

Demeur, M., et al. (1956) N.C., 4, 509.

Dixon, D.R., Bandtel, K.C., (1956) P.R., 104, 1730.

Feld, B.T., (1953), P.R., 89, 330.

Fischer, J., March, R., & Marshall, L., (1958) P.R., 109, 533.

Gell-Mann, M., (1955), Bull. Am. Phys. Soc., 30, No.8, E - 2.

Goldberger, M.L., (1955) P.R., 99, 979.

Goldhaber, M., Grodzins, L., & Sunyar, A.W., (1957), P.R., 106, 826 & P.R., 109, 1015.

Goldschmidt-Clermont, Y., P.R., 91, 468.

Gunst, S.B., & Page, L.A., (1953) P.R., 92, 970.

Hamilton, J., & Woolcock, W.S., (1960) P.R., 118, 291.

Hisdal see Sirlin (1957).

Hogg, W., (1958) Thesis, University of Glasgow.

Hogg, W., & Bellamy, E.H., (1958) Proc. Phys. Soc., 72, 895.

Imhof, W., Knapp, E.A., & Perez-Mendez, V., (1958) R.S.I., 29, 476.

Jakobson, M., Schulz, A., & Steinberger, J., (1951), P.R., 81, 894.

Jenkins, T.L., Luckey, D., Palfrey, T.R., & Wilson, R.R., (1954), P.R., 95, 179.

Karlamov et al. (1959) Rochester Conference Report.

Keck et al. (1952), P.R., 85, 410.

Knapp, E., Imhoff, W., Kennedy, W., & Perez-Mendez, V., (1957), P.R., 107, 323.

Koester, J.L., & Mills, F.E., (1957), P.R., 105, 1900.

Knapp, E., Kenney, R.W., Perez-Mendez, V., (1958), P.R., 114, 605.

Koller & Sachs, (1959), P.R., 116, 760.

Kuchner, J.A., Merrison, A.W., & Tornabene, S., (1959), Proc. Phys. Soc., A., 73, 545.

Lax, M., & Fleshback, H., (1951), P.R., 81, 189.

Laudau, L., (1957), N.P., 3, 127.

Lebow, I.L., Feld, B.T., Frisch, D.H., & Osborne, L.S., (1952), P.R., 85, 681.

Lee, T.D., & Yang, C.N., (1957), P.R., 105, 1671.

Lehmann, (1959), N.C.S., 14, 177.

Leiss, J., & Penner, A.S., (1958)University of Illinois - "Analysis of Photonuclear Cross Sections".

Lewis, G.M., & Azuma, R., (1959) Proc. Phys. Soc.,73, 873.

Littauer, R.M., & Walker, D., (1952), P.R. 86, 838.

Loeffler, Palfrey, Tautfest, (1959) N.I. 50,

Low, F.E., (1955) P.R. 97, 1392.

Luckey, D., Jenkins, T., Wilson, R.R., P.R.91, 468.

McDiarmid, J., (1957) P.R. 109, 1794.

McFarlane, W., Barden, S.E., & Oldroyd, D.L., (1955), Nature, 176, 666.

McMillan, E.M., Peterson, J.M., & White, R.S., (1949), Science, 110, 579.

McVoy, K.M., & Dyson, F.J., (1957) P.R. 106, 1360.

Malmberg, J.H., & Robsinson C.S., (1958), P.R.109, 158.

Madey, R., (1955), R.S.I. 26, 971.

Martin, R.L., (1952), P.R. 87, 1052.

Merrison et al. (1960), Private Communication.

Moravcsik, M.J., (1956), P.R. 104, 1451.
(1957), P.R. 105, 267.
(1957), P.R. 107, 600.

Motz, H., Crowe, K.M., & Friedman, R.M., (1955)P.R.98,268
(1955) P.R. 99, 673.

Nagle, D.E., Hildebrand, R.H., & Plano, R.J., (1957) (1957), P.R. 105, 718.

Newton, R.G., (1956), P.R. 103, 385.

Noyes, H.P., (1956), P.R. 101, 320

Oehme & Taylor (1959), P.R. 113, 371.

Orear, J., (1954), P.R. 96, 176; (1956), N.C. 4, 856

Palfrey (1959), see Loeffler (1959).

Panofsky, W.K.H., Aamodt, R.L., & Hadley, J., (1951), P.R. 81, 565.

Sakurai, J.J., (1959) Progress in Nuc. Phys., Vol. 7, 243.

Samios, N.P., (1960), P.R.L., 4, 470.

Sands, M., Teasdale, J.G., & Walker, R.L.,
(1954) P.R. 95, 592.
(1954) P.R. 96, 849.

Sona, P.G., (1958), Frascati, Nota interna N.3.

Steinberger, J., & Bishop, A.S., (1950), P.R. 78, 494.

Stork, D.H., (1954), P.R. 93, 868.

Taylor, R., (1960), P.R. 107, 835.

Tolhock, H.A., (1956) Revs. Mod. Phys., 28, 277.

Walker, R.L., Oakley, D.C., & Tollestrup, A.V., (1955) P.R. 97, 1279.

Watson, K.M., (1952), P.R. 85, 852.

Watson, K.M., Keck, J.C., Tollestrup, A.V., & Walker,R.L., (1956), P.R. 101, 1159.

White, S., Repp, G.W., & Nelson, J., P.R. 91, 468.

White,R.S., Jacobson, M.J., & Schulz, A.G., (1952) P.R. 88, 836.

Wilson, R.R., (1952), P.R. 86, 125.

Wolfe, Silverman & De Wire (1955) R.S.I. 26, 504.